2012-05-03

# Targeting the Histone Acetyl-Transferase, RTT109, for Novel Anti-Fungal Drug Development: A Dissertation

Jessica Lopes da Rosa-Spiegler
*University of Massachusetts Medical School*

# TARGETING THE HISTONE ACETYL-TRANSFERASE, RTT109, FOR NOVEL ANTI-FUNGAL DRUG DEVELOPMENT

A Dissertation Presented
By

**JESSICA RAMOS LOPES DA ROSA-SPIEGLER**

Submitted to the Faculty of the
University of Massachusetts Graduate School of Biomedical Sciences, Worcester
in partial fulfillment of the requirements of the degree of

DOCTOR OF PHILOSOPHY

May 3, 2012

HISTONE MODIFYING ENZYME AND FUNGAL PATHOGENICITY

**TARGETTING THE HISTONE ACETYL-TRANSFERASE, RTT109, FOR NOVEL ANTI-FUNGAL DRUG DEVELOPMENT**

A Dissertation Presented By

Jessica Lopes da Rosa-Spiegler

The signatures of the Dissertation Defense Committee signifies completion and approval as to style and content of the Dissertation

---

Paul Kaufman, Ph.D., Thesis Advisor

---

Richard Bennett, Ph.D., Member of Committee

---

Anthony Imbalzano, Ph.D., Member of Committee

---

Oliver Rando, M.D., Ph.D., Member of Committee

---

Nicholas Rhind, Ph.D., Member of Committee

The signature of the Chair of the Committee signifies that the written dissertation meets the requirements of the Dissertation Committee

---

Craig Peterson, Ph.D., Chair of Committee

The signature of the Dean of the Graduate School of Biomedical Sciences signifies that the student has met all graduation requirements of the School

---

Anthony Carruthers, Ph.D.
Dean of the Graduate School of Biomedical Sciences

Interdisciplinary Graduate Program

May 3, 2012

**Dedication**: This accomplishment is dedicated to the 1.5 million inhabitants of my home country, Guiné Bissau. “Piquinino na tamanho. Garande na fama.”; To the Guineans and Cape-Verdeans who just the generation before mine fought for our freedom from oppression and colonial rule; To the people today who still fight for and believe in a stable and peaceful future for Guiné Bissau. Thank you.

Equally, I dedicate my efforts and work to my amazing husband, Jason Spiegler. You have supported me and been my number 1 cheerleader since we met 9 years ago. You inspire me to be my best. Now, our children, Autumn and (extremely soon to be here) “Baby Brother” are my motivation in all I do.

**Acknowledgments**: I first must thank my mentor, Dr. Paul D. Kaufman for his inspiring knowledge base, which is what enticed me to join his lab. Dr. Kaufman has been a superb mentor, relentlessly encouraging and patiently understanding. I most appreciate his thoughtfulness and clear direction that has allowed me to move forward and make some accomplishments in my 5 years in the lab. I feel greatly privileged to have been under his mentorship.

I would also like to thank the members of the Kaufman lab, present and past, that I have had the fortune to work with, particularly Corey Smith, Eric Campeau, Ahmed Fazly, Xiaoming Sun, Judith Erkmann, Toshiaki Tsubota, Timothy Matheson, and Amie Jordan. I am still waiting for my PDK medallion chain.

Also, I must thank the people I daily encounter in the LRB that make my days fun and keep me grounded in this hectic scientific research world: Amaline, “Chocolate” Eric, Evelyn, Nina, Carlye, Hubert and Ester.

Finally, last but most important, I thank my parents Maria Manuela and Mario Lopes da Rosa for all the advantages they have provided me and my siblings in our lives. They have propelled me into attaining the highest degree I could. They have always made the choice to give me the best opportunities in the home, in life, and in school. Everything I am proud of being today is thanks to them.

**Abstract**

Discovery of new antifungal chemo-therapeutics for humans is limited by the large degree of conservation among eukaryotic organisms. In recent years, the histone acetyl-transferase Rtt109 was identified as the sole enzyme responsible for an abundant and important histone modification, histone H3 lysine 56 (H3K56) acetylation. In the absence of Rtt109, the lack of acetylated H3K56 renders yeast cells extremely sensitive to genotoxic agents. Consequently, the ability to sustain genotoxic stress from the host immune system is crucial for pathogens to perpetuate an infection. Because Rtt109 is conserved only within the fungal kingdom, I reasoned that Rtt109 could be a novel drug target.

My dissertation first establishes that genome stability provided by Rtt109 and H3K56 acetylation is required for *Candida albicans* pathogenesis. I demonstrate that mice infected with *rtt109*$^{-/-}$ cells experience a significant reduction in organ pathology and mortality rate. I hypothesized that the avirulent phenotype of *rtt109* $^{-/-}$ cells is due to their intrinsic hypersensitivity to the genotoxic effects of reactive oxygen species (ROS), which are utilized by phagocytic cells of the immune system to kill pathogens. Indeed, *C. albicans rtt109* $^{-/-}$ cells are more efficiently killed by macrophages *in vitro* than are wild-type cells. However, inhibition of ROS generation in macrophages renders *rtt109* $^{-/-}$ and wild-type yeast cells equally resilient to killing. These findings support the concept that ability to resist genotoxic stress conferred by Rtt109 and H3K56 acetylation is a virulence factor for fungal pathogens and establish Rtt109 as an opportune drug- target for novel antifungal therapeutics.

Second, I report the discovery of a specific chemical inhibitor of Rtt109 catalysis as the initial step in the development of a novel antifungal agent. We established a collaboration with the Broad Institute (Cambridge, MA) to perform a high-throughput screen of 300,000 compounds. From these, I identified a single chemical, termed KB7, which specifically inhibits Rtt109 catalysis, with no effect on other HAT enzymes tested. KB7 has an IC50 value of approximately 60 nM and displays noncompetitive inhibition regarding both acetyl-coenzyme A and histone substrates. With the genotoxic agent camptothecin, KB7 causes a synergistic decrease in *C. albicans* growth rate. However, this effect is only observed in an efflux-pump mutant, suggesting that this compound would be more effective if it were better retained intracellularly. Further studies through structure-activity relationship (SAR) modifications will be conducted on KB7 to improve its effective cellular concentration.

## TABLE OF CONTENTS

## LIST OF TABLES

## LIST OF FIGURES

## LIST OF MULTIMEDIA FILES

**Supplemental Table 2.S7:** List of gene ontology terms enriched in microarray data from cells grown in YPD media

**Supplemental Table 2.S8:** List of gene ontology terms enriched in microarray data from cells exposed to hydrogen peroxide

**Supplemental Table 2.S9:** Array-wide microarray data in GEO "Matrix" format for the four biological replicates of YPD-grown cells

**Supplemental Table 2.S10:** Array-wide microarray data in GEO "Matrix" format for the four biological replicates of $H_2O_2$-exposed cells

## PREFACE

Not included in this dissertation is the following publication:

**Lopes da Rosa, J**., Holik, J., Green, E.M., Rando, O.J., and **Kaufman, P.D.** (2011) Overlapping Regulation of CenH3 Localization and Histone H3 Turnover by CAF-1 and HIR Proteins in *Saccharomyces cerevisiae.* Genetics 187 (1) 9-19.

# CHAPTER 1

## Introduction

**Acknowledgement:** The following introductory chapter contains excerpts (section 2 and 3) from a published review article written by myself and Dr. Paul D. Kaufman: Lopes da Rosa, J. and Kaufman, P.D. (2012) Chromatin-mediated *Candida albicans* virulence. Biochim Biophys Acta, 1819 (3-4).

## 1. General Background

Eukaryotic genomes are assembled into a nucleoprotein complex called chromatin. Organization of DNA into chromatin allows for the compaction of large genomes into relatively small nuclei. The nucleosome, the fundamental repeating unit of chromatin is a protein octamer of two histone H2A- H2B dimers flanking a histone $(H3\text{-}H4)_2$ tetramer wrapped by 147 base pairs of DNA (Davey et al., 2002; Luger et al., 1997). Histones are generally inhibitory to biological processes because of their extensive contacts with the DNA. Several general molecular mechanisms are used to counter this inhibition and generate access to DNA in chromatin. First, nucleosomes are moved along the DNA fiber or are evicted by ATPase "remodeling" enzymes, thereby regulating DNA accessibility (reviewed in (Smith and Peterson, 2005)). Second, histones undergo a wide variety of covalent modifications to modulate nucleosome assembly, transcription, formation of silenced heterochromatin, and DNA repair (reviewed in (Allard et al., 2004; Kouzarides, 2007; Millar and Grunstein, 2006; Moore and Krebs, 2004)). Post-translation modifications (PTMs) on histones involve acetylation, methylation, phosphorylation, ubiquitylation and sumoylation. These modifications often provide binding sites for trans-acting proteins (reviewed in (Ruthenburg et al., 2007)). In the case of histone H4 lysine 16 acetylation, the modification also directly alters the higher-order folding properties of chromatin (Shogren-Knaak et al., 2006). Together, increased DNA accessibility and protein recruitment facilitate chromatin function (reviewed in (Kouzarides, 2007;

Sinha and Peterson, 2009)). Chromatin also contributes directly to genome stability as the platform for kinetochore formation, the structures that attach to microtubules for chromosome segregation during mitosis (reviewed in (Cheeseman and Desai, 2008)).

In recent years, various studies have highlighted the relationship between chromatin maintenance and virulence of eukaryotic pathogens. Single cell eukaryotic pathogens must adapt to various environmental stimuli to successfully propagate in the mammalian host, evade attacks from its immune system and ensure future transmission to the next host. These processes often require dramatic morphological changes, expression of virulence-associated genes, and repair of damaged DNA caused by the hostile host environment. Many of these events involve chromatin alterations that are crucial for successful pathogenesis. There are several thorough and current reviews on chromatin modification of eukaryotic single cell pathogens such as *Plasmodium falciparum* (Cui and Miao, 2010; Lopez-Rubio et al., 2007), *Trypanosoma brucei* (Figueiredo et al., 2009; Lopez-Rubio et al., 2007) and *Toxoplasma gondii* (Dixon et al., 2010) that establish precedence for chromatin functions affecting pathogenesis. It is now also clear that chromatin maintenance is important for virulence in fungal pathogens, specifically *Candida albicans* (discussed below).

*C. albicans* is the most prevalent human fungal pathogen (Pfaller and Diekema, 2007). As ubiquitous opportunistic pathogens, *Candida* species are the fourth leading cause of hospital-acquired infections (Pfaller and Diekema, 2007), often stemming from implanted medical devices or organ transplants (Neofytos et al., 2010). In

healthy individuals, *C. albicans* adheres to and colonizes the mucosal lining of the human gut as a commensal organism. If the ecological balance is disturbed through the use of antibiotics or severe immuno-deficiency, *C. albicans* can overgrow and cause irksome but benign mucosal infections such as vaginitis, diaper rash or oral thrush. However, *Candida* species can also cause life-threatening infections. Fungal cells can spread into the circulatory system, leading to systemic candidiasis (candidemia). Although very rare, the mortality rate for systemic candidiasis is as high as 49%, despite anti-fungal treatment (Gudlaugsson et al., 2003). Furthermore, resistance to the currently available anti-fungal medications is rising (Cannon et al., 2007; Cowen et al., 2002; Pfaller et al., 2011). This situation makes candidiasis infections a significant public health concern, and thus novel anti-fungal drug targets are of great interest. Most anti-*Candida* drugs target cell membrane or cell wall synthesis, so identification of alternative physiological pathways that affect pathogenicity is an important goal for biomedical research.

With the intention of obtaining novel anti-fungal drugs, specifically against *C. albicans*, I have targeted a chromatin maintenance protein called Rtt109. Rtt109 has no functional homologues outside of the fungal kingdom and was first intensely studied for its crucial role in resistance to DNA damage in yeast. As a histone-modifying enzyme, Rtt109 represents a novel pathway to target for anti-fungal drug development. In this dissertation, I establish the role of Rtt109 in pathogenicity *in vivo* and characterize the first Rtt109 chemical inhibitor through *in vitro* enzymology studies.

## 2. Aspects of chromatin that promote pathogenicity through transcription regulation

### *2.1 Overview*

*C. albicans* is a dimorphic fungus. Under normal laboratory conditions (30°C, rich media), the cells grow with a budded yeast morphology. In response to various triggers, such as serum, nitrogen starvation or DNA damage, the cells filament to form pseudohyphae or true hyphae forms (Kumamoto and Vinces, 2005; Shi et al., 2007; Sudbery, 2011). The ability to change morphologically is important for pathogenicity, suggesting that the different shapes and characteristics of these cells are beneficial in different niches during infection (Reviewed in (Gow et al., 2012; Romani et al., 2003)). For instance, filamentous cells are best suited to infiltrate tissue (Brand, 2012; Gow et al., 2012). As a result of cellular morphology, *C. albicans* form different colony shapes on agar. Morphological changes, specifically between yeast and filamentous forms are regulated through transcription. A number of hyphae-specific genes encoding structural proteins and transcription factors have been identified that control this transition (reviewed in (Calderone and Fonzi, 2001; Ernst, 2000; Whiteway and Bachewich, 2007)). Several studies have highlighted the role of chromatin modification to promote regulation of these different transcription states (see below).

### *2.2 Set1 Methyltransferase*

The first account of a histone modifying enzyme affecting *C. albicans* pathogenicity was discovered in an interesting fashion. Cheng et al. performed an immunological screen using sera from HIV-positive patients suffering from oral candidiasis against proteins expressed from a *C. albicans* genomic library (Cheng et al., 2003). The histone methyltransferase (HMT), Set1, was one of three immunogens that were identified. A unique species-specific 208 amino acid N-terminus domain proved to be immunogenic in humans, allowing for this discovery (Raman et al., 2006).

Set1 is a well-conserved HMT that targets histone H3 lysine 4 (H3K4) resulting in mono-, di-, or tri- methylation (Briggs et al., 2001). Set1 and H3K4-methylation are generally associated with active gene transcription (Guillemette et al., 2011), but are also involved in DNA damage resistance (Faucher and Wellinger, 2010). Although, *C. albicans set1*$^{-/-}$ mutants lose all detectable H3K4 methylation, these cells exhibit few morphological phenotypes except for hyperfilamentation when embedded in agar (Raman et al., 2006). However, *set1*$^{-/-}$ mutants are significantly less successful at adhering to mammalian cells *in vitro*, at colonizing organs in mice, and at causing mortality in murine systemic candidiasis (Raman et al., 2006).

### *2.3 Gcn5-containing complexes*

Gcn5 is a well-conserved histone acetyl-transferase that provides HAT activity to several transcription activator complexes such as SAGA and ADA (Brownell et al., 1996). Gcn5-mediated acetylation also promotes genome stability by catalyzing

PTMs related to nucleosome assembly (Burgess et al., 2010). In *C. albicans*, inactivation of the SAGA/ADA complexes, by eliminating the core subunit Ada2, results in decreased histone H3 lysine 9 (H3K9)- acetylation (a mark of active transcription for many inducible loci), increased sensitivity to oxidative stress and fluconazole, and a defective response to *in vitro* filamentation stimuli (Pukkila-Worley et al., 2009; Sellam et al., 2009). Ada2 occupies the promoter of many oxidative stress-induced and fluconazole-induced genes. Accordingly, *ada2*$^{-/-}$ cells display reduced transcription of these genes. As a result, these mutants cause less mortality in mice and *Caenorhabditis elegans* infection models (Pukkila-Worley et al., 2009; Sellam et al., 2009).

Likewise, in the fungal pathogen *Cryptococcus neoformans*, Gcn5 is essential for pathogenicity in the murine inhalation model of cryptococcosis (O'Meara et al., 2010). *Gcn5* mutant strains display increased sensitivity to $H_2O_2$ and elevated temperatures, but not to other stresses such as starvation or high salt (O'Meara et al., 2010). Most interestingly, *gcn5* mutants are deficient in capsule formation, the mechanism by which this organism protects itself from being phagocytosed (O'Meara et al., 2010).

### *2.4 Sirtuin deacetylases in heterochromatin silencing*

A major reoccurring theme in unicellular eukaryotic pathogens is the regulation of genes located in heterochromatin that encode variant surface proteins (Merrick and Duraisingh, 2006). Heterochromatin is a region of the genome that is

stably silenced because of heritable chromatin conformation. Certain pathogens, such as *Plasmodium falciparum* and *Trypanosoma brucei,* evade the immune system by expressing only one of numerous variants of a single coat protein gene, via a mechanism termed allelic exclusion (reviewed in (Lopez-Rubio et al., 2007; Verstrepen and Fink, 2009)). In both these organisms, the regulated loci are sub-telomeric and regulation is dependent on the formation of heterochromatin. In *P. falciparum*, this allelic exclusion requires the sirtuin-family histone deacetylase, Sir2 and in *T. brucei*, Rap1, the telomeric DNA binding protein is required (Duraisingh et al., 2005; Freitas-Junior et al., 2005; Tonkin et al., 2009; Yang et al., 2009). In *C. albicans*, loss of heterochromatin silencing through homozygous deletion of *SIR2* causes unstable inheritance of colony morphology (Pérez-Martín et al., 1999). Thus far, no transcriptional effects of *SIR2* deletion have been reported for *C. albicans*.

*Candida glabrata*, another human fungal pathogen, possesses two sub-telomeric gene clusters that code for seven Epithelia Adhesin (*EPA*) membrane proteins (Castaño et al., 2005; De Las Peñas et al., 2003). *EPA1* is the only *EPA* gene expressed in laboratory cultured cells and is essential for adhesion to mammalian cells *in vitro*. However, *epa1*$^{-/-}$ cells are not deficient in pathogenicity (Cormack et al., 1999). Other *EPA* genes (*EPA2-6*) are silent in cultured cells but can be de-repressed upon loss of telomeric heterochromatin silencing by deleting *SIR2*, *SIR3* or *RAP1* (De Las Peñas et al., 2003; Domergue et al., 2005). Interestingly, silencing of the *EPA6* genes is determined by the amount of nicotinic acid (NA) in the environment (Domergue et al., 2005). *C. glabrata* is auxotrophic for NA and therefore cannot

synthesize $NAD^+$ to allow $NAD^+$-dependent sirtuin deacetylases, like Sir2, to function. *EPA6* is selectively expressed during the mouse model for *C. glabrata* urinary tract infection, but not during systemic candidiasis or in culture (Domergue et al., 2005). Tissue culture media provides sufficient NA, however, urine does not. This explains why *EPA6* is selectively expressed in NA depleted environment and why deletion of the *EPA* cluster leads to significant avirulence in the case of urinary tract infections. In conclusion, there is a direct link between de-repression of sirtuin-mediated silenced virulence genes with the appropriate environmental cues in *C. glabrata*.

*2.5 SWI/SNF and Chromatin remodeling*

Chromatin maintenance not only involves histone modification, but it also involves chromatin remodeling to change local nucleosome density. The multi-subunit complex, SWI/SNF promotes transcription of inducible genes by sliding and evicting nucleosomes on DNA, providing access for transcriptional machinery (Côté et al., 1994; Kwon et al., 1994). Deletion of either *SWI1*, encoding DNA binding/transcription co-activator, or *SNF2*, encoding the ATPase subunit, results in complete loss of pathogenicity in murine systemic candidiasis (Mao et al., 2006). In culture, these mutants cannot express hyphae (filamentation)-specific genes in response to stimuli such as serum or nutrient starvation, and as a result do not filament (Mao et al., 2006). Normally, Snf2 is recruited to hyphae-specific genes (*HWP1, ALS3, ECE1*) under these conditions by the combined action of the NuA4

HAT complex and the hyphae-specific transcription factor Efg1 (Lu et al., 2008). Via ChIP assays, both Efg1 and NuA4 can be found at these hyphae-specific genes regardless of cellular morphology (Lu et al., 2008). However, NuA4 requires Efg1 to reside at these promoters, indicating that Efg1 recruits NuA4 and that this in turn recruits SWI/SNF to allow transcription of hyphae-specific genes (Lu et al., 2008). Therefore, the hyphae-specific transcription factor Efg1, which promotes pathogenicity in murine systemic candidiasis (Lo et al., 1997), requires both a histone modification and a chromatin remodeling to transcribe filament-specific genes. It is likely that a multitude of chromatin proteins contribute to other virulence-related gene expression by similar mechanisms.

*2.6 Regulation of white-opaque switching*

The clinical isolate WO-1 *C. albicans* "switching strain" exists in two morphological states: round cells that form white round colonies and elongated cells that form opaque flat colonies (Slutsky et al., 1987). (These morphological phenotypes are distinct from those described above in *sir2*$^{-/-}$ cells (Pérez-Martín et al., 1999)). Increased pathogenicity is attributed to either cell type depending on the site of infection, hinting that phenotypic switching could be a virulence factor to better colonize distinct environments (reviewed in (Morschhäuser, 2010; Soll, 2009)). White-opaque switching, regulated by transcriptional feedback loops and the master regulator WOR1, remain stable over many generations (reviewed in (Lohse and Johnson, 2009; Morschhäuser, 2010). This type of stable inheritance suggested that

some aspects of chromatin regulation might be involved, and therefore several investigators have directly tested whether histone-modifying enzymes affect white-opaque phenotypic switching (Hnisz et al., 2009; Klar et al., 2001; Srikantha et al., 2001). Notably, destabilization of the SET3C HDAC complex, by deleting the genes encoding either core subunits *SET3* or *HOS2*, decreases white-opaque switching in WO-1 strains. These *set3*$^{-/-}$ and *hos2*$^{-/-}$ cells also exhibit hypersensitivity to filamentation stimuli such as low nutrient agar (Lee's media) or elevated growth temperature (37°C) (Hnisz et al., 2010; Hnisz et al., 2009). Despite having a Set domain common to methyltransferase enzymes, Set3 doesn't seem to have histone methyltransferase activity. Instead, the SET3C complex possesses HDAC activity through the Hos2 and Hst1 subunits. In *S. cerevisiae,* this complex has a primary role in repressing genes involved in sporulation, a meiotic process that does not occur in *C. albicans* (Pijnappel et al., 2001). Nevertheless, *set3*$^{-/-}$ *C. albicans* are hyperfilamentous and cause significantly less mortality during murine systemic candidiasis (Hnisz et al., 2010). SET3C is believed to be the homologue of human HDAC3/SMRT, and it will be of great interest to determine the virulence-associated loci that are regulated by this complex.

## 3. Aspects of chromatin that promote pathogenicity through genome stability

### *3.1 Overview*

In collaboration with the receptor-mediated immune system, the innate immune system plays an integral part in clearing mammals of pathogens. Phagocytes,

such as macrophages and neutrophils, engulf antibody-coated or complement-coated microbes into a membrane-bound compartment called a phagosome and eventually subject them to various toxic molecules (Pereira and Hosking, 1984) (reviewed in (Mansour and Levitz, 2002; Netea et al., 2008)). These toxins include reactive oxygen species (ROS) such as hydroxyl radicals (•OH), superoxide anions ($O_2^-$) and hydrogen peroxide ($H_2O_2$) that are generated through oxidative burst by the membrane-bound NADPH-oxidase enzyme (reviewed in (Missall et al., 2004)). *In vitro*, generation of ROS by phagocytes promotes *C. albicans* killing (Ferrante, 1989; Frohner et al., 2009; Hu et al., 2006; Lopes da Rosa et al., 2010; Sasada and Johnston, 1980; Sasada et al., 1987; Thompson and Wilton, 1992). *In vivo*, mice that are deficient in the NADPH-oxidase enzyme as a model for chronic granulomatous disease, an illness that leads to elevated susceptibility to mycosal infections, are more susceptible to pulmonary and systemic candidiasis (Aratani et al., 2002a; Aratani et al., 2002b). Accordingly, *C. albicans* mutant cells that lack the superoxide dismutase or catalase enzymes to neutralize these toxic molecules (*sod5*$^{-/-}$ and *cta1*$^{-/-}$ mutants, respectively) are less resistant to macrophages and less pathogenic in murine systemic candidiasis (Frohner et al., 2009; Martchenko et al., 2004; Wysong et al., 1998). Together, these investigations established that proteins required for fungi to withstand ROS-mediated damage are important for pathogenesis. Furthermore, because ROS directly damage DNA, genotoxic stress is likely to be a factor in these situations.

Multiple DNA repair pathways are crucial for *C. albicans* pathogenesis. Defects in homologous recombination in *rad52*$^{-/-}$ mutants and in non-homologous end

joining in *lig4*$^{-/-}$ mutants causes avirulence in murine systemic candidiasis (Chauhan et al., 2005). Further, multiple DNA repair genes, along with oxidative stress genes, are up-regulated when *C. albicans* comes into contact with macrophages *in vitro* (Lorenz et al., 2004). However, *C. albicans* mutants that lack base excision repair (BER) proteins (*apn1*$^{-/-}$, *ntg1*$^{-/-}$ and *ogg1*$^{-/-}$) are not hypersensitive to $H_2O_2$ or exposure to macrophages (Legrand et al., 2008). One interpretation for the latter results is that overlapping functionality with other proteins results in minimal phenotypes in cells lacking a single BER protein (Legrand et al., 2008). In any case, these results support the notion that the ability to survive genotoxic stress by *C. albicans* is indeed a virulence factor.

To evade killing in the phagosome, *C. albicans* changes morphology from budded cells to hyphal or pseudohyphal filaments, thereby rupturing out of the phagocyte (reviewed in (Calderone and Fonzi, 2001; Romani et al., 2003; Vázquez-Torres and Balish, 1997). Various environmental stimuli can induce filamentation *in vitro*, including genotoxic stress caused by DNA damage or DNA replication blocks (Bai et al., 2002; Nasution et al., 2008; Shi et al., 2007). Filamentation from replication stress or DNA damage depends on the checkpoint proteins Rad53 and Rad9 (Shi et al., 2007), linking the ability to escape phagocytes to signaling pathways that sense and respond to DNA damage (Shi et al., 2007). In sum, the mechanisms for sensing DNA damage, escaping the phagosome, and repairing DNA damage generated by host-generated ROS are interconnected in *C. albicans* and are imperative for successful pathogenesis.

*3.2 Genotoxic stress and histone post-translation modification*

Histone post-translation modifications (PTM) are frequently studied as marks associated with gene expression. However, their contributions to DNA damage checkpoint signaling and DNA repair are also substantial (Allard et al., 2004; Moore and Krebs, 2004). A notable example is acetylation of histone H3 lysine 56 (H3K56), synthesized by the histone acetyl-transferase, Rtt109 (Collins et al., 2007; Driscoll et al., 2007; Han et al., 2007a) (further discussed in detail in section 4 and in Chapter 2).

Our laboratory was first to demonstrate that loss of H3K56 acetylation via deletion of *RTT109* in *C. albicans* strikingly reduces mortality in mice subjected to systemic candidiasis (Lopes da Rosa et al., 2010) (see Chapter 2). Furthermore, *rtt109*$^{-/-}$ cells are incapable of efficiently colonizing the kidneys during acute (24 hours) or prolonged (20 days) infections (Lopes da Rosa et al., 2010; Wurtele et al., 2010). Notably, the poor pathogenicity of *rtt109*$^{-/-}$ cells correlates with an inability to withstand phagocyte-generated ROS (Lopes da Rosa et al., 2010). Although, *rtt109*$^{-/-}$ cells are significantly more susceptible to macrophages *in vitro* than wild-type cells, preventing macrophage-generated ROS renders *rtt109*$^{-/-}$ mutants equally resistant as wild-type cells (Lopes da Rosa et al., 2010). These data demonstrate that the genotoxic stress protection provided by Rtt109 and H3K56ac is important for *C. albicans* to survive phagocytosis by macrophages, providing a mechanistic explanation for the defect in pathogenesis.

In *C. albicans*, the $NAD^+$- dependent sirtuin HDAC, *HST3,* is an essential gene and is solely responsible for hydrolyzing acetylated H3K56 (H3K56-ac) (Wurtele et al., 2010). Heterozygous *hst3*$^{+/-}$ mutants are hypersensitive to genotoxic stress (Wurtele et al., 2010). Deletion of both *RTT109* alleles prevents the *hst3*$^{-/-}$ lethal phenotype, indicating that hyper-accumulation of H3K56-ac is lethal in *C. albicans* (Wurtele et al., 2010). Accordingly, nicotinamide (NAM), an inhibitor of $NAD^+$-dependent HDACs, is toxic to *C. albicans* and a variety of other human pathogenic fungi including several other *Candida* species and *Aspergillus fumigatus* (Wurtele et al., 2010). Interestingly, hyper-accumulation of H3K56-ac is not fatal in *Saccharomyces cerevisiae,* as *hst3Δ, hst4Δ* mutants are viable (Celic et al., 2006; Maas et al., 2006).

Rtt109 affects multiple processes in pathogenic fungi, because it also affects morphological white-opaque "switching" events (described above) in *Candida albicans* (Stevenson and Liu, 2011). *rtt109*$^{-/-}$ opaque cells are not stable and have an increased switching frequency to white cells. Conversely, increasing H3K56-ac levels by deletion of a copy of *HST3* or exposure to sub-lethal concentrations of NAM promotes opaque formation (Stevenson and Liu, 2011).

*3.3 Genome plasticity and the spindle assembly checkpoint*

A major function of chromatin modification and remodeling is to ensure genome stability, specifically the proper inheritance of genomic information in macro-structural units called chromosomes. *C. albicans,* however, is notorious for

generating aneuploidy in culture (Ahmad et al., 2008; Selmecki et al., 2005). In certain cases, genome instability is purposely beneficial to *C. albicans*. For example, *C. albicans* readily loses a copy of chromosome 5 (Chr5) in order to survive on the alternative carbon sources, sorbose (Janbon et al., 1998; Rustchenko et al., 1994). *C. albicans* also manipulates Chr5 to attain resistance to fluconazole, a clinically used anti-fungal drug. Two extra arms of Chr5L flanked by a neo-centromere (5 i(5L)) is generated and stably perpetuated to provide additional copies of ergosterol synthesis genes (Selmecki et al., 2006). Another remarkable example is that *Candida* centromeres can be moved to neighboring locations under the appropriate genetic selection (Ketel et al., 2009).

It is unclear how these frequent chromosome alteration events are regulated. One possibility could have been a relaxed spindle assembly checkpoint. The spindle assembly checkpoint ensures that all kinetochores are properly attached to a spindle, prior to anaphase, to ensure accurate segregation of chromosomes to each daughter cell (reviewed in (McAinsh et al., 2003)). Bai et al. hypothesized that because pathogenic fungi face extensive chromosomal damage from phagocyte-generated ROS, the spindle assembly checkpoint pathway would be imperative for pathogenicity (Bai et al., 2002). Indeed, homozygous deletion of *MAD2*, a protein essential for SAC function, renders *C. albicans* hypersensitive to $H_2O_2$ and results in complete loss of virulence in murine systemic candidiasis (Bai et al., 2002). Therefore, like the DNA damage checkpoint (Shi et al., 2007), the spindle assembly checkpoint in *C. albicans* functions to promote pathogenesis. However, these findings

do not support a relaxed spindle assembly checkpoint as the source of genome plasticity in *C. albicans*.

## 4. Rtt109 (Regulator of Ty1 Transposition 109)

### *4.1 Function of Rtt109*

Rtt109 was not initially recognized as an enzyme based on primary sequence similarity to other histone acetyl-transferase (HAT) enzymes. In fact, Rtt109 was first identified in a screen for repressors of Ty1 transposition, where disruption of the previously uncharacterized open reading frame caused elevated transposition events (Scholes et al., 2001). Rtt109 was eventually implicated in H3K56 acetylation via genome-wide Western blot surveys of the yeast deletion collection for mutants that lack H3K56-ac (Han et al., 2007a; Schneider et al., 2006).

Rtt109 has several distinguishing properties; it has no close sequence homologues outside of the fungal kingdom and requires one of two histone chaperones, Vps75 or Asf1, to stimulate its catalytic activity (Albaugh et al., 2010; Kolonko et al., 2010; Recht et al., 2006; Tsubota et al., 2007). *In vivo*, Rtt109 is solely responsible for H3K56 acetylation, and requires the eukaryotically conserved histone chaperone Asf1 (anti-silencing factor 1) for catalysis (Recht et al., 2006). Rtt109 also partially contributes to cellular levels of N-terminal tail modifications, H3K9, H3K23 and H3K27 acetylation (marks associated with newly deposited histone), and requires the NAP (nucleosome assembly protein) family histone chaperone, Vps75 to do so (Berndsen et al., 2008; Fillingham et al., 2008). *In vitro*,

Rtt109-Asf1 are only effective on H3 in the context of an H3-H4 dimer or tetramer (Han et al., 2007b; Tsubota et al., 2007), whereas histone H3 alone or H3 peptides are not efficiently used as substrates (unpublished data, JLS). This limitation is most likely due to the interaction between Asf1 and H4 domains of the H3-H4 dimer as observed in the co-crystal structure (English et al., 2006). *In vitro*, Rtt109-Vps75 complexes are very efficient at catalyzing acetylation of all known Rtt109 targets on tetramers, histone H3 alone, and N-terminal H3 peptides. However, Rtt109, regardless of activating cofactor, cannot efficiently acetylate H3K56 on nucleosomes (Han et al., 2007c).

Rtt109 has a very strong affinity for Vps75; Kd = 10 ± 2 nM (Albaugh, 2010). Rtt109-Vps75 complexes are readily purified from yeast or co-expressing *E. coli* cells. However, Rtt109 has a much weaker interaction with Asf1, and Rtt109-Asf1 complexes have only been co-purified from yeast using cross-linkers (Han et al., 2007b). The strong interaction with Vps75 may be beneficial to Rtt109, as it stabilizes the Rtt109 protein *in vivo* (Fillingham et al., 2009). Vps75 also partially escorts Rtt109 into the nucleus via its nuclear localization signal (Keck and Pemberton, 2011). Rtt109 itself does not possess a canonical NLS and the role of Asf1 or histones have not been addressed as a potential nuclear escort partner.

### *4.2 Description of H3K56*

Most modifications occur on N-terminal histone tails that protrude outside the DNA gyres of the nucleosome. The globular domain of histones is comprised of 3 α-

helical histone fold domains each separated by an unstructured loop. Histone H3 additionally has an α-helix between the N-terminal tail and the first histone fold domain. This region makes extensive interactions with DNA, in contrast to the N-terminal tails, insinuating that these residues are relevant to nucleosome stability and flexibility. Through mass spectrometry analysis and genetic manipulations novel globular domain modifications were discovered (Garcia et al., 2007; Hyland et al., 2005; Xu et al., 2005; Zhang et al., 2003).

By mass spectrometry, 28% of H3 in asynchronous populations of *S. cerevisiae* are H3K56- acetylated (Xu et al., 2005). H3K56 is the first residue of the α-N-helix that interacts with DNA after the N-terminal tail. Lysine 56 interacts with the phosphodiester backbone of DNA through a water molecule at the entry and exit points of the nucleosome (Davey et al., 2002; Luger et al., 1997). Acetylation of H3K56 would presumably disrupt the electrostatic interaction between the positively charged histone protein and the negatively charged DNA backbone. Mutations that reverse the positive charge of lysine to a negative charge (H3k56e) are lethal (Erkmann and Kaufman, 2009). Acetylation of H3K56 does not alter the structure of the nucleosome, as observed through crystal structure studies (Watanabe et al., 2010). However, acetylation of H3K56 results in an overall less dense chromatin structure (Driscoll et al., 2007; Kamieniarz and Schneider, 2009; Masumoto et al., 2005; Neumann et al., 2009; Xu et al., 2007b). In accordance, *in vitro* studies show that formation of nucleosome arrays is not affected by K56 acetylation, but interactions between nucleosome arrays are disrupted (Watanabe et al., 2010).

In *Saccharomyces cerevisiae,* all newly synthesized histones are acetylated on H3K56, resulting in genome-wide distribution during S-phase (Celic et al., 2006; Kaplan et al., 2008; Maas et al., 2006; Masumoto et al., 2005). H3K56 is also abundant in other yeast species such as *Schizosaccharomyces pombe*, *C. albicans* and *Pneumocystis carinii* (Kottom et al., 2011; Lopes da Rosa et al., 2010; Recht et al., 2006; Xhemalce et al., 2007). Genome-scale views across the budding yeast cell cycle detects H3K56-ac in waves following DNA replication forks and also at sites of replication-independent histone exchange, demonstrating that this is a short-lived mark of new histone incorporation (Kaplan et al., 2008; Masumoto et al., 2005). The rapid decay of this mark depends on sirtuin (Sir2 family) NAD+-dependent histone deacetylase (HDAC) enzymes, Hst3 and Hst4 in *S. cerevisiae* (Celic et al., 2006; Maas et al., 2006). Outside of S-phase, H3K56-ac is incorporated via histone turnover during transcription elongation at actively transcribed loci (Schneider et al., 2006) and especially at inducible loci (Rufiange et al., 2007).

*4.3 Phenotypes associated to defects in H3K56 acetylation*

Point mutation of the H3K56 residue into an amino acid that cannot be acetylated (H3K56R) or that mimics constitutive acetylation (H3K56Q) leads to hypersensitivity to genotoxic stress and DNA damaging agents, including endogenous DNA damage (Hyland et al., 2005; Masumoto et al., 2005). Accordingly, the proteins that synthesize (Rtt109 & Asf1) and hydrolyze (Hst2, Hst3 and Hst4) H3K56-ac are required for genotoxic stress resistance in *S. cerevisiae, Schizosaccharomyces pombe*

and *C. albicans* (Driscoll et al., 2007; Han et al., 2007a; Lopes da Rosa et al., 2010; Recht et al., 2006; Schneider et al., 2006; Wurtele et al., 2010; Xhemalce et al., 2007). Deletion of the hydrolyzing HDACs leads to frequent chromosome loss in *S. cerevisiae* (Celic et al., 2006; Thaminy et al., 2007) and is lethal in *C. albicans* (Wurtele et al., 2010), demonstrating the importance of H3K56-ac transient nature. Nevertheless, H3K56-ac abundance is prolonged past S-phase under DNA damaging conditions until DNA has been repaired (Maas et al., 2006; Masumoto et al., 2005). *rtt109* mutants are not DNA damage checkpoint deficient (Driscoll et al., 2007; Masumoto et al., 2005). They activate the DNA damage and replication checkpoints through the Rad53 kinase followed by DNA repair as in wild-type (Chen and Tyler, 2008; Driscoll et al., 2007). However, histone deposition after a single site-specific double-strand break repair is slowed in *rtt109Δ* cells (Chen and Tyler, 2008; Williams et al., 2008) indicating that H3K56-ac plays a role in restoring chromatin after damage.

In general, histone turnover is slowed in *rtt109* and *asf1* mutants (Kaplan et al., 2008) because H3K56-ac enhances histone deposition onto DNA via the replication-dependent histone chaperones CAF-1 (chromatin assembly factor 1) and Rtt106 (Li et al., 2008; Su et al., 2012; Zunder et al., 2012). *rtt109*Δ experience spontaneous DNA damage, marked by elevated histone H2A(S129) phosphorylation and Rad52 foci (Driscoll et al., 2007; Han et al., 2007a; Lopes da Rosa et al., 2010). Replication fork stability is compromised in cells unable to acetylate H3K56. Stalled replication forks collapse when cells are depleted of deoxynucleotides by the effects

of the S-phase blocking agent hydroxy urea (HU) (Han et al., 2007b; Recht et al., 2006). However, these mutants can recover from transient S-phase blocks, as opposed to direct DNA damage caused by camptothecin or methyl methane sulfonate (Wurtele et al., 2012). In addition, cells unable to acetylate H3K56 have increased accumulation of extrachromosomal rDNA circles (Han et al., 2007b) a consequence of natural replication fork barriers on rDNA repeats that would be problematic for unstable stalled replication forks. Follow up on these findings may clarify a role for H3K56-ac and Rtt109 in DNA damage versus DNA replication.

*4.4 H3K56-ac in mammalian cells*

Detection of H3K56-ac in humans is controversial, but clearly much less abundant than in yeast, if present at all (Garcia et al., 2007; Xu et al., 2005; Yu et al., 2012). Early mass spectrometry analysis of HeLa cells (Henrietta Lacks' cervical cancer cell line) approximated that 1% of H3 were K56- acetylated (Xie et al., 2009). However, 0.8% of H3K56 is reported to be methylated, as detected by the same technique, making the specific identification of the modification technically ambiguous (Garcia et al., 2007; Yu et al., 2012). In contrast, other well-described histone acetylation marks in HeLa cells occur on 3.8- 22.9% of H3 (Horwitz et al., 2008). A later re-examination of H3K56-ac in HeLa and K562 (a human erythroleukemic cell line) cell lines using more stringent and controlled quantifications for mass spectrometry showed that only 0.03% of H3 possessed the modification. The level of acetylation did not change despite treatment with various

HDAC inhibitors (Drogaris et al., 2012). Additionally, the same laboratory showed that misleading results can arise from anti-H3K56-ac antibody cross-reaction when HDAC inhibitors increased acetylation marks on other lysine residues in the context of non-H3K56 peptides (Drogaris et al., 2012). Issues with antibody specificity had previously been reported specifically when H3K56-ac was detected on recombinant H3 (Ozdemir et al., 2006). Furthermore, transduction of HeLa cells with inducible yeast *RTT109* and *ASF1* lentivirus yields no detectable H3K56-ac signal by Western blot using our specific anti- H3K56-ac anti-serum, despite appropriate expression of the two proteins and the addition of various HDAC inhibitors (unpublished data, JLS). Overall, these data suggest that H3K56ac is not a prevalent modification in humans. Nevertheless, various studies utilizing antibodies for Western blot and immuno-fluorescence detection in human cells have associated H3K56-ac with cell differentiation (Dovey et al., 2010; Dutta et al., 2010; Xie et al., 2009), DNA damage (Battu et al., 2011; Miller et al., 2010; Tjeertes et al., 2009; Vempati, 2011; Vempati et al., 2010; Yuan et al., 2009) and cell-specific transcription regulation (Kong et al., 2011; Lo et al., 2011). What is not contested is that a homologue of Rtt109 does not exist in the human genome. The consensus is that both the well conserved eukaryotic HAT, Gcn5 and the mammalian p300 are responsible for H3K56 acetylation in human cells (Kong et al., 2011; Tjeertes et al., 2009; Vempati et al., 2010). Although, the efficiency of p300 activity towards H3K56 compared to H4 N-terminal tail residues *in vitro* is extremely poor (unpublished data, JLS).

## 5. A HAT inhibitor as a novel anti-fungal agent

### *5.1 HAT families*

There are three known families of HAT enzymes, based on primary sequence: p300/CBP, GNAT (Gcn5- related N-acetyl transferase) and MYST (MOZ, Ybf2/Sas3, Sas2, Tip60). Rtt109 has no primary sequence similarity to the HAT families and the canonical Motif A (acetyl coA binding pocket) of HATs is unrecognizable through sequence analysis in Rtt109. Our laboratory, as well as others, first reported histone acetyl-transferase activity of Rtt109 through biochemical assays (Collins et al., 2007; Driscoll et al., 2007; Han et al., 2007a; Tsubota et al., 2007; Xhemalce et al., 2007). Later on, through crystal structure studies, it became evident that the central core region of Rtt109 is structurally similar to that of the well-conserved eukaryotic Gcn5 HAT (Lin and Yuan, 2008) and that overall Rtt109 shares a three dimensional fold with p300 (Stavropoulos et al., 2008; Tang et al., 2011; Tang et al., 2008), a HAT only conserved in mammals. Similar to p300, Rtt109 also uses auto-acetylation to activate catalysis (Karanam et al., 2006; Thompson et al., 2004). Due to these similarities, some laboratories group Rtt109 with the p300/CBP family. However, the polarity and chemistry of their active sites (Marmorstein and Trievel, 2009; Wang et al., 2008) and the catalytic mechanisms of Rtt109 and p300 are distinct (Albaugh et al., 2010; Berndsen and Denu, 2008; Kolonko et al., 2010; Lin and Yuan, 2008; Tang et al., 2008).

### *5.2 HAT enzymatic mechanisms*

Thus far, HAT catalysis events all involve de-protonation of the target histone lysine residue, followed by its nucleophilic attack of the acetyl group on acetyl coenzyme A (Hodawadekar and Marmorstein, 2007; Marmorstein and Trievel, 2009). Initial studies of Esa1, a MYST family HAT, suggested a ping-pong mechanism, which involves a covalent link between the acetyl group and the enzyme prior to nucleophilic attack by the de-protonated histone lysine (Yan et al., 2002) (Figure 1.1). Current evidence, however, supports that both GNAT and MYST family enzymes use a sequential mechanism involving a ternary intermediate complex where both substrates are simultaneously associated to the enzyme without formation of a covalent bond (Figure 1.1) (Berndsen et al., 2007; Tanner et al., 2000; Tanner et al., 1999). p300, on the other hand, operates a Theorell-Chance ("hit-and- run") mechanism that involves formation of an intermediate enzyme-acetyl coenzyme A complex, followed by transient association with the protein substrate (Figure 1.1) (Liu et al., 2008). In this case, a ternary intermediate complex is not formed. Rtt109 follows a random sequential mechanism similar to that observed for Gcn5 and Esa1. Specifically, either substrate can bind Rtt109 in any order to form a ternary complex for catalysis (Albaugh et al., 2010).

Rtt109 enzymology is intriguing. As an enzyme Rtt109 is very inefficient in the absence of its histone chaperone cofactors. Rtt109 depends on histone chaperones Asf1 or Vps75 to increase catalytic efficiency [Kcat/ Km ($M^{-1}$ $S^{-1}$) = 1.5 x $10^3$ (Rtt109); 8.4 x $10^4$ (Rtt109-Vps75); 2 x $10^4$ (Rtt109-Asf1)] (Berndsen et al., 2008; Tsubota et al., 2007). The chaperones have a less significant effect on Km for

**Figure 1.1 Enzyme mechanisms of histone acetyl-transferases**

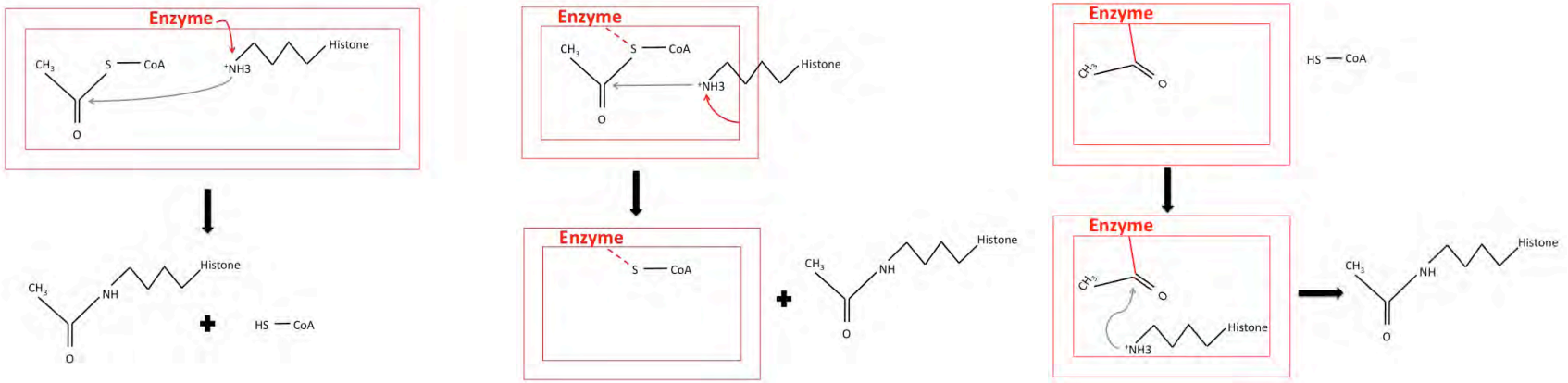


**Sequential mechanism**
*(Rtt109 & Gcn5)*

•Formation of tertiary complex (enzyme, histone & Ac-CoA substrates)

•Ordered or non-ordered substrate binding

**Theorell-Chance mechanism**
*(p300)*

•Formation of binary complex (enzyme & Ac-CoA)

•Ordered substrate binding

•Transient histone association for catalysis

**Ping-pong mechanism**

•Covalently linked acetyl group from Ac-CoA to enzyme

•Transfer of acetyl group to histone from enzyme

tetramers, which is consistent with Rtt109's ability to bind histones directly, although with 10 fold less affinity than Vps75 or Asf1 (Han et al., 2007c; Park and Luger, 2008). The role of the chaperones may indeed be to solely stimulate catalysis, as opposed to simply recruiting histones.

Additionally, Rtt109 must be acetylated at lysine 290 to be functional (Stavropoulos et al., 2008). Rtt109 auto-acetylates itself intra-molecularly and independently of histone chaperones (Albaugh et al., 2011). K290 auto-acetylation occurs 50 times slower than histone acetylation (Albaugh et al., 2011). Mutation of K290 on Rtt109 to prevent acetylation increases the Km and the Kd for acetyl-coenzyme A by $\geq$ 10 fold (Albaugh et al., 2011). Attempts to investigate the status of Rtt109-K290 as a means of H3K56-ac regulation throughout the cell cycle were unsuccessful due to low antibody sensitivity (unpublished data, JLS). It would be very interesting to determine if and how Rtt109-K290 acetylation regulates H3K56-ac status *in vivo*.

*5.3 HAT inhibitors and potential applications*

Because of their strong impact on genome function, the relationship between human diseases and histone acetylation is an active topic of investigation (Dekker and Haisma, 2009; Timmermann et al., 2001). However, advances in chemotherapeutic developments are most promising for histone de-acetylase (HDAC) inhibitors (Dokmanovic et al., 2007). Only few studies have focused on identifying HAT inhibitors as a novel source of chemotherapeutic drugs (Dekker and Haisma, 2009).

Several synthetic and natural compounds have been characterized as HAT inhibitors (Reviewed in (Cole, 2008; Dekker and Haisma, 2009)). Acetyl-coA bi-substrate adducts are cell-impermeable transition state and product analogs that can inhibit HAT enzyme activity *in vitro* (Lau et al., 2000). However, neither lysine-coenzyme A nor an H3K56-coenzyme A bisubstrate analogue inhibit Rtt109 catalysis (Tang et al., 2008). More recently, a small molecule inhibitor of p300 was identified through a virtual ligand screen, and this also has no effect on Rtt109 (Bowers et al., 2010). Curcumin (from tumeric), anarcadic acid (from cashew nut oil) and garcinol (from the *Garcinia indica* fruit) are natural compounds that have inhibitory effects towards all three HAT family members, including p300, Gcn5, and Tip60 (Balasubramanyam et al., 2003; Balasubramanyam et al., 2004; Cui et al., 2007; Mantelingu et al., 2007; Marcu et al., 2006; Sun et al., 2006). However, their multiple targets make them unsuitable as specific inhibitors. In short, none of the known HAT inhibitors are promising lead compounds for chemical manipulation to develop a specific Rtt109 inhibitor.

Compounds that inhibit Rtt109 are predicted to cause sensitivity to DNA damage in yeast cells. An analogous situation exists for the human MYST-family HAT, TIP60. TIP60 is recruited to sites of DNA damage and acetylates multiple histone residues during DNA repair (Sun et al., 2005). Notably, inhibition of TIP60 by anacardic acid sensitizes human cells to DNA damaging agents (Sun et al., 2006). Since Rtt109 promotes *C. albicans* pathogenesis (Lopes da Rosa et al., 2010), a chemical inhibitor of the enzyme is expected re-capitulate this phenotype and make

for a novel anti-fungal drug candidate. Examination of protein databases reveals homologs of Rtt109 only among other fungal species. The close homology of the fungal Rtt109 enzymes, including residues essential for catalytic activity (Han et al., 2007a; Tsubota et al., 2007), suggest that inhibitory compounds are likely to be effective against Rtt109 proteins from multiple fungal species. Furthermore, the dissimilarity between Rtt109 and enzymes of other HAT families indicate that a specific inhibitor will have minimal activity and toxicity towards mammalian proteins.

# CHAPTER 2

## Histone acetyltransferase Rtt109 is required for *Candida albicans* pathogenesis

**Acknowledgments:** The following chapter is a published manuscript with the following citation reference:
Lopes da Rosa, J.L., Boyartchuk, V.L., Zhu, L.J. and Kaufman, P.D. (2010) Histone acetyltransferase Rtt109 is required for *Candida albicans* pathogenesis. PNAS 107 (4), 1594-1599.
Supplemental data and methods are included except for Supplemental Table 2.S7, 2.S8, 2.S9, 2.S10 which are Available online at http://www.pnas.org/content/107/4/1594/suppl/DCSupplemental.
Microarray data are posted on the gene expression omnibus (GEO) database at http://www.ncbi.nlm.nih.gov/geo/ accession number GSE18936.
I solely performed and analyzed all experiments presented with the exception of the following: Injections of pathogens into mice (Dr. Victor L. Boyartchuk); Microarray bioinformatics (Dr. L. Julie Zhu).
The manuscript was written by Dr. Paul D. Kaufman and myself, with contribution from Dr. Zhu for the bioinformatics section of the experimental procedures.

**ABSTRACT**

*Candida albicans* is a ubiquitous opportunistic pathogen that is the most prevalent cause of hospital-acquired fungal infections. In mammalian hosts, *C. albicans* is engulfed by phagocytes that attack the pathogen with DNA-damaging reactive oxygen species (ROS). Acetylation of histone H3 lysine 56 (H3K56) by the fungal-specific histone acetyltransferase Rtt109 is important for yeast model organisms to survive DNA damage and maintain genome integrity. To assess the importance of Rtt109 for *C. albicans* pathogenicity, we deleted the predicted homologue of Rtt109 in the clinical *C. albicans* isolate, SC5314. *C. albicans rtt109* $^{-/-}$ mutant cells lack acetylated H3K56 (H3K56ac) and are hypersensitive to genotoxic agents. Additionally, *rtt109* $^{-/-}$ mutant cells constitutively display increased H2A S129 phosphorylation and elevated DNA repair gene expression, consistent with endogenous DNA damage. Importantly, *C. albicans rtt109* $^{-/-}$ cells are significantly less pathogenic in mice and more susceptible to killing by macrophages *in vitro* than are wild-type cells. Via pharmacological inhibition of the host NADPH oxidase enzyme, we show that the increased sensitivity of *rtt109* $^{-/-}$ cells to macrophages depends on the host's ability to generate ROS, providing a mechanistic link between the drug sensitivity, gene expression and pathogenesis phenotypes. We conclude that Rtt109 is particularly important for fungal pathogenicity, suggesting a novel target for therapeutic antifungal compounds.

**INTRODUCTION**

The basic repeating unit of eukaryotic chromatin, termed the nucleosome, is composed of 146 base pairs of DNA wrapped around an octamer of core histone proteins, containing two copies each of H2A, H2B, H3 and H4 (Luger et al., 1997). Post-translational modifications (PTM) of histone molecules promote various chromatin functions including replication, repair, transcription, and silencing (Groth et al., 2007; Li et al., 2007; Millar and Grunstein, 2006). In the yeasts *Saccharomyces cerevisiae* and *Schizosaccharomyces pombe,* newly synthesized histone H3 molecules are abundantly acetylated on lysine 56 (Kaplan et al., 2008; Masumoto et al., 2005; Xhemalce et al., 2007). In *S. cerevisiae*, H3K56 acetylation is required for replication fork stability (Duro et al., 2008; Tsubota et al., 2007), reassembly of chromatin after DNA damage repair, and histone association with chromatin assembly proteins (Chen and Tyler, 2008; Erkmann and Kaufman, 2009; Kim and Haber, 2009; Li et al., 2008). A fungal-specific histone acetyl-transferase (HAT) enzyme, termed Rtt109 and its stimulatory histone chaperone co-factor, Asf1, are required for H3K56 acetylation (Driscoll et al., 2007; Han et al., 2007a; Recht et al., 2006; Tsubota et al., 2007). *S. cerevisiae* mutants lacking Rtt109 or Asf1 display delayed cell cycle progression (Driscoll et al., 2007), spontaneous DNA damage (Fillingham et al., 2008; Masumoto et al., 2005; Prado et al., 2004), unstable replication forks, and are extremely sensitive to DNA damaging agents (Tsubota et al., 2007). In accordance, point mutation of H3 lysine 56 to arginine, which cannot be

acetylated and mimics a positively charged, unacetylated lysine, results in similar phenotypes (Masumoto et al., 2005; Recht et al., 2006). Therefore, acetylation of H3K56 is a particularly important PTM for fungal growth.

*C. albicans* is an opportunistic pathogen that poses a considerable public health problem, with an estimated 40% mortality rate for systemic candidiasis (Gudlaugsson et al., 2003; Pfaller and Diekema, 2007). Antifungal drug resistance is a major clinical problem, and few drugs are available to battle *Candida* infections (Cannon et al., 2007). H3K56 acetylation appears to be much less abundant in mammals than in yeasts (Garcia et al., 2007; Xie et al., 2009; Zhang et al., 2003) and close homologues of Rtt109 are not detected outside of the fungal kingdom (Bazan, 2008; Tang et al., 2008). Therefore, we hypothesized that Rtt109 might provide a new target for antifungal therapeutics, and we began to investigate the importance of H3K56 acetylation in fungal pathogenicity.

During the course of a systemic infection, *C. albicans* cells are engulfed by host phagocytes, where they are exposed to ROS (Vázquez-Torres and Balish, 1997). ROS contribute to efficient killing of *C. albicans* both in cultured cells and whole organisms (Aratani et al., 2002b; Donini et al., 2007; Stevenhagen and van Furth, 1993; Thompson and Wilton, 1992). ROS directly damage DNA, as well as cellular proteins and lipids (Haghnazari and Heyer, 2004; Salmon et al., 2004). Upon incubation with macrophages, *C. albicans* DNA repair genes are transcriptionally induced (Lorenz et al., 2004), suggesting that DNA damage

indeed occurs in the phagosome and that hypersensitivity to genotoxic stress would be disadvantageous to the pathogen. Because H3K56 acetylation is essential for yeast to survive genotoxic stress, we investigated the role of Rtt109 in *C. albicans* pathogenicity.

## RESULTS

### *C. albicans* ORF19.7491 encodes the Rtt109 functional homologue

We identified *C. albicans* ORF19.7491 as the likely Rtt109 functional homologue through primary sequence homology. Also, the recent high-resolution structures of *S. cerevisiae* Rtt109 (Stavropoulos et al., 2008; Tang et al., 2008) highlight several catalytic domains that are well-conserved between the two species (Fig. 2.S1A). *C. albicans* is an obligate diploid that lacks a classical sexual cycle, so two sequential rounds of gene deletion are required to generate homozygous mutants. For this, we employed the *Candida*-adapted Flp/FRT sequence-specific recombination system to replace the target locus (Reuss et al., 2004). This system leaves behind a single 34 bp FRT site after excision (Fig. 2.S1b). All genotypes were confirmed using PCR (Fig. 2.S1C, Table 2.S3). Immunoblot analysis demonstrated that H3K56ac was lost in homozygous *rtt109* $^{-/-}$ mutant cells, whereas in *RTT109* $^{+/-}$ heterozygous cells H3K56ac was maintained (Fig. 2.1A). To verify that the phenotypes observed resulted from the intended deletion, we generated a "complemented" strain, *RTT109* $^{FH/-}$, by re-introducing a 2xFlag-6xHIS-tagged *RTT109* gene at the endogenous locus of the

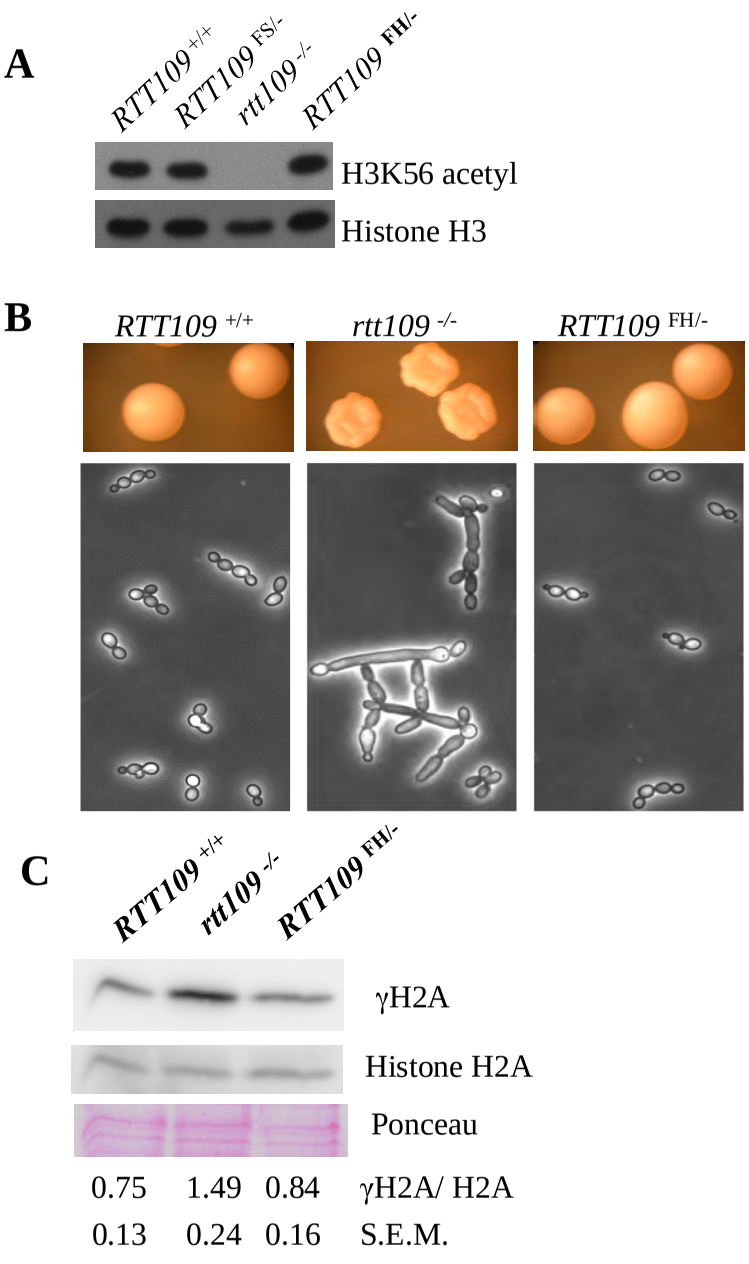


**Figure 2. 1. Loss of Rtt109 results in filamentous growth and constitutive DNA damage signaling**. (A) Immunoblot analysis of acetylated H3K56 from whole cell extracts of the indicated strains grown to log-phase. The blot was stripped and re-probed for total histone H3 as a loading control. (B) Colony and single cell morphology of indicated strains. Yeast cells were grown on agar or in liquid rich media at 30º before being photographed. Micrographs are at 640x magnification. (C) Immunoblot analysis of phosphorylated H2A-serine 129 (γH2A) and total histone H2A for a representative set of samples. Quantification presented below the gel represents the mean ratio +/- S.E.M. of γH2A to total H2A measured by densitometry using ImageJ software for 4 independent experiments for each strain. The Ponceau stained membrane serves as an internal loading control. (D) Growth curve of log-phase cultures of the indicated strains. Doubling time was derived by linear regression on the Log (10) scale.

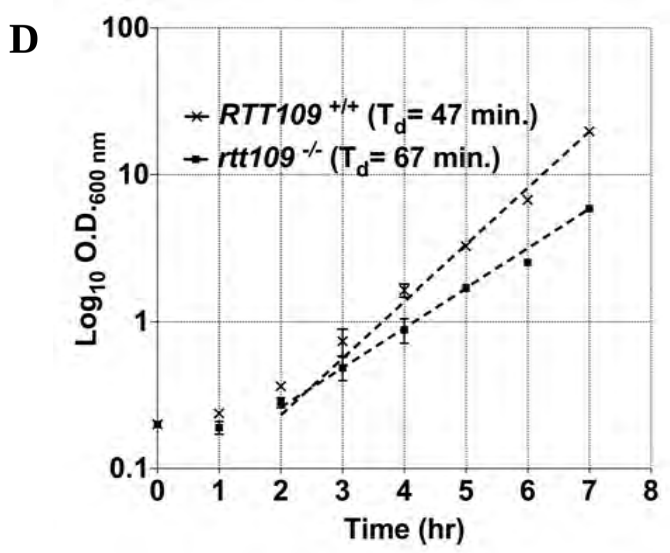

homozygous mutant (Fig. 2.S1B and 2.S1C). As anticipated, H3K56ac was restored in the complemented *RTT109* $^{FH/-}$ strain (Fig. 2.1A). We conclude that *C. albicans* ORF19.7491 encodes a functional Rtt109 homologue.

### *C. albicans rtt109* $^{-/-}$ cells are sensitive to genotoxic agents

*C. albicans* can grow in multiple morphological states. Individual cells appear as budded or filamentous cells (Sudbery et al., 2004). The ability to switch among these morphologies is required for *C. albicans* pathogenicity (Laprade et al., 2002; Lo et al., 1997), suggesting that multiple morphologies contribute to host infection. Filamentous growth can be triggered by various stimuli including oxidative stress (Nasution et al., 2008), activation of the DNA damage and replication checkpoints due to exogenous or endogenous DNA damage (Andaluz et al., 2006; Shi et al., 2007), or by cell cycle delays resulting from perturbed microtubule dynamics or spindle checkpoint activation (Finley and Berman, 2005; Finley et al., 2008), (reviewed in (Berman, 2006)).

We therefore examined single cell and colony morphology of *rtt109* $^{-/-}$ mutants. Unlike the smooth wild-type and *RTT109* $^{FH/-}$ colonies, *rtt109* $^{-/-}$ colonies were wrinkled, suggesting a heterogeneous population (Fig. 2.1B). By examining individual cells, we observed that a large proportion of *rtt109* $^{-/-}$ cells were filamentous (Fig. 2.1B). In contrast, wild-type and *RTT109* $^{FH/-}$ *C. albicans* populations were homogeneous budded cells. In *S. cerevisiae*, inability to acetylate H3K56 leads to spontaneous DNA damage (Driscoll et al., 2007; Han et

**Figure 2. 2. *Candida albicans rtt109* $^{-/-}$ cells are hypersensitive to genotoxic agents but not all antifungal drugs.** (a) Five-fold serial dilutions of the indicated strains on rich media (YPD) supplemented with campthotecin (CPT), methyl methane sulfonate (MMS) and hydrogen peroxide ($H_2O_2$). Plates were photographed after 2 days at 30°. (b-e) Percent growth inhibition in the presence of indicated drugs in RPMI 1640 was measured after 16-18 hrs at 35° by optical density 600 nm. Results are mean of triplicates ± s. d.

**Figure 2. 2.** ***Candida albicans rtt109*** $^{-/-}$ **cells are hypersensitive to genotoxic agents but not all antifungal drugs.**

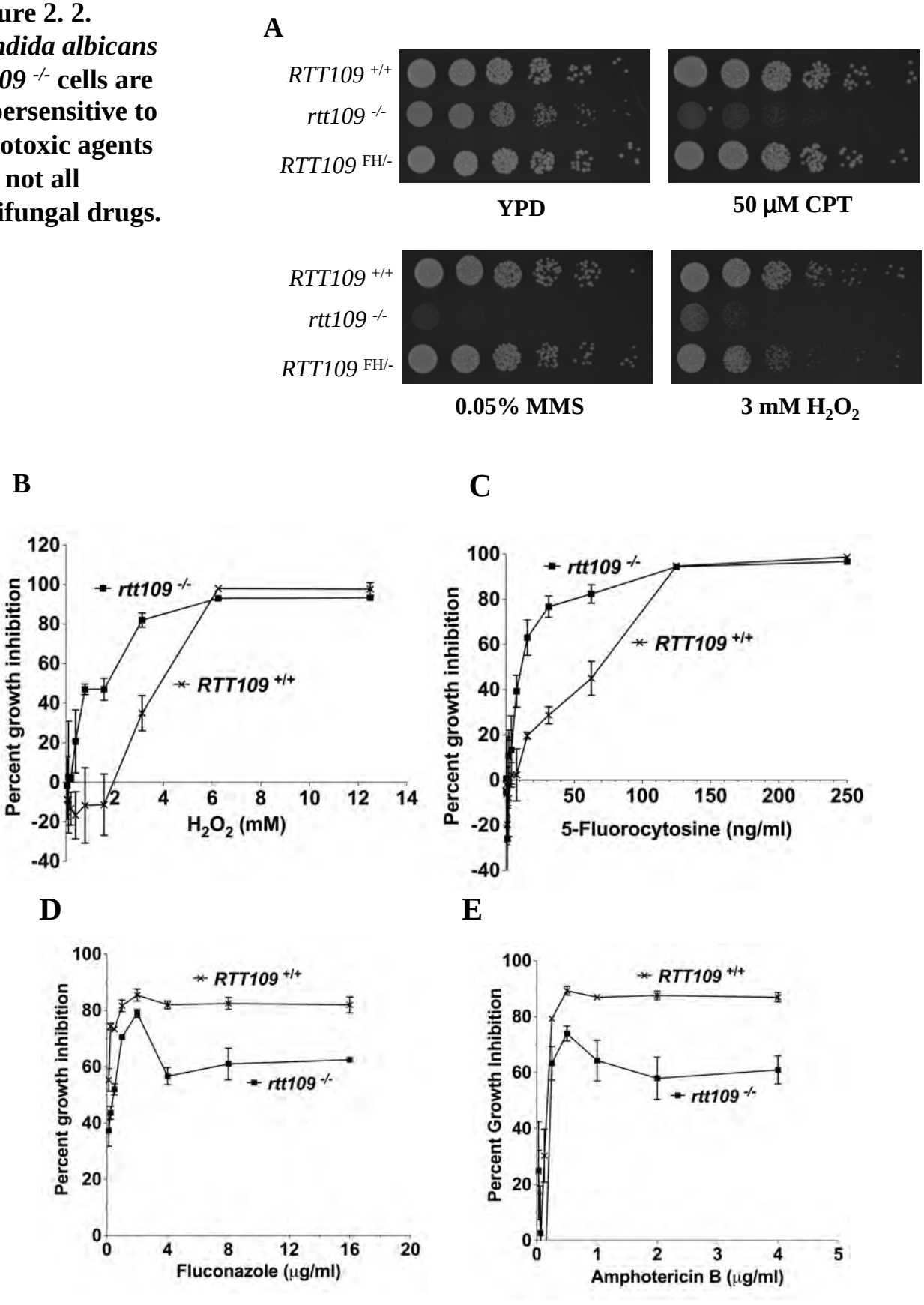

al., 2007a) and constitutive checkpoint activation (Driscoll et al., 2007), which as a result delay G2-M progression (Driscoll et al., 2007). We therefore suspected that constitutive DNA damage causes the aberrant morphology of *C. albicans rtt109*$^{-/-}$ mutants. We examined the mutant cells for phosphorylation of histone H2A serine 129 (γH2A), a well-conserved modification that is triggered by DNA double strand breaks (Redon et al., 2003). Low levels of γH2A are constitutively present in *S. cerevisiae asf1Δ* and *rtt109Δ* strains (Fillingham et al., 2008; Prado et al., 2004). Indeed, *C. albicans rtt109* $^{-/-}$ mutants displayed elevated amounts of γH2A in the absence of exogenous DNA damaging agents (Fig. 2.1C). As expected for cells that undergo constitutive checkpoint activation, *C. albicans rtt109* $^{-/-}$ mutants had a moderately longer doubling time (Fig. 2.1D). We conclude that loss of Rtt109 stimulates *C. albicans* filamentation, likely via an increase in spontaneous DNA damage and loss of genomic stability. Accordingly, *C. albicans rtt109* $^{-/-}$ cells were hypersensitive to the genotoxic agents campthotecin (CPT), a topoisomerase poison, and methyl methane sulfonate (MMS), a DNA alkylating agent (Fig. 2.2A). *C. albicans rtt109* $^{-/-}$ mutants were also hypersensitive to hydrogen peroxide ($H_2O_2$), one of the ROS employed by phagocytes to kill engulfed *C. albicans* (Vázquez-Torres and Balish, 1997) (Fig. 2.2A and 2.2B).

Flucytosine (5-fluorocytosine; 5FC) is a clinically approved antifungal agent used to treat systemic candidiasis (Pfaller and Diekema, 2007). As a nucleotide analogue, it impedes DNA synthesis (Polak and Scholer, 1975),

suggesting that mutants defective for replication fork stability may be more sensitive to this compound. We therefore tested sensitivity to 5FC and observed that the minimal inhibitory concentration was diminished for *rtt109* $^{-/-}$ mutants (Fig. 2.2C). These data suggest that impairing Rtt109 could improve the effectiveness of 5FC in a chemotherapeutic setting. Notably, *rtt109* $^{-/-}$ mutants were not hypersensitive to the antifungal drugs fluconazole or amphotericin B (Fig. 2.2D and 2.2E), both of which affect cell membrane synthesis (Cannon et al., 2007). These data reinforce the notion that pharmacological sensitivities of the *rtt109* $^{-/-}$ mutant cells are specifically related to genome stability.

### *C. albicans* pathogenicity is diminished in the absence of Rtt109

Murine systemic candidiasis is a well-established model to study pathogenesis by *C. albicans* (de Repentigny, 2004; Spellberg et al., 2005). We infected BALB/cByJ mice with 1.0 x $10^5$ wild-type, *rtt109* $^{-/-}$ or *RTT109* $^{FH/-}$ cells by tail vein injection. We monitored morbidity and mortality twice daily and observed that the *rtt109* $^{-/-}$ cells were significantly deficient in causing fatal pathogenesis compared to wild-type (p-value 0.0435) and *RTT109* $^{FH/-}$ complemented (p-value 0.0377) strains (Fig. 2.3A). The difference in lethality caused by *rtt109* $^{-/-}$ and wild-type strains was even more significant ($p < 0.001$) when mice were infected with 1.5 x $10^5$ cells (Fig. 2.3B). To determine whether these phenotypes correlated with proliferation of the pathogen in the animal, we retrieved single kidneys from infected animals and assessed fungal burden at 3

**Figure 2. 3. *rtt109*$^{-/-}$ mutant cells display reduced pathogenicity in mice and increased sensitivity to macrophages.** BALB/cByJ female mice were infected with 1.0 x $10^5$ (a) or 1.5 x $10^5$ (b) yeast cells via venous tail injection with the indicated C. albicans strains. Renal fungal load of mice infected with 1.0 x $10^5$ of the indicated strains 3 dpi (c) or 20 dpi (d). Five-fold serial dilutions of homogenized left kidney were plated on rich media agar for 24 hrs at 30°. (e) ZBM2 macrophage-derived cells were incubated for 15-16 hours with the indicated C. albicans strains at an MOI of 1:15 in the presence or absence of diphenyleneiodonium chloride (DPI). The macrophages were osmotically lysed and dilutions of the co-culture were plated onto rich media. Colony forming units (cfu) were compared to cultures of yeast incubated in parallel in the absence of macrophages. Results are mean ± s.e.m. (RTT109 $^{+/+}$ n=5; rtt109 $^{-/-}$ n=5; p-value =0.025).

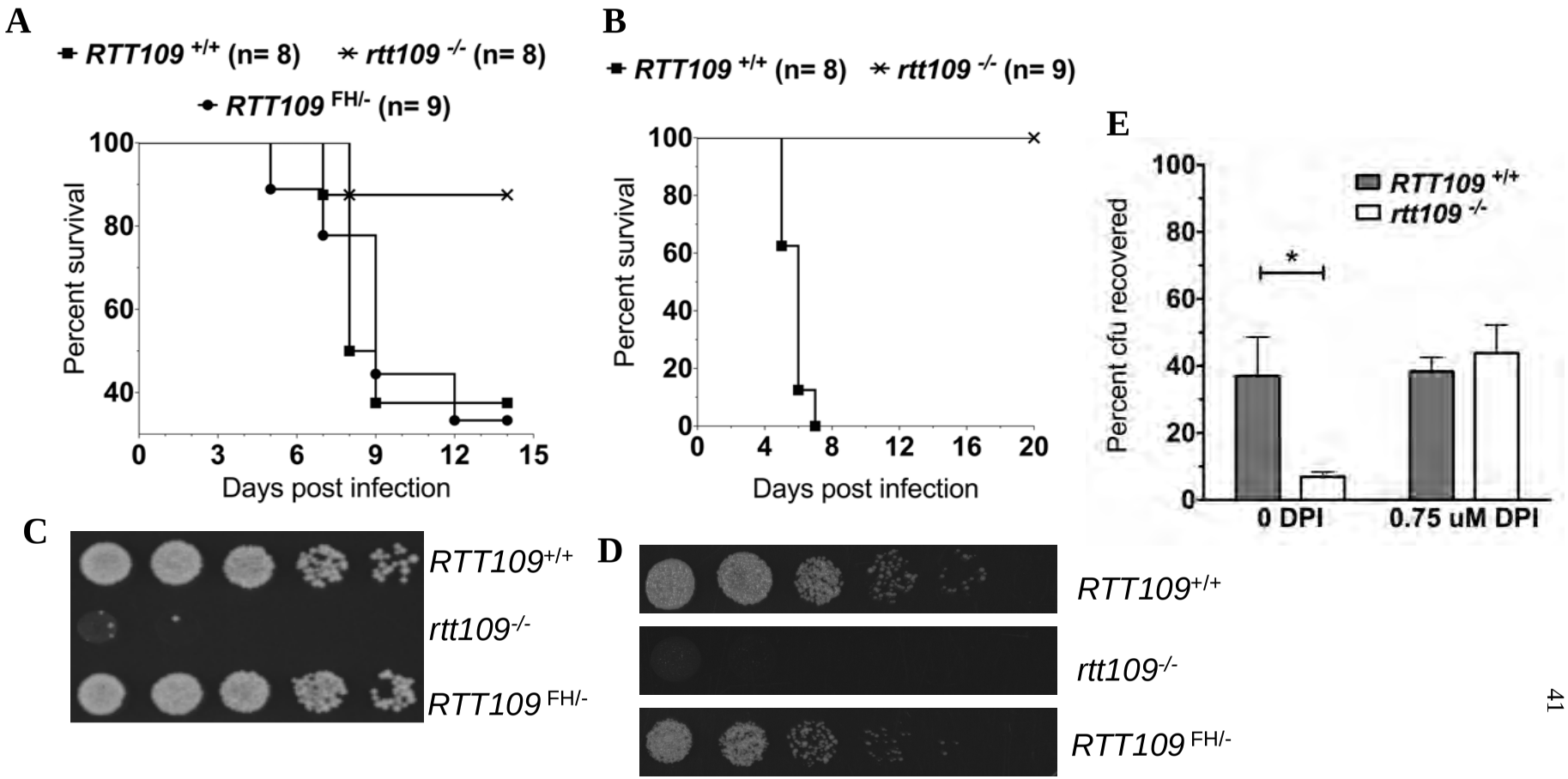

and 20 days post infection by serial dilution of tissue homogenates on YPD agar (Fig. 2.3C and 2.3D). We observed that mice infected with wild-type or complemented *C. albicans* strains had comparable renal fungal loads. In contrast, mice infected with the *rtt109* $^{-/-}$ mutant carried negligible amounts of yeast. We conclude that *C. albicans* requires Rtt109 for efficient pathogenesis in mice.

### *C. albicans rtt109* $^{-/-}$ cells are more susceptible to ROS-mediated killing by macrophages

Macrophages play an important role in controlling *C. albicans* infections (Vázquez-Torres and Balish, 1997). To determine whether macrophage-mediated growth inhibition could contribute to the observed decrease in *C. albicans rtt109* $^{-/-}$ pathogenicity, we quantified yeast cell survival after exposure to a mouse-derived macrophage-like cell line, ZBM2. After a 15-16 hour co-incubation at a ratio of 1 fungal cell per 15 ZBM2 cells, proliferation of *rtt109* $^{-/-}$ cells was significantly more inhibited by macrophages than were wild-type *C. albicans* cells (p-value 0.025; Fig. 2.3E). We repeated these experiments in the presence of an NADPH-oxidase inhibitor (DPI; diphenyleneiodium chloride) to inhibit generation of ROS by the macrophages (Hancock and Jones, 1987). Previous work has shown that inhibition of NADPH-oxidase in phagocytes by DPI decreases the fungicidal activity against *C. albicans* (Donini et al., 2007; Stevenhagen and van Furth, 1993). We determined that in the presence of DPI, survival of macrophage killing by the *rtt109* $^{-/-}$ cells was increased to the same

level observed for wild-type cells (Fig. 2.3E). We conclude that without Rtt109, *C. albicans* is more susceptible to killing by mammalian host macrophages because of the ROS deposited into phagosomes of macrophages.

### *rtt109*$^{-/-}$ cells display an altered profile of metabolic gene expression and constitutively induce DNA repair genes

To gain further insight into the altered phenotypes of the *rtt109*$^{-/-}$ mutant cells, we performed microarray analysis of gene expression. We first compared logarithmically growing wild–type and *rtt109*$^{-/-}$ mutant cells in rich (YPD) media, focusing on genes that displayed a greater than two-fold change with a p-value <0.01 (see Materials and Methods). Among this group was a large number of genes involved in the response to DNA damage, almost all of which displayed elevated expression in the *rtt109*$^{-/-}$ mutant cells (Table 2.S4A). In contrast, many of the genes most highly down-regulated in the mutant cells were related to carbohydrate metabolism (Table 2.S4B), To extend these observations, GO-term analysis was performed to quantify the enrichment of genes associated with biological processes. Many of the enriched GO-terms significantly overlapped, such that all of the enriched biological process terms can be generally categorized as being involved in carbohydrate metabolism, DNA damage and repair, or mitochondrial function (Fig. 2.4). Together, the transcription data suggests two major trends: complex miss-regulation of energy metabolism in mutant cells, and constitutive DNA damage signaling.

**Figure 2. 4. *rtt109* $^{-/-}$ mutant cells have an altered transcription profile significantly enriched in carbohydrate metabolism and DNA repair related GO terms.** Enriched gene ontology terms were calculated from all genes with a p-value <0.01 and fold change of $\log_2 \leq$-1.0 or $\geq$1.0. These GO terms have an adjusted B.H. p-value from 6.58E-4 (top) to 8.00E-3 (bottom) and represent overlapping genes (see Table S7). The percent of genes increased or decreased in rtt109 $^{-/-}$ is represented within each GO term bar.

**Figure 2. 4. *rtt109* $^{-/-}$ mutant cells have an altered transcription profile significantly enriched in carbohydrate metabolism and DNA repair related GO terms.**

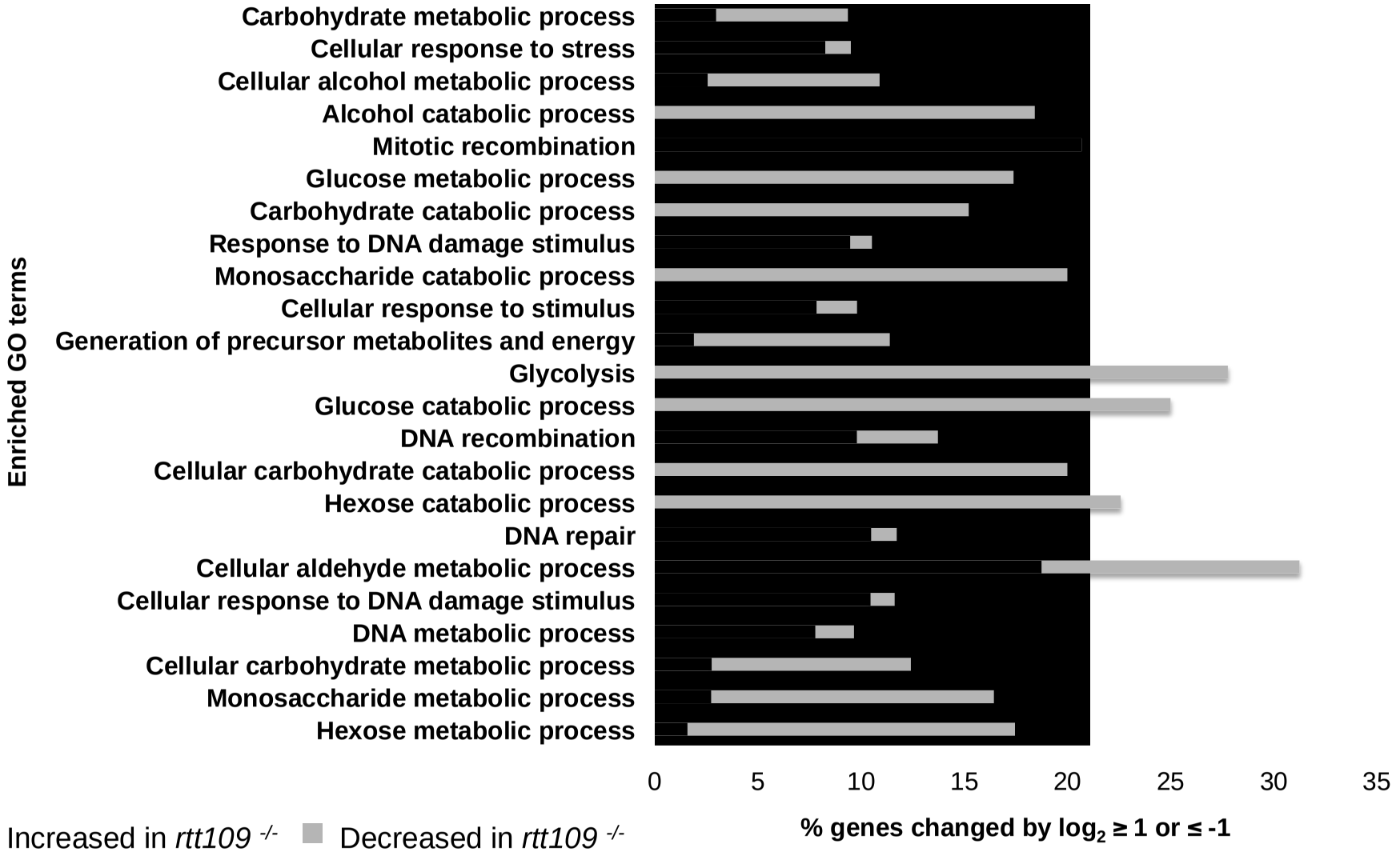

To investigate the sensitivity of *rtt109* $^{-/-}$ cells to ROS, we also analyzed gene expression changes in cells exposed to 0.4 mM hydrogen peroxide for 10 minutes, a treatment that has previously been shown to induce a DNA damage response (Enjalbert et al., 2003; Enjalbert et al., 2006). Under these conditions, we observed that there were many more genes with elevated rather than reduced RNA levels in the *rtt109* $^{-/-}$ mutant cells (Table 2.S5). We note that the broad group of DNA repair genes that was elevated in the YPD-grown mutant cells was not observed in the comparison of strains grown in the presence of $H_2O_2$, likely because both strains in this experiment are responding to $H_2O_2$-mediated DNA damage. Notably, genes that specifically respond to oxidative stress (e.g. superoxide dismutases encoded by *SOD3*, *SOD4*, and *SOD5*) were more highly induced in mutant cells, leading to significant enrichment of multiple GO terms related to oxidative stress (Fig. 2.5). Therefore, *rtt109* $^{-/-}$ mutant cells appear able to sense and mount a vigorous transcriptional response to oxidative stress, but appear unable to survive in phagocytes or mice.

Additionally, in the presence of $H_2O_2$ the mutant cells up-regulate genes related to cell wall synthesis (Fig. 2.5). In contrast, enriched GO terms related to cell adhesion, interaction and biofilm formation mostly included genes down-regulated in the mutant cells. It remains a possibility that some of these complex increases and decreases could contribute to the loss of pathogenicity in *rtt109* $^{-/-}$ mutant cells (Fig. 2.3). However, given the pharmacological data showing that *rtt109* $^{-/-}$ mutant cells are sensitive to killing by macrophages because of host-

**Figure 2. 5. Exposure to hydrogen peroxide results in an altered transcription profile significantly enriched in cell wall synthesis and oxidative stress related GO terms in *rtt109* $^{-/-}$ mutant cells.** Enriched gene ontology terms were calculated from all genes with a p-value <0.01 and changed by $\log_2 \leq -1$ and $\geq 1$ upon $H_2O_2$ exposure compared to wild-type. These GO terms have an adjusted B.H. p-value 3.56E-5 (top) to 7.76E-3 (bottom) and represent overlapping genes (see Table S8). The percent of genes increased or decreased in *rtt109* $^{-/-}$ is represented within each GO term bar. *The following GO terms were merged based on their having the exact same genes increased or decreased, the same number of genes represented in the genome and the same B.H. p-value: chitin biosynthetic process, cell wall chitin metabolic process; amino sugar metabolic process, glucosamine metabolic process, N-acetylglucosamine metabolic process, cell wall polysaccharide metabolic process; glucosamine biosynthetic process, N-acetylglucosamine biosynthetic process, amino sugar biosynthetic process; fatty acid oxidation, lipid oxidation. .

**Figure 2. 5. Exposure to hydrogen peroxide results in an altered transcription profile significantly enriched in cell wall synthesis and oxidative stress related GO terms in *rtt109* $^{-/-}$ mutant cells.**

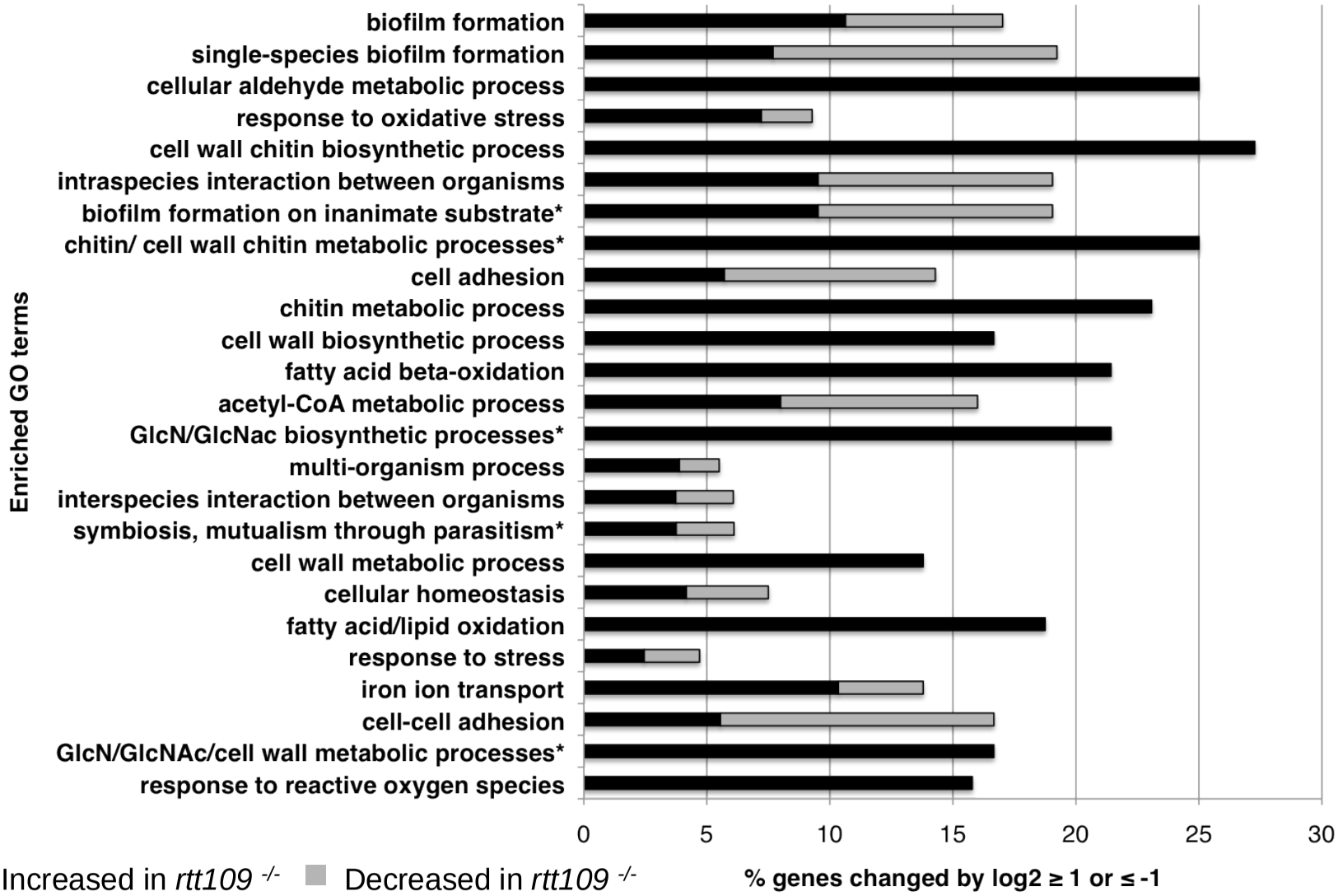

generated reactive oxygen species (Fig. 2.3E), we favor the idea that increased sensitivity to oxidative stress is the major cause of this phenotype.

Several genes that displayed transcriptional differences by microarray were validated through RT-PCR experiments. These genes included *RTT109, RAD51, IFE2, HHO1, HTZ1, SOD5, DDR48, ALS1* and *PCK1* (Fig. 2.S2). Similar alterations in RNA levels were detected by the microarrays and by RT-PCR for both the unperturbed and $H_2O_2$-stressed samples. We conclude that we have accurately detected gene expression changes in our experiments.

**DISCUSSION**

We have identified the *C. albicans* Rtt109 acetyltransferase that modifies H3K56 (Fig. 2.1A). Importantly, we show that Rtt109 is required for efficient pathogenesis in mice, and our *in vitro* data suggest that increased susceptibility to macrophages makes *rtt109* $^{-/-}$ mutant cells less pathogenic (Fig. 2.3). Our results are consistent with previous data suggesting that efficient DNA repair is required for pathogenesis. For example, *C. albicans rad52* $^{-/-}$ mutants are unable to perform homologous recombination as a mode of DNA repair, and are less pathogenic in mice (Chauhan et al., 2005). Our data specifically emphasize the importance of reactive oxygen species generated in mammalian host phagosomes for killing *C. albicans.* Previously, mice that lack the NADPH oxidase enzyme responsible for generating ROS in phagocytes were shown to experience greater rates of mortality during systemic *C. albicans* infections (Aratani et al.,

2002b). Here, we demonstrate that the increased sensitivity of *rtt109*$^{-/-}$ cells to macrophages requires NADPH oxidase function (Fig. 2.3E). We conclude that H3K56 acetylation by Rtt109 is a new example of how the ability to withstand genotoxic agents is important for *C. albicans* pathogenesis.

Genome-wide expression profiling of *C. albicans* in the presence of several types of host cells has been performed (reviewed in (Brown et al., 2007; Kumamoto, 2008)). These studies indicate that alterations in metabolism and stress response genes often occur upon interaction with host cells. For example, after phagocytosis, glycolytic genes are down-regulated and fatty acid oxidation and glyoxylate cycle genes are up-regulated (Fradin et al., 2005; Lorenz et al., 2004)}. Phagocytic cells are particularly important for this response, because erythrocytes and mononuclear cells have little effect on *C. albicans* gene expression, but an enriched population of polymorphonuclear cells (mostly neutrophils and eosinophils) down regulates glycolytic genes, including *HXK2* (hexokinase II) and *PGI1* (phosphoglucoisomerase), as well as glyoxylate cycle genes, including *MLS1* (malate synthase). Neutrophils also induce an oxidative stress response, including activation of *SOD5*, a cell surface-associated superoxide dismutase (Fradin et al., 2005). Similar trends are also seen in the *rtt109*$^{-/-}$ mutant cells. Together, the coordinated down-regulation of glycolysis and up-regulation of the glyoxylate cycle in mutant cells grown in rich media containing a large amount of glucose suggests that *rtt109*$^{-/-}$ mutant cells are less well able to utilize sugars for metabolism, and rely more on glyoxylate cycle

enzymes to convert fats to carbohydrates. As noted above, there are also complex alterations of gene expression related to mitochondrial and peroxisomal metabolism and cell wall synthesis. How much the metabolic alterations in *rtt109*$^{-/-}$ mutant cells contribute to the pathogenesis phenotype has yet to be resolved. Some of these alterations may be via indirect changes to chromatin, because we also observed that two histone isoform genes, *HHO1* and *HTZ1*, display reduced RNA levels in the mutant cells in YPD (Fig. 2.S2; Table 2.S4). However, because *rtt109*$^{-/-}$ cells became as resistant to macrophages as were wild-type cells upon inhibition of host NADPH oxidase (Fig. 2.3E), we favor the hypothesis that the sensitivity of *rtt109*$^{-/-}$ cells to exogenous DNA damaging agents (Fig. 2.2), reflected by their constitutive response to endogenous damage (Fig. 2.1C, 2.4 and Table 2.S4), largely explains why Rtt109 is important for pathogenesis.

Recent analyses of telomere-proximal gene silencing in the budding yeast *S. cerevisiae* has suggested that elevated levels of H3K56 acetylation antagonizes epigenetic silencing of telomere-proximal genes (Xu et al., 2007a; Yang et al., 2008), although deletion of *RTT109* has little effect on silencing (Yang et al., 2008). To determine whether loss of Rtt109 in *C. albicans* might cause position-dependent alteration of gene expression at telomeres, we paid particular attention to telomere-proximal genes in these analyses (Table 2.S6). Genes with elevated and reduced transcript levels in *rtt109*$^{-/-}$ cells were observed, and there did not appear to be any smooth trends that originate from the chromosome

ends in these data sets; this is especially evident at the chrR right telomere. Moreover, many of the altered genes near telomeres can be explained by trends suggested from the GO term analyses. For example, there are several stress-, damage- and hyphal-induced genes that display elevated expression in the mutant cells (e.g. *XYL2, DFM1,* orf19.7531*, SOD3*, and to a lesser extent, *RAD3 and NAG1*). Although it remains an open possibility that H3K56ac may play a role in position-dependent gene expression at some of the altered loci we have detected, our data suggest that the most salient changes in gene expression are related to DNA damage induction and alterations in cellular metabolism rather than chromosomal position.

Because Rtt109 is well-conserved among fungal species (Fig. 2.S1), we propose that Rtt109 is a strong candidate target for therapeutic intervention against fungal pathogens, not limited to *C. albicans*. Although mammalian p300/CBP HAT enzymes are distant Rtt109 homologues, many catalytically important residues in p300/CBP are distinct from those in Rtt109 (Tang et al., 2008). In fact, compounds that inhibit p300/CBP have no effect on Rtt109 (Tang et al., 2008), indicating that the potential for discovering specific inhibitors of fungal Rtt109 enzymes is promising.

**Experimental Procedures:**

**Yeast culture**. Strains were constructed as described in the Supplementary Material. *C. albicans* strains were grown in Yeast Extract Peptone (YEP; 0.1%

yeast extract, 0.2% peptone) supplemented with 2% dextrose (YPD; rich media) or 2% maltose. When indicated, yeast cells were cultured in Yeast nitrogen base (YNB; 0.67% yeast nitrogen base, 0.77% complete synthetic media, and 2% dextrose) or Yeast Carbon Base (YCB; 0.234% yeast carbon base, 0.2% yeast extract, 0.4% BSA, pH 4) media at 30°. Where mentioned, media were supplemented with 200 μg $ml^{-1}$ nourseothricin (ClonNat, Werner BioAgents) or 10 μg $ml^{-1}$ mycophenolic acid (Sigma-Aldrich, Inc.).

**Immunobloting.** Alkaline whole cell lysates (Fig. 2.1A) were obtained as previously described (Kushnirov, 2000). Samples were separated on 17% polyacrylamide SDS gels, transferred onto polyvinylidene fluoride and probed with rabbit anti-H3K56ac (1:2000, Abcam), or rabbit anti-H3 (1:1000, Abcam). Whole cell lysates (Fig. 2.1C) were obtained from 50 ml log-phase cultures in YPD and washed twice in whole cell extract buffer (20 mM Hepes pH 7.0, 350 mM NaCl, 10% glycerol, 0.1% tween-20) in the presence of 1 μg $ml^{-1}$ aprotinin, 0.16 mg $ml^{-1}$ benzamidine, 0.5 μg $ml^{-1}$ leupeptin, 0.7 μg $ml^{-1}$ pepstatin and 0.17 mg $ml^{-1}$ phenylmethylsulphonyl fluoride (PMSF). Pellets were resuspended with 1 ml whole extract buffer. An equal volume of glass beads was added and cells were agitated on a mini bead-beater at 4°C, for four 1-minute pulses. Glass beads were then separated from the lysate by centrifugation at 2,500 x g, at 4°C for 5 minutes. Next, insoluble material was pelleted by centrifugation at 18,000 x g, at 4°C for 10 minutes. The soluble supernatant was recovered and protein

concentrations were determined by Bradford assay. 15 μg of protein was used for immunoblotting with rabbit anti-H2A-phosphorylated S129 (1:4000, Abcam) or rabbit anti- H2A (1:3000, Abcam) antibodies.

**Antifungal sensitivity assay.** To determine minimal inhibitory concentrations of amphotericin B (AMB; Fluka, Sigma-Aldrich), fluconazole (FCZ; Sigma-Aldrich) and 5-fluorocytosine (5FC; Sigma-Aldrich), we followed the EUCAST broth dilution method as previously described (Cuenca-Estrella et al., 2003). Briefly, AMB and FCZ were reconstituted in DMSO, and 5FC in water. Two-fold serial dilutions of antifungal agents (or vehicle) were prepared in RPMI1640, 2% dextrose, 165 mM MOPS, pH 7.0, in triplicate in a microtiter plate. 2.5 x $10^4$ log-phase yeast cells were subsequently added to each well and incubated for 16-18 hours at 35°. Growth was determined by optical density at wavelength 600 nm and compared to cells exposed to vehicle alone.

**Murine Candidiasis.** BALB/cByJ female mice (Jackson Lab), 6-8 weeks old, were injected in the tail vein with log-phase *C. albicans* cells suspended in 400 μl PBS. Moribund mice were sacrificed by cervical dislocation. To assess fungal load, the left kidney was sterilely dissected and homogenized in 0.02% Triton-X 100. Five-fold serial dilutions of the homogenized tissue were plated on YPD agar for 24 hours at 30° and photographed.

All animals were maintained under specific pathogen-free conditions in the animal facilities at UMass Medical School (UMMS). All experiments involving live animals were carried out in accordance with the guidelines set forth by the UMMS Department of Animal Medicine and the Animal Use protocol approved by the Institutional Animal Care and Use Committee (IACUC).

**Macrophage growth inhibition assay.** A macrophage cell line, termed ZBM2, was derived from C57BL/6J bone marrow and immortalized by retroviral transduction of SV40 large T antigen. The cell line was maintained in DMEM supplemented with 10% heat inactivated fetal bovine serum, 10% L-929 cell conditioned media, 100 units $ml^{-1}$ penicillin and 100 μg $ml^{-1}$ streptomycin.

Macrophage cells were plated at a density of 2 x $10^6$ per 35 $mm^2$ dish and allowed to adhere for 5 hours. Log- phase *C. albicans* grown in YEP were washed in DMEM media, plated to a 1:15 macrophage ratio in a final volume of 2 mL and incubated at 37° in 5% $CO_2$ overnight. Samples were collected into 14 ml 0.02% Triton-X100 (v/v) in water to osmotically lyse macrophages. Dilutions of each sample were plated onto YPD and placed at 37° to assess colony-forming units (CFU). Percent growth inhibition was calculated relative to yeast cultures incubated in parallel without macrophages. Experiments with diphenyleneiodium chloride (DPI) were performed similarly with the inclusion of 0.75 μM DPI from a 31.8 mM stock solution in DMSO. Conditions without DPI

included the same final concentration of 0.002% DMSO. All experiments were repeated at least four separate times.

**Statistics.** The survival data for the positive control and the experimental groups (Fig. 2.3A -B) were compared using the Mantel-Cox method. Statistical analysis of macrophage growth inhibition assay (Fig. 2.3E) was determined by paired two-tailed Student t-test. The software used was GraphPad Prism.

**RNA extraction and microarray hybridization**

Four independent pairs of biological replicate samples were analyzed to compare RNA levels in wild-type and *rtt109* $^{-/-}$ cells. Two experiments were performed: first, in unperturbed cells grown in YPD and second, in cells exposed to $H_2O_2$. To account for dye effects, two of the four samples for each experiment were analyzed using Cy3 labeling of the wild-type sample and Cy5 labeling of the mutant sample; the dyes were swapped for the other two biological replicates.

In the first experiment, wild-type and *rtt109* $^{-/-}$ cultures were grown at 30°C in 50 ml YPD to a matching O.D. 600 nm for each of the four biological replicates, with the final O.D. 600 nm ranging from 0.6-0.9 for the different experiments. Pellets were flash frozen with liquid nitrogen and stored at -80°C until further processing. RNA was purified by acid-phenol extraction followed by ethanol, ammonium acetate precipitation as previously described (Sexton et al., 2007). DNA oligonucleotide *C. albicans* microarray slides were purchased from

The Genome Center at Washington University (http://genome.wustl.edu/services/microarray/candida_albicans). 10 μg RNA was labeled by reverse transcription using the 3DNA Array 350 system (Genisphere) and hybridization and washing were performed per the manufacturer's instructions. Scanning was performed immediately after washing using GenePix software at a PTM ranging from 490-630 (Cy3; 532nm) and 650-960 (Cy5; 635nm).

In the second experiment, RNA was analyzed from $H_2O_2$-exposed cells. In this case, the final O.D. 600nm ranged from 0.5- 0.9 before exposure to 0.4 mM $H_2O_2$ in YPD for 10 minutes at 30°C. The cells were immediately centrifuged into a pellet and flash frozen with liquid nitrogen for storage. RNA was then prepared and analyzed as above.

**Bioinformatic analysis of RNA expression**

Limma package (limma_2.18.0, (Smyth, 2004)) from Bioconductor was used for preprocessing and model fitting. A linear model was fit to the background-corrected, loess-normalized and log-transformed expression data. The dye effect and mutant effect were tested as explanatory variables to determine whether the expression level of each gene differed between mutant and wild type samples, after the dye effect was removed statistically. Three features for each gene were printed on the array, resulting in three estimated log-fold changes for each gene. Genes with at least one feature having a p-value < 0.01 for mutant

effect and a fold change ≥2 were considered potentially differentially expressed in mutant and were included for subsequent Gene Ontology (GO) enrichment test.

The gene and GO term association list was downloaded from http://www.candidagenome.org (version 1.633 and taxon: 5476) with duplicates removed. All the ancestor GO terms were added to the association list using GO.db package (GO.db_2.2.11) from Bioconductor. GO enrichment analysis was performed using the hypergeometric test in R (V 2.9.0). GO terms with at least ten associated genes in the genome and a p-value adjusted using B-H method (Benjamini and Hochberg, 1995) < 0.01 were considered significantly enriched.

**Acknowledgements**. We thank Åshild Vik and Joachim Morschauser for strains and plasmids. This work was supported by NIH R01 GM55712 (PDK), NIH F31 AI 078726 (JLS) and NIH R01 AI060991 (VB). JLS and PDK conceived the experiments, analyzed the data and wrote the paper, JLS performed the experiments except for the mouse injections, which VB performed. VB also helped with experimental design and edited the manuscript. LJZ designed, analyzed the microarray experiments and edited the manuscript.

**Supplementary Figure Legends**

**Supplemental Figure 2.S1**. **Identification, deletion and restoration of ORF19.7491, the *Candida albicans* homologue of the histone acetyltransferase Rtt109.** (**a**) Amino acid sequence alignment of *C. albicans* (C.a.) ORF19.7491 and *S. cerevisiae* (S.c.) Rtt109 performed with ClustalW2 software. Residues shaded in dark gray are identical. Residues shaded in light gray indicate charge and size conservation. Residues involved in catalysis are indicated by a rectangle (Han et al., 2007a; Stavropoulos et al., 2008; Tang et al., 2008; Tsubota et al., 2007). (**b**) Diagram of altered alleles at the *C. albicans RTT109 locus*. (**c**) PCR confirmation of the indicated strains. (Oligonucleotides used: X = OPK1110, Y = OPK1111, Z = OPK1112. See Table S3).

**Supplemental Figure 2.S1. Identification, deletion and restoration of ORF19.7491, the *Candida albicans* homologue of the histone acetyltransferase Rtt109.**

**A**

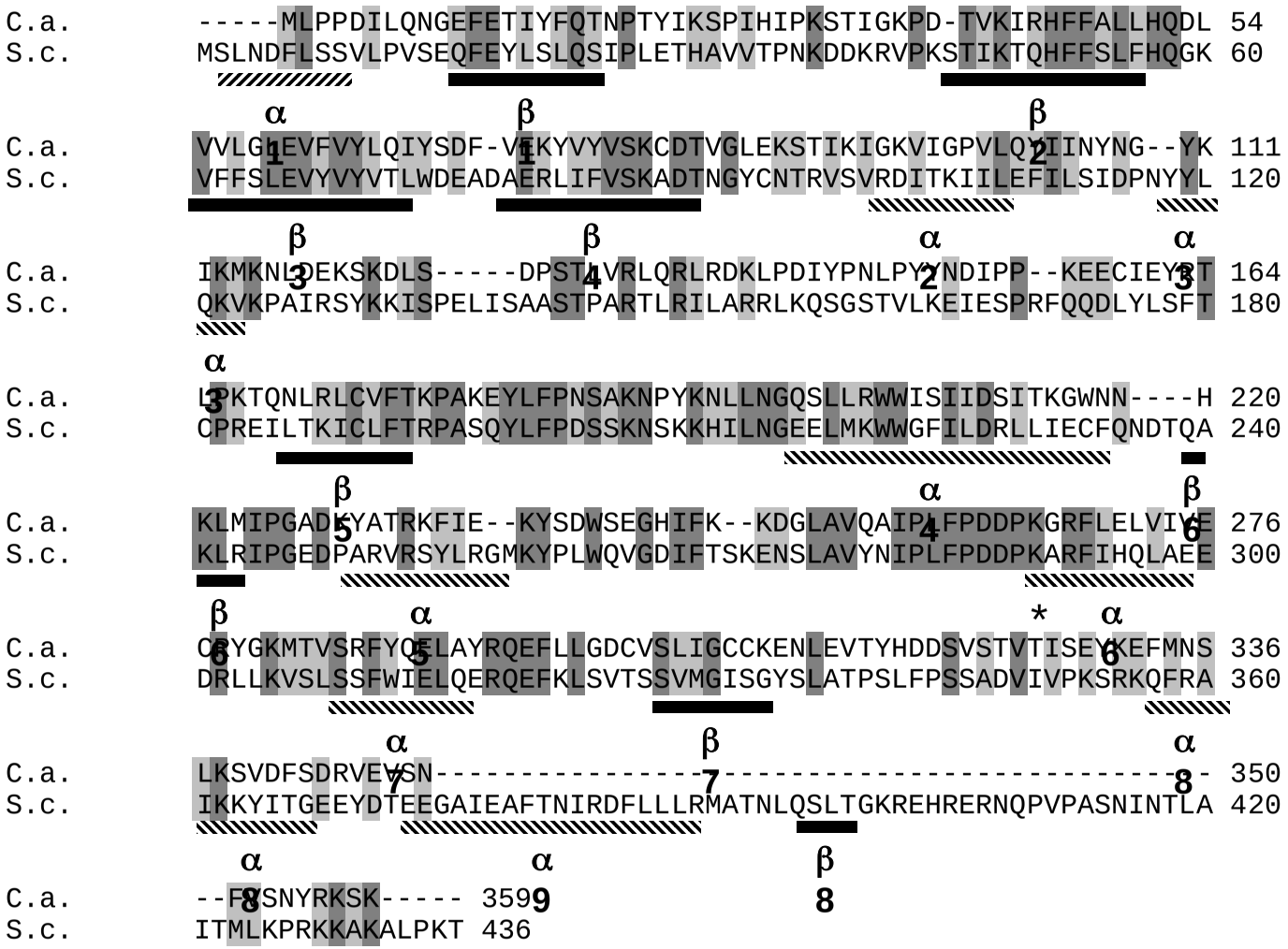

**Supplemental Figure 2.S1. Identification, deletion and restoration of ORF19.7491, the *Candida albicans* homologue of the histone acetyltransferase Rtt109.**

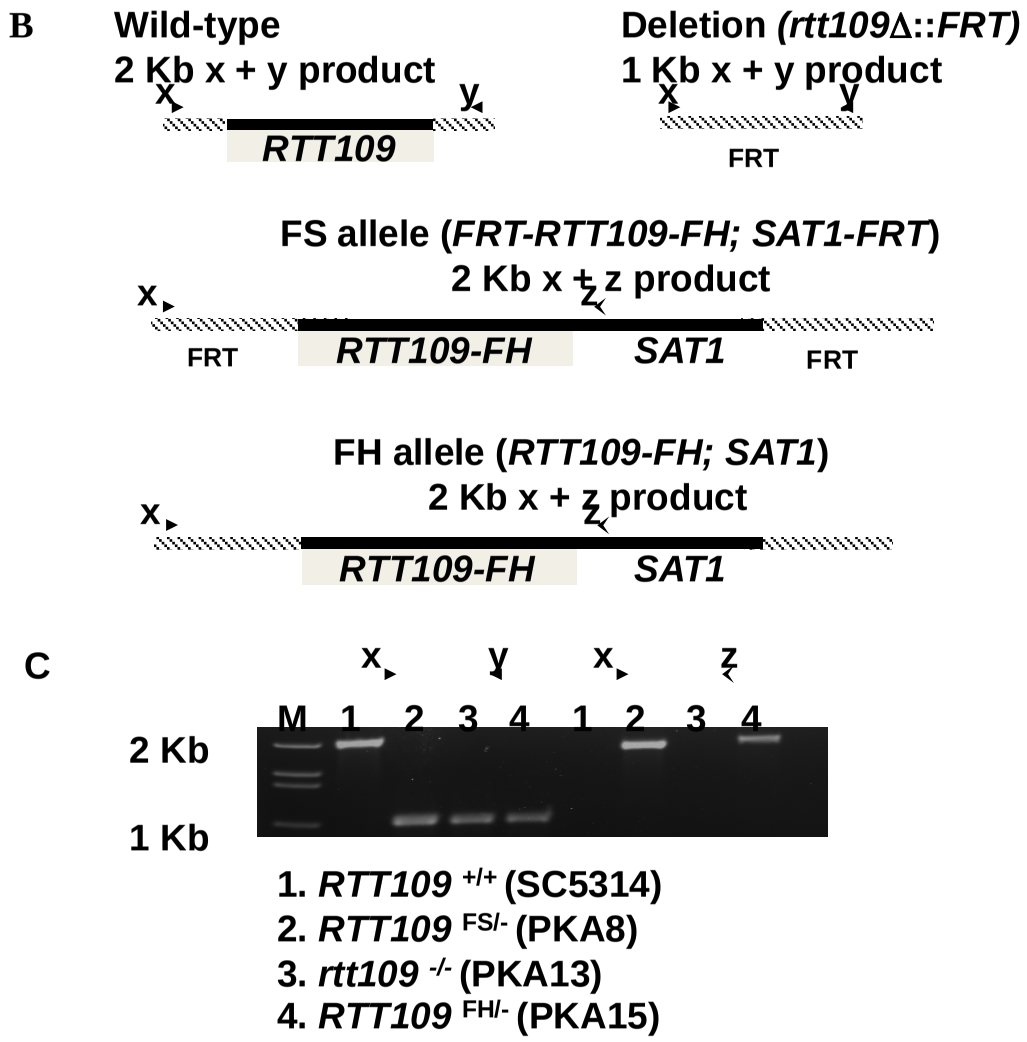

**Supplemental Figure 2.S2. RT-PCR validation of microarray results. (a-c). Cells grown in YPD.** (**a**) RT-PCR detection of 18S rRNA (*RDN18*) in an RNA preparation that had been used for microarray analysis. *RTT109* was also assayed in these multiplex reactions as an internal control for strain identity. PCR reactions were also performed with cDNA samples made in mock reactions omitting reverse transcriptase ("no RTase"). Using the same cDNA samples analyzed in panel (**a**), we also assayed (**b**) *RAD51* (microarray $Log_2$ Fold Change= 1.51), a transcript more abundant in *rtt109* $^{-/-}$ cells and (**c**) *IFE2* ($Log_2$FC= -2.73), *HHO1* ($Log_2$FC= -1.54), and *HTZ1* ($Log_2$FC= -1.71), which are less abundant in *rtt109* $^{-/-}$ cells. PCR products were loaded on 8% native gels in two-fold decreasing volumes. Signals were quantified by densitometry using LabWorks software. Each band was quantified with the values presented normalized to the signal obtained from the least-diluted sample from wild-type cells. **(d-f)** Cells exposed to hydrogen peroxide**.** RNA samples from cells exposed to hydrogen peroxide were prepared and analyzed as described above. (**d**) Multiplex PCR for 18S rRNA (*RDN18*) and *RTT109*. Detection of transcripts (**e**) elevated *SOD5* ($Log_2$FC= 3.30), *DDR48* ($Log_2$FC= 2.14), *PCK1* ($Log_2$FC= 1.76) and (**f**) reduced *ALS1* ($Log_2$FC= -1.58) in *rtt109* $^{-/-}$ cells.

**Supplemental Figure 2.S2. RT-PCR validation of microarray results. (a-c). Cells grown in YPD.**

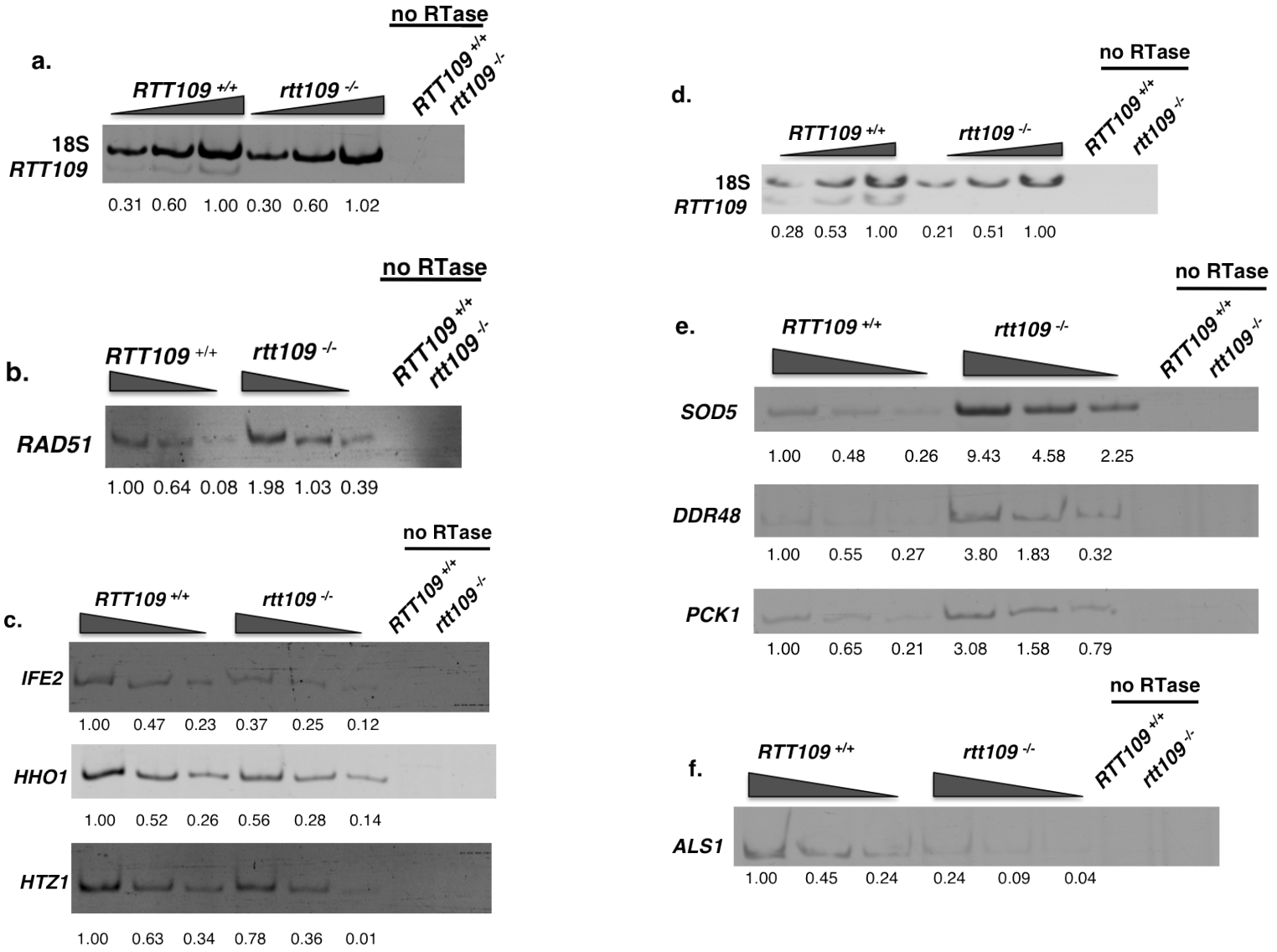

**Supplemental Table 2.S3: Primers and *C. albicans* strains used in this study**

**(a) DNA primers**

| | |
|---|---|
| OPK1110 (X) | ccttgtttaggagtgaatgg |
| OPK1111 (Y) | tcaacagtaatgtctgtcta |
| OPK1112 (Z) | aaacaacaaacatttttggg |
| RDN18 (f) | cacgacggagtttcacaaga |
| RDN18 (r) | cgatggaagtttgaggcaat |
| RTT109 (f) | ctaatgattcctggggcaga |
| RTT109 (r) | ctgtaccgccaaaccatctt |
| RAD51 (f) | ggtgaattgagtgccagaca |
| RAD51 (r) | taatgaccacggcaatacca |
| IFE2 (f) | tgaaccattggcagtgtcat |
| IFE2 (r) | actttgtgccctttcaatgc |
| HHO1 (f) | agaaagctgccaccaaaaag |
| HHO1 (r) | tggagcagctttggtttctt |
| HTZ1 (f) | gtgcatggaggaaaaggaaa |
| HTZ1 (r) | gagcaggattacaattcccg |
| ASL1 (f) | cctgctggttatcgtccatt |
| ALS1 (r) | gacgactgccagcacaagta |
| SOD5 (f) | ctccaaaggcagtccatcat |
| SOD5 (r) | gggcaatcctttcaaatcaa |
| DDR48 (f) | ggtttcggtaaagacgacga |
| DDR48 (r) | cgtcattggaagagccaaa |
| PCK1 (f) | gttgccaccagtctccaaat |
| PCK1 (r) | tgcggagaatgtagcttgtg |

**(b)** Strain genotypes

| | | |
|---|---|---|
| *RTT109* $^{+/+}$ (SC5314) | Wild-type | |
| *RTT109* $^{FS/-}$ (PKA8) | *rtt109*D::FRT / *rtt109*D::*FRT-RTT109*-2xFlag-6xHis, *SAT1*-FRT | This study |

| | | |
|---|---|---|
| *RTT109* $^{FS/-}$, *FLP* (PKA11) | *rtt109*D::FRT / *rtt109*D::FRT-*RTT109*-2xFlag-6xHis-SAT1-FRT; pSAP2::eCaFLP-MPA$^{R}$ | This study |
| *rtt109* $^{-/-}$ (PKA13) | *rtt109*D::FRT / *rtt109*D::FRT; pSAP2::eCaFLP-MPA$^{R}$ | This study |
| *RTT109* $^{FH/-}$ (PKA15) | *rtt109*D::FRT / *rtt109*D::*RTT109*-2xFLAG-6xHis, *SAT1* | This study |

**Supplemental Table 2.S4.** Genes with altered RNA levels in *rtt109* $^{-/-}$ compared to wild-type *C. albicans* cells during logarithmic growth in YPD media. Listed here are the mean $\log_2$ fold changes in RNA levels (*rtt109* $^{-/-}$ / wild type) estimated from the four biological replicates, so (a) positive values indicate greater RNA levels in the mutant cells, and (b) negative values indicate lower RNA levels in the mutant cells. These are all the genes we detected with an average fold-change of $\log_2$ equal or greater than 1 with a p-value < 0.01 in at least 2 of the 3 array features. Open reading frames not yet characterized in *C. albicans*, but identified as an orthologue of a *Saccharomyces cerevisiae* protein by the Candida Genome Database are indicated with "Sc" preceding the gene name.

**(a) Genes with greater RNA levels in the mutant cells**

| Gene name and description | Mean $\log_2$ fold change |
|---|---|
| CTN1, mitochondrial carnitine acetyltransferase | 2.81 |
| HSP12, heat shock protein | 2.52 |
| BMT3 Beta-Mannosyl transferase | 2.23 |
| orf19.7306, conserved uncharacterized protein | 2.10 |
| SPS4, sporulation-specific protein | 2.04 |
| SAP7, secreted aspartyl proteinase 7 | 2.00 |
| DNA2, DNA helicase involved in DNA replication | 1.82 |
| PST1, Protoplast-Secreted protein | 1.79 |
| PHO89, Na+/Pi symporter | 1.77 |
| CAT2, carnitine acetyltransferase | 1.77 |
| orf19.2769, hyphal-induced (ScPBI2, proteinase B inhibititor) | 1.77 |

| | |
|---|---|
| orf19.7531, conserved uncharacterized protein | 1.74 |
| FOX3, Putative peroxisomal 3-oxoacyl CoA thiolase | 1.73 |
| orf19.4795, hypothetical protein | 1.72 |
| SOD4, Cu/Zn superoxide dismutase | 1.71 |
| orf19.4171, conserved uncharacterized protein | 1.70 |
| orf19.5141, hypothetical protein | 1.69 |
| EST2, telomerase reverse transcriptase | 1.69 |
| FLO5, putative cell wall protein | 1.66 |
| MDR1, benomyl/methotrexate resistance protein | 1.66 |
| LYS22, homocitrate synthase | 1.66 |
| orf19.4070, hypothetical protein | 1.59 |
| RAD16, nucleotide excision repair protein | 1.59 |
| DIP53, dicarboxylic amino acid permease | 1.56 |
| PSF1, DNA-dependent DNA replication, GINS complex subunit | 1.55 |
| ARO10, pyruvate decarboxylase | 1.55 |
| RAD51, DNA repair protein; RecA homolog | 1.51 |
| ARG1, argininosuccinate synthetase | 1.47 |
| MPH1, RNA helicase involved in DNA repair | 1.46 |
| RAD7, nucleotide excision repair protein | 1.45 |
| orf19.5780, conserved uncharacterized membrane protein | 1.45 |
| MLH1, DNA mismatch repair protein | 1.44 |
| PRI1, p48 polypeptide of DNA primase | 1.41 |
| TES1, acyl-CoA thioesterase | 1.41 |
| orf19.1449, uncharacterized ORF (ScDDI2/ ScDDI3, DNA damage inducible) | 1.40 |
| CIS36, hypothetical protein weakly similar to C-terminus of PIR3-like proteins | 1.34 |
| orf19.3627, conserved uncharacterized protein | 1.34 |
| MDH99, dehydrogenase | 1.33 |
| PSA2, mannose-1-phosphate guanyltransferase | 1.32 |
| orf19.251, stress-induced (ScHSP31, Heat shock protein) | 1.32 |
| UGA22, succinate-semialdehyde dehydrogenase; involved in utilization of | 1.31 |

| | |
|---|---|
| GABA as a nitrogen source | |
| DCD1, deoxycytidylate deaminase | 1.30 |
| IFD1, conserved aryl-alcohol dehydrogenase | 1.30 |
| BDE99, 1,4-butanediol diacrylate esterase | 1.26 |
| CVT9, oligomeric, coiled-coil, peripheral membrane protein | 1.26 |
| orf19.6083, hypothetical protein | 1.26 |
| ATF1, alcohol acetyltransferase | 1.26 |
| AMO2, copper-containing amine oxidase | 1.25 |
| orf19.6263, Predicted membrane transporter (ScMCH4, Mono carboxylate transporter | 1.24 |
| EAP1, Enhanced Adherence to Polystyrene; glycosylphosphatidylinositol-anchored cell wall protein involved in adhesion to human epithelial cells | 1.23 |
| CPA2, carbamoyl phosphate synthetase large subunit, arginine biosynthesis | 1.23 |
| CHS8, chitin synthase 8 | 1.18 |
| orf19.346, alanine transaminase (ScALT1) | 1.17 |
| GRP3, induced by osmotic stress | 1.16 |
| RBK1, ribokinase | 1.16 |
| PRC2, carboxypeptidase Y precursor | 1.16 |
| orf19.4830, hypothetical protein | 1.15 |
| RNH2, ribonuclease H | 1.15 |
| orf19.6117, similar to ER protein | 1.15 |
| ZMS1, homolofous to Zinc Finger Protein C2H2 | 1.14 |
| orf19.4634, N-type ATP pyrophosphatase superfamily (ScNCS6) | 1.14 |
| ABP2, unknown function, induced by alpha-factor | 1.13 |
| orf19.3292, conserved uncharacterized protein (ScMXR2, Methionine sulfoxide reductase) | 1.12 |
| MEC1, cell cycle checkpoint protein | 1.09 |
| ARA1, D-arabinose dehydrogenase | 1.08 |
| orf19.4749, hypothetical protein | 1.07 |
| orf19.4316, Trimethyllysine dioxygenase, the first enzyme in the carnitine biosynthesis pathway | 1.05 |

| | |
|---|---|
| MNN13, mannosyltransferase | 1.03 |
| MEF2, mitochondrial elongation factor G- like protein | 1.01 |

## (b) Genes with lower RNA levels in the mutant cells

| Gene name and description | Mean $Log_2$ fold change |
|---|---|
| STM1, purine motif triplex-binding protein; specific affinity for guanine-rich quadruplex nucleic acids | -4.08 |
| SCW10, soluble cell wall protein similar to mannoprotein MP65 | -3.69 |
| UCF1, Up-regulated by CAMP in Filamentous | -2.75 |
| IFE2, Zn-containing alcohol dehydrogenase | -2.73 |
| HXK2, hexokinase II | -2.68 |
| RHD3, conserved protein repressed in hyphal development | -2.44 |
| HXT6, hexose transporter | -2.26 |
| SAH1, S-adenosyl-L-homocysteine hydrolase | -2.23 |
| COX12, cytochrome c oxidase subunit VIb | -2.16 |
| ZRT2, low affinity zinc transporter | -2.04 |
| CAM1, translation elongation factor eEF1 gamma, protein level decreased in stationary phase cultures | -1.95 |
| orf19.1196, conserved uncharacterized protein with ser/thr kinase domain (ScPKH3, Pkb-activating Kinase Homolog) | -1.88 |
| HTZ1, histone variant involved in chromatin and transcriptional control | -1.71 |
| orf19.4450.1, hypothetical protein identified by cDNA isolation | -1.67 |
| BUB3, cell cycle arrest protein | -1.61 |
| HHO1, histone H1 | -1.54 |
| PIR1, cell wall structural constituent with tandem repeats | -1.52 |
| orf19.5626, conserved uncharacterized protein | -1.48 |
| ADAEC, (ScAGA1, agglutinin subunit) | -1.47 |
| orf19.3448, hypothetical protein | -1.39 |
| orf19.5267, Putative cell wall protein | -1.38 |
| PCK1, phosphoenolpyruvate carboxykinase | -1.35 |
| MAE1, mitochondrial malate dehydrogenase | -1.33 |

| | |
|---|---|
| GPM2, phosphoglycerate mutase | -1.32 |
| RTT109, Regulator of Ty1 Transposition, Histone acetyltransferase critical for cell survival in the presence of DNA damage during S phase | -1.32 |
| FDH1, formate dehydrogenase | -1.29 |
| PCL7, cyclin like protein interacting with PHO85 | -1.27 |
| orf19.3713, dubious protein | -1.23 |
| SAM4, AdoMet-homocysteine methyltransferase | -1.18 |
| AOX2, alternative oxidase | -1.18 |
| CDR4, ABC transporter | -1.16 |
| orf19.5136, conserved uncharacterized protein | -1.15 |
| NRG1, transcriptional repressor | -1.13 |
| FGR41, putative GPI-anchored protein | -1.13 |
| MAD1, coiled-coil protein involved in the spindle-assembly checkpoint | -1.12 |
| orf19.3302, conserved uncharacterized protein, (ScPIG2, Putative type-1 protein phosphatase targeting subunit that tethers Glc7p type-1 protein phosphatase to Gsy2p glycogen synthase) | -1.09 |
| orf19.1653, hypothetical protein | -1.09 |
| orf19.951, hypothetical protein, transcription downregulated upon yeast-hyphal switch | -1.06 |
| orf19.5282, hypothetical protein decreased expression in hyphae compared to yeast-form cells | -1.05 |
| orf19.2398, hypothetical protein | -1.04 |

**Supplemental table 2.S5:** Genes with elevated expression in *rtt109* $^{-/-}$ compared to wild-type *C. albicans* cells during exposure to hydrogen peroxide. Criteria for inclusion of genes are as described for Table S4.

## (a) Genes with greater RNA levels in the mutant cells

| Gene name and description | MEAN $log_2$ fold change |
|---|---|
| SOD5, copper-zinc superoxide dismutase | 3.304 |
| IFD1, conserved aryl-alcohol dehydrogenase | 3.252 |
| LDG8, uncharacterized protein, regulated by peroxide stress | 2.770 |
| orf19.7306, protein of aldo-keto reductase family | 2.309 |
| SOD4, Cu/Zn superoxide dismutase | 2.289 |
| PGA13, Putative GPI-anchored protein | 2.167 |
| DDR48, flocculent specific protein | 2.136 |
| IFD6, aryl-alcohol dehydrogenase | 2.010 |
| orf19.1691, conserved uncharacterized protein | 1.864 |
| MLS1, malate synthase | 1.778 |
| PCK1, phosphoenolpyruvate carboxykinase | 1.760 |
| orf19.2213, conserved uncharacterized protein | 1.671 |
| PRN1, RNA pol II transcription cofactor | 1.648 |
| orf19.5514, conserved uncharacterized protein | 1.645 |
| orf19.2724, conserved uncharacterized protein | 1.628 |
| PST1, 1,4-benzoquinone reductase; brefeldin A resistance protein; Protoplast-Secreted protein | 1.623 |
| orf19.6484, hypothetical protein | 1.606 |
| TCD4, sulfonate dioxygenase | 1.549 |
| PSA2, mannose-1-phosphate guanyltransferase | 1.537 |
| FRE2, ferric reductase | 1.524 |

| | |
|---|---|
| IFD4, aryl-alcohol dehydrogenase | 1.499 |
| ARO10, pyruvate decarboxylase | 1.485 |
| AHP1, alkyl hydroperoxide reductase | 1.482 |
| PHR1, pH regulated GPI-anchored membrane protein that is required for morphogenesis | 1.453 |
| GST3, glutathione S- transferase | 1.441 |
| orf19.2515, hypothetical protein | 1.417 |
| orf19.3351, hypothetical protein | 1.354 |
| ALD5, aldehyde dehydrogenase | 1.348 |
| orf19.3902, hypothetical protein | 1.332 |
| orf19.6117, uncharacterized ER protein | 1.310 |
| MSN4, zinc finger transcription factor | 1.285 |
| ECE1, secreted cell elongation protein | 1.281 |
| VPS45, vacuolar protein sorting associated protein | 1.270 |
| orf19.5686, hypothetical protein | 1.260 |
| FTH1, iron permease | 1.251 |
| MDH99, dehydrogenase | 1.250 |
| CLN3, G1 cyclin | 1.246 |
| orf19.2512, possibly spurious ORF | 1.241 |
| YTA7, ATPase | 1.222 |
| orf19.2202, uncharacterized ORF | 1.212 |
| orf19.5141 hypothetical protein | 1.207 |
| UGA22, succinate-semialdehyde dehydrogenase; involved in utilization of GABA as a nitrogen source | 1.193 |
| orf19.4873, hypothetical protein | 1.189 |
| RBR1, Glycosylphosphatidylinositol (GPI)-anchored cell wall protein required for filamentous growth at acidic pH | 1.188 |
| PRN3, RNA pol II transcription cofactor | 1.181 |
| orf19.6592, Predicted membrane transporter, member of the aromatic acid:proton symporter (AAHS) family | 1.174 |
| SNQ2, ABC transporter | 1.171 |

| | |
|---|---|
| IQG1, RAS GTPase-activating-like | 1.125 |
| orf19.3615, conserved uncharacterized protein | 1.114 |
| ACS1, acetyl-coenzyme A synthetase | 1.112 |
| orf19.6311, hypothetical protein | 1.105 |
| orf19.2769, hyphal-induced (ScPBI2, proteinase B inhibititor) | 1.103 |
| PRN4, RNA pol II transcription cofactor | 1.081 |
| RNH2, ribonuclease H | 1.075 |
| ZTA1, NADPH:quinone reductase; zeta-crystallin | 1.071 |
| orf19.5799, conserved uncharacterized protein | 1.066 |
| EEP1, conserved hypothetical protein | 1.065 |
| orf19.6315, hypothetical protein | 1.062 |
| ALD6, mitochondrial aldehyde dehydrogenase | 1.058 |
| SAP7, secreted aspartyl proteinase 7 | 1.052 |
| FAV2, uncharacterized, filament-induced protein | 1.023 |

## (b) Genes with lower RNA levels in the mutant cells

| **Gene name and description** | **Mean $Log_2$ fold change** |
|---|---|
| RTT109, Regulator of Ty1 Transposition, Histone acetyltransferase critical for cell survival in the presence of DNA damage during S phase | -3.375 |
| orf19.675, conserved uncharacterized protein, similar to cell wall proteins, induced in core stress response | -2.306 |
| ALS1, agglutinin like protein 1 | -1.582 |
| PRY2, homology to plant PR-1 class of proteins | -1.261 |
| ALS4, agglutinin like protein 4 | -1.152 |
| FGR41, putative GPI-anchored protein | -1.124 |

**Supplemental table 2.S6: telomere-proximal genes.** Open reading frames within at least 16kb of each telomere are listed, starting from most telomere-proximal at the top of the list for each telomere. The mean $log_2$ fold changes in RNA levels (*rtt109* $^{-/-}$ / wild type) are indicated on the right. Values for genes with greater expression in the mutant cells (positive $log_2$ fold change values) > 1.0 are indicated in green and **bold**. Genes with less expression in the mutant cells (negative $log_2$ fold change values) < 1.0 are indicated in red and **bold**. For selected genes, the approximate distance from the telomere end is indicated for comparison. Open reading frames not yet characterized in *C. albicans*, but identified as an orthologue of a *Saccharomyces cerevisiae* protein by the Candida Genome Database website are indicated with "Sc" preceding the gene name.

| Telomere: approx. distance from end | Gene name | Systematic name | Gene functions / homologies | Mean $log_2$ FC (YPD) | Mean $log_2$ FC ($H_2O_2$) |
|---|---|---|---|---|---|
| **chrR R** | | | | | |
| | CTA26 | orf19.7680 | Putative transcriptional activator, tel-proximal gene family | 0.39 | 0.24 |
| | ATP16 | orf19.7678 | ScATP16; mitochondrial ATP synthase | **-1.35** | 0.09 |
| ~2kb | XYL2 | orf19.7676 | xyulose reductase, stress induced (scSOR1; Sorbitol dehydrogenase) | **1.03** | **1.42** |
| | | orf19.7675 | (scMRPL25; Mitochondrial ribosomal protein of the large subunit) | 0.23 | 0.31 |
| | | orf19.7673 | (scSMD1; RNA splicing factor) | **-1.61** | -0.22 |
| ~4.5kb | | orf19.7672 | (scDFM1; ER unfolded protein response) | **1.02** | 0.20 |
| | | orf19.7670 | Putative Ca2+/H+ antiporter (scVNX1) | 0.27 | 0.31 |
| | MAL2 | orf19.7668 | Alpha- glucosidase that hydrolyzes sucrose | 0.47 | 0.68 |

| | | | | | |
|---|---|---|---|---|---|
| | IAH1 | orf19.7667 | Involved in acetate metabolism | 0.03 | 0.18 |
| | | orf19.7666 | Anion:cation symporter (scSEO1) | -0.67 | -0.44 |
| | | orf19.7665 | (ScCox16; Mitochondrial inner membrane protein, required for assembly of cytochrome c oxidase) | 0.30 | -0.09 |
| | | orf19.7664 | | -0.42 | -0.24 |
| | | orf19.7663 | (ScCSM1; Nucleolar protein that forms a complex with Lrs4p and then Mam1p at kinetochores during meiosis I to mediate accurate homolog segregation) | -0.10 | 0.02 |
| | RTT103 | orf19.7662 | (ScRTT103; plays a role in transcription termination by RNA polymerase II) | 0.02 | 0.07 |
| | HMI1 | orf19.7661 | ATP-dependent 3' - 5' helicase involved in maintenance of mitochondrial DNA | 0.00 | 0.04 |
| | | | | | |
| **chrR L** | | | | | |
| | | orf19.7545 | | -0.18 | 0.08 |
| | TLO1 | orf19.7544 | tel-proximal gene family | -0.37 | 0.01 |
| ~15 kb | INO2 | orf19.7539 | transcription factor | 0.92 | 0.24 |
| | PIF1/2 | orf19.7538 | (scRRM3; DNA helicase involved in rDNA replication) | 0.40 | 0.30 |
| | BNR1 | orf19.7537 | | 0.15 | 0.31 |
| | MIS12 | orf19.7534 | | -0.09 | -0.24 |
| ~24 kb | | orf19.7531 | Hyphae-induced | **1.74** | -0.08 |
| | EPL1 | orf19.7529 | Subunit of the NuA4 histone acetyltransferase complex | 0.16 | 0.04 |
| | | | | | |
| **chr1 L** | | | | | |
| | | orf19.6115 | dubious ORF | 0.18 | 0.01 |
| | | orf19.6114 | dubious ORF | 0.39 | 0.32 |
| | | orf19.6113 | dubious ORF | 0.05 | 0.44 |
| | CTA2 | orf19.611 | Putative transcriptional activator , | -0.72 | 0.20 |

| | | | | | |
|---|---|---|---|---|---|
| | | 2 | tel-proximal gene family | | |
| | | orf19.6110 | dubious ORF | 0.13 | 0.66 |
| | TUP1 | orf19.6109 | Transcriptional corepressor | -0.01 | 0.31 |
| | MVD | orf19.6105 | Mevalonate diphosphate decarboxylase | -0.36 | 0.27 |
| | | orf19.6103 | (ScSPO73; Meiosis-specific protein of unknown function) | -0.21 | 0.02 |
| ~15 kb | | orf19.6102 | (ScACA1; Transcription factor of the ATF/CREB family) | 0.14 | 0.51 |
| | | | | | |
| **chr1 R** | | | | | |
| | | orf19.7278 | similar to Tca2 retrotransposon | -0.53 | -0.25 |
| ~1 kb | TLO4 | orf19.7276.1 | tel-proximal gene family | -0.54 | 0.97 |
| | FGR24 | orf19.7275 | Protein encoded in retrotransposon Zorro2 with similarity to retroviral endonuclease-reverse transcriptase proteins | 0.09 | 0.10 |
| | | orf19.7274 | Predicted ORF in retrotransposon Zorro2 with similarity to retroviral reverse transcriptase proteins | 0.44 | 0.11 |
| | | orf19.7272 | dubious ORF | 0.08 | 0.10 |
| | | orf19.7271 | dubious ORF | 0.09 | 0.38 |
| | | orf19.7270 | | -0.38 | 0.00 |
| | PAA11 | orf19.7269 | (ScPAA1; Polyamine acetyltransferase) | -0.03 | 0.21 |
| | | orf19.7267 | | 0.67 | 0.04 |
| ~10 kb | | orf19.7266 | | 0.66 | 0.41 |
| | UBP10 | orf19.7265 | | -0.18 | 0.23 |
| | RPN11 | orf19.7264 | (ScRPN11; Metalloprotease subunit of the 19S regulatory particle of the 26S proteasome lid) | 0.65 | 0.44 |
| | | orf19.7263 | | -0.24 | 0.49 |
| | GDI1 | orf19.7261 | (ScGDI1; GDP dissociation inhibitor, regulates vesicle traffic in secretory pathways) | -0.21 | -0.07 |
| | | | | | |

| | | | | | |
|---|---|---|---|---|---|
| **chr2 R** | | | | | |
| | | orf19.5370 | | -0.41 | 0.31 |
| | HEM12 | orf19.5369 | (ScHEM12; Uroporphyrinogen decarboxylase) | -0.02 | -0.13 |
| | | orf19.5368 | (scYDR049w; putative transcription factor) | 0.09 | 0.20 |
| | RDH54 | orf19.5367 | Protein described as having role in DNA recombination, repair | 0.39 | -0.11 |
| | | orf19.5365 | | -0.50 | -0.13 |
| | ECM2 | orf19.5364 | (ScECM2; Pre-mRNA splicing factor) | -0.31 | -0.35 |
| | | | | | |
| **chr2 L** | | | | | |
| | TLO5 | orf19.1925 | tel-proximal gene family | -0.68 | 0.16 |
| | RRN3 | orf19.1923 | (ScRRN3; Protein required for transcription of rDNA by RNA polymerase I) | 0.32 | 0.15 |
| | CIS301 | orf19.1920 | (ScYJL160c; member of the PIR (proteins with internal repeats) family of cell wall proteins) | 0.35 | -0.13 |
| | AES6 | orf19.1917 | | -0.01 | 0.10 |
| | MPP10 | orf19.1915 | (ScMPP10; Component of the SSU processome and 90S preribosome) | -0.35 | -0.17 |
| | FAV3 | orf19.1914 | Induced by mating factor in MTLa/MTLa opaque cells | -0.26 | -0.01 |
| | | orf19.1913 | | -0.07 | -0.13 |
| | PGA52 | orf19.1911 | Putative GPI-anchored protein | 0.10 | -0.27 |
| | | orf19.1910 | | 0.40 | -0.02 |
| ~15 kb | EMC9 | orf19.1907 | | 0.68 | 0.30 |
| | | | | | |
| **chr3 L** | | | | | |
| | | orf19.5475 | dubious ORF | -0.13 | 0.52 |
| | | orf19.5474 | dubious ORF | 0.34 | 0.22 |
| | | orf19.5472 | dubious ORF | 0.14 | 0.00 |
| | YRF1 | orf19.546 | | 0.62 | 0.66 |

| | | | | | |
|---|---|---|---|---|---|
| | | 9 | | | |
| | TLO7 | orf19.5467 | tel-proximal gene family | -0.44 | 0.33 |
| | RPS24 | orf19.5466 | Predicted ribosomal protein | 0.08 | 0.05 |
| | YJU2 | orf19.5465 | (ScYJU2; Essential protein required for pre-mRNA splicing) | -0.39 | 0.01 |
| ~17 kb | | orf19.5464 | | **1.03** | 0.01 |
| | SEC6 | orf19.5463 | (ScSEC6; Essential 88kDa subunit of the exocyst complex) | -0.12 | -0.13 |
| | | | | | |
| **chr3 R** | | | | | |
| | | orf19.6192 | dubious ORF | 0.79 | 0.26 |
| | TLO8 | orf19.6191 | tel-proximal gene family | -0.71 | 0.25 |
| | SRB1 | orf19.6190 | Essential GDP-mannose pyrophosphorylase | -0.16 | 0.06 |
| | FMP22 | orf19.6189 | | -0.12 | -0.02 |
| | | orf19.6188 | | 0.11 | -0.14 |
| | | orf19.6187 | | -0.03 | -0.08 |
| ~10kb | | orf19.6186 | | 0.86 | 0.89 |
| | IND1 | orf19.6185 | | 0.11 | -0.30 |
| | | orf19.6184 | | -0.02 | 0.42 |
| | | | | | |
| **chr4L** | | | | | |
| | TLO9 | orf19.362 | tel-proximal gene family | 0.48 | 0.76 |
| | VMA6 | orf19.364 | vacuolar ATPase | 0.46 | 0.71 |
| | RAD17 | orf19.366 | (ScRAD17; Checkpoint protein, involved in the activation of the DNA damage and meiotic pachytene checkpoints) | -0.04 | 0.46 |
| | CNH1 | orf19.367 | Na+/H+ antiporter | -0.37 | -0.38 |
| | | orf19.371 | | -0.17 | 0.32 |
| | | orf19.372 | | 0.36 | 0.48 |
| | | orf19.374 | (scTRE2; Protein that functions with Tre1p to regulate ubiquitylation and vacuolar degradation of the metal transporter Smf1p) | -0.80 | -0.08 |

| | | | | | |
|---|---|---|---|---|---|
| | BDA1 | orf19.376 | | **1.22** | 0.21 |
| | PHR3 | orf19.377 | (ScGAS4; 1,3-beta-glucanosyltransferase) | 0.10 | 0.19 |
| ~16 kb | | orf19.5633 | | -0.43 | 0.52 |
| | FRP1 | orf19.5634 | Predicted ferric reductase | 0.24 | 0.59 |
| **chr4R** | | | | | |
| | | orf19.3073 | | 0.35 | 0.08 |
| | TLO10 | orf19.3074 | tel-proximal gene family | -0.18 | 0.21 |
| | | orf19.3076 | (ScTVP15; Integral membrane protein localized to late Golgi vesicles) | -0.87 | -0.03 |
| ~6.5kb | VID21 | orf19.3077 | Subunit of the NuA4 histone acetyltransferase complex | -0.31 | 0.59 |
| | | orf19.3080 | | 0.54 | 0.90 |
| | | orf19.3084 | | -0.16 | 0.32 |
| | CDC1 | orf19.3083 | (ScCDC1; Putative lipid phosphatase of the endoplasmic reticulum) | 0.96 | 0.45 |
| ~16kb | SEC10 | orf19.3086 | (ScSEC10; Essential 100kDa subunit of the exocyst complex) | -0.81 | -0.27 |
| | | | | | |
| **chr5L** | | | | | |
| | TLO11 | orf19.5700 | tel-proximal gene family | -0.39 | 0.36 |
| | | orf19.5698 | Putative ribosomal protein (ScMRPL1) | -0.10 | -0.11 |
| ~6.5kb | GAA1 | orf19.5693 | (ScGAA1; Subunit of the GPI:protein transamidase complex) | 0.10 | 0.63 |
| | | orf19.5692 | | 0.03 | 0.00 |
| | CDC11 | orf19.5691 | Septin | -0.15 | 0.38 |
| | | orf19.5689 | (ScSEC28; Epsilon-COP subunit of the coatomer) | -0.48 | 0.29 |
| | | orf19.5688 | absent from array | | |
| ~12 kb | | orf19.5686 | | 0.97 | **1.44** |
| | THS1 | orf19.5685 | Putative threonyl-tRNA synthetase | -0.43 | -0.12 |

| | | | | | |
|---|---|---|---|---|---|
| | | orf19.5684.1 | absent from array | | |
| | | orf19.5684 | (ScMRPL28; Mitochondrial ribosomal protein of the large subunit) | 0.05 | 0.15 |
| | | orf19.5683 | (ScYHR140W ; Putative integral membrane protein) | 0.56 | -0.31 |
| | | | | | |
| **chr5R** | | | | | |
| | | orf19.4055 | Protein similar to *S. cerevisiae* Ybr075wp | -0.05 | 0.48 |
| | CTA24 | orf19.4054 | Putative transcriptional activator | -0.69 | 0.21 |
| | HTS1 | orf19.4051 | Putative tRNA-His synthetas | -0.42 | 0.03 |
| | DES1 | orf19.4048 | delta-4 sphingolipid desaturase | 0.11 | -0.55 |
| | EST1 | orf19.4045 | Telomerase subunit | -0.19 | -0.28 |
| | | orf19.4046 | Putative transcription factor containing a Zn(2)-Cys(6) binuclear cluster | 0.44 | 0.20 |
| ~10 kb | MUM2 | orf19.4044 | Protein similar to *S. cerevisiae* Mum2p | 0.55 | 0.34 |
| ~11 kb | | orf19.4043 | | 0.32 | 0.69 |
| | | | | | |
| **chr6L** | | | | | |
| | NRG2 | orf19.6339 | Protein similar to ScNrg2p transcription factor, which regulates invasive growth in S. cerevisiae | 0.03 | 0.16 |
| | | orf19.6338 | dubious ORF | 0.43 | 0.24 |
| | TLO13 | orf19.6337 | tel-proximal gene family | 0.12 | 0.63 |
| | PGA25 | orf19.6336 | Putative GPI-anchored protein | -0.09 | 0.18 |
| | | orf19.6329 | | -0.23 | -0.15 |
| | | orf19.6328 | (ScACN9; Protein of the mitochondrial intermembrane space) | -0.23 | 0.05 |
| | HET1 | orf19.6327 | Putative sphingomyelin transfer protein | -0.79 | -0.16 |
| | | orf19.6326 | | -0.34 | 0.38 |

| | | | | | |
|---|---|---|---|---|---|
| ~13kb | | orf19.6325.1 | | 0.76 | 0.64 |
| | VID27 | orf19.6324 | Protein similar to *S. cerevisiae* Vid27p | -0.09 | 0.02 |
| | HPA2 | orf19.6323 | (ScHPA3; D-Amino acid N-acetyltransferase) | -0.34 | 0.19 |
| | | | | | |
| **chr6R** | | | | | |
| | | orf19.2163 | (scYBR074w; Putative metalloprotease) | 0.26 | 0.41 |
| | NAG4 | orf19.2160 | Putative transporter, N-AcetylGlucosamine | -0.09 | 0.75 |
| | NAG3 | orf19.2158 | Putative transporter, N-AcetylGlucosamine | 0.01 | -0.35 |
| | DAC1 | orf19.2157 | | -0.04 | -0.18 |
| | NAG1 | orf19.2156 | N-acetylglucosamine-6-phosphate (GlcNAcP) deacetylase | 0.76 | 0.64 |
| | HXK1 | orf19.2154 | N-acetylglucosamine (GlcNAc) kinase | 0.22 | 0.38 |
| | NAG6 | orf19.2151 | N-AcetylGlucosamine | -0.16 | 0.33 |
| | | | | | |
| **chr7L** | | | | | |
| | | orf19.7125 | | -0.18 | 0.24 |
| | RVS161 | orf19.7124 | Required for endocytosis | -0.11 | 0.25 |
| | | orf19.7123 | | 0.33 | 0.06 |
| ~3kb | | orf19.7121 | | 0.76 | 0.31 |
| ~6kb | RAD3 | orf19.7119 | 5' to 3' DNA helicase, involved in nucleotide excision repair and transcription | 0.96 | 0.64 |
| | ADK2 | orf19.7118 | (ScADK2; Mitochondrial adenylate kinase) | -0.45 | 0.10 |
| | | orf19.7116 | (ScLEO1; Component of the Paf1 complex) | -0.70 | -0.43 |
| | SAC7 | orf19.7115 | Protein described as a GTPase activating protein for RHO1 | 0.38 | 0.00 |
| | CSA1 | orf19.7114 | Surface antigen on elongating hyphae and buds | -0.64 | 0.21 |
| | FRP2 | orf19.7112 | Protein described as ferric reductase | 0.12 | 0.02 |
| ~16kb | SOD3 | orf19.7111.1 | Cytosolic manganese-containing superoxide dismutase | 0.64 | **1.29** |

| | | | | | |
|---|---|---|---|---|---|
| | FIS1 | orf19.7111 | (ScFIS1; Protein involved in mitochondrial membrane fission and peroxisome abundance) | -0.20 | 0.34 |
| | | | | | |
| **chr7R** | | | | | |
| | TLO16 | orf19.7127 | tel-proximal gene family | -0.41 | 0.47 |
| ~6.5kb | | orf19.7127.1 | | 0.66 | 0.76 |
| | SYS1 | orf19.7128 | (ScSYS1; Integral membrane protein of the Golgi) | -0.17 | 0.03 |
| ~8kb | | orf19.7130 | | **1.10** | -0.33 |
| | BBH1 | orf19.7131 | Butyrobetaine dioxygenase | 0.74 | 0.39 |
| | SPT6 | orf19.7136 | transcription elongation factor | -0.61 | -0.32 |
| | | orf19.7139 | | 0.10 | 0.22 |
| | CMT1 | orf19.7140 | | 0.42 | 0.55 |
| | UFE1 | orf19.7141 | Possibly involved in retrograde transport between the Golgi and the ER | 0.31 | -0.07 |

**Available online at**

http://www.pnas.org/content/107/4/1594/suppl/DCSupplemental

**Supplemental Table 2.S7:** List of gene ontology terms enriched in microarray data from cells grown in YPD media. GO terms with at least ten associated genes in the genome and B.H. adjusted p-value < 0.01 were included, calculated for genes with RNA levels changed by $\log_2 \leq -1$ or $\log_2 \geq 1$ with a p-value < 0.01.

**Supplemental Table 2.S8:** List of gene ontology terms enriched in microarray data from cells exposed to hydrogen peroxide. GO terms with at least ten associated genes in the genome and B.H. adjusted p-value < 0.01 were included, calculated for genes with RNA levels changed by $\log_2 \leq -1$ or $\log_2 \geq 1$ with a p-value < 0.01.

**Supplemental Table 2.S9:** Array-wide microarray data in GEO "Matrix" format for the four biological replicates of YPD-grown cells.

**Supplemental Table 2.S10:** Array-wide microarray data in GEO "Matrix" format for the four biological replicates of $H_2O_2$-exposed cells.

**Supplemental Methods:**

**Deletion of RTT109 in *C. albicans***

To delete ORF19.7491 (*RTT109*) by gene replacement, we digested pSFL2 (Reuss et al., 2004) to release the FRT-flanked MAL promoter-driven FLP and *SAT1* drug resistance (*natR*) cassette. This cassette was inserted between 460 bp of genomic DNA flanking both sides of the *C. albicans RTT109* open reading frame, yielding pPK564. We transformed SC5314 by electroporation as previously described (Reuss et al., 2004) with *SmaI*-digested pPK564. Cells were recovered on YPD agar overnight and replica plated onto YPD supplemented with 200 μg $ml^{-1}$ nourseothricin (*nat*). We verified proper insertion of the construct at the *RTT109* locus by PCR using oligonucleotides targeted outside the region of homology (OPK1110 & OPK1111) and inside pPK564 (OPK1112) (Fig. 2.S1b and 2.S1c; Table 2.S3; data not shown). To induce FRT-specific recombination, we grew the cells overnight in YEP supplemented with 2% maltose, plated single colonies on YPD agar and identified clones that lost resistance to nourseothricin. We verified deletion of the *FLP, SAT1* insert by PCR using the oligonucleotides mentioned above to identify a heterozygous *RTT109* $^{+/-}$ strain (data not shown).

We were not able to disrupt the second *RTT109* gene using the strategy described above, suggesting that deletion of both *RTT109* alleles is heavily selected against, and that traditional insertional mutagenesis may be too infrequent in this case. Therefore, we took a two-step approach, first replacing the remaining *RTT109* gene with one flanked by FRT sites. To do this, we made a

2xFLAG-6xHis tagged *RTT109* allele adjacent to the *SAT1* drug resistance gene, flanked by FRT sites and 460 bp of homology downstream and upstream the *RTT109* ORF (pPK585, carrying what we term the FLP-Sensitive *RTT109*$^{FS}$ allele). We replaced the remaining copy of *RTT109* in the heterozygous strain with *RTT109*$^{FS}$ by introducing *SmaI*-digested pPK585 by electroporation and selecting nat$^{R}$ colonies as described above. We verified proper insertion by PCR (Fig. 2.S1c). We also confirmed the presence of the 6xHis-2xFLAG-tagged Rtt109 protein in this isolate (PKA8) by metal affinity chromatography and immunoblotting (data not shown). To provide an inducible source of FLP, we constructed pPK592 by replacing the *URA3* gene in pSFL213 (Staib et al., 2000) with the *IMH3* (MPA$^{R}$) gene, generating a SAP2 promoter-driven FLP selectable with mycophenolic acid (MPA). We transformed PKA8 with *XbaI-SacI*-digested pPK592 by electroporation and selected on YNB media supplemented with 10 μg ml$^{-1}$ MPA, yielding PKA11. Finally, to generate *rtt109* $^{-/-}$ homozygous strains, we induced SAP2 promoter-driven transcription of eCaFLP by growing PKA8 cells in YCB media supplemented with 10 μg ml $^{-1}$ MPA overnight, and screened for loss of the RTT109$^{FS}$ allele by determining which colonies displayed nourseothricin sensitivity. Candidate homozygous delete mutants were then screened by PCR and immunoblotting, yielding PKA13 (Fig. 2.S1c and Fig. 2.1a).

The complemented strain, *RTT109* $^{FH/-}$ (PKA15), was made by inserting an *RTT109*-2xFLAG-6xHis allele (abbreviated as RTT109$^{FH}$) into PKA13 at a previously deleted *rtt109*D::FRT endogenous locus. To ensure this allele would

be stable in the presence of FLP, we removed both flanking FRT sites from pPK585, yielding pPK602. pPK602 was digested with *SmaI*, electroporated into PKA13 and $nat^R$ colonies were selected as described for pPK585. Proper insertion was confirmed by PCR (Fig. 2.S1c), and complementation of Rtt109 function was demonstrated by H3K56ac immunoblot (Fig. 2.1a) and metal chromatography followed by anti-Flag immunoblot analysis to detect Rtt109-2xFlag-6xHis expression (data not shown).

**RT-PCR microarray validation**

RNA samples purified for microarrays were used for RT-PCR. cDNA was prepared from 2 μg RNA with SuperScript II Reverse Transcriptase (Invitrogen) with oligo dT (Sigma) following the manufacture's instructions.

# CHAPTER 3

## Discovery of a specific Rtt109 chemical inhibitor

**Acknowledgement:** The following chapter includes a description of some work done in collaboration with the Small Molecule Facility at UMass Medical School (Worcester, MA) and the Chemical Biology Platform at the Broad Institute (Cambridge, MA). Specifically, Dr. Hong Cao operated the robots at the UMass Small Molecule Facility during the pilot high throughput screen described below. The subsequent screen, also described below, was conducted at the Broad Institute by the Chemical Biology Platform group with proteins manufactured in our lab by a previous Research Assistant, Amie Jordan. Unless indicated, all other protein purifications and experimental procedures were performed by myself.

## Introduction

Histone acetyl-transferase (HAT) enzymes catalyze post-translation modifications (PTM) through the transfer of an acetyl group from acetyl-coenzyme A (Ac-CoA) to the ε-amine group of a histone lysine residue. PTMs on histones, which include methylation, phosphorylation, ubiquitination, in addition to acetylation, have important consequences for genome stability and function (Reviewed in (Gardner et al., 2011; Kouzarides, 2007; Mersfelder and Parthun, 2006; Peterson and Laniel, 2004; Ransom et al., 2010; Zhu and Wani, 2010)). For instance, acetylation of specific histone amino acids can promote appropriate gene expression (Brownell et al., 1996), chromatin conformation (Shogren-Knaak et al., 2006), DNA replication (Li et al., 2008) and DNA repair (Chen et al., 2008).

Recently, Rtt109, a HAT enzyme solely conserved in the fungal kingdom, was shown to be required for fungal pathogenicity (Lopes da Rosa et al., 2010; Wurtele et al., 2010). Rtt109 is entirely responsible for histone H3 lysine 56 (H3K56) acetylation in yeast (Han et al., 2007a; Lopes da Rosa et al., 2010; Schneider et al., 2006; Xhemalce et al., 2007). H3K56 is located on the α-helix between the N-terminal tail and the histone fold domain of histone H3, making it one of few PTM sites not located on the unstructured N-terminal tail of histones. *In vivo,* the histone chaperone Asf1 is required to stimulate Rtt109 acetylation of H3K56 (Han et al., 2007a; Recht et al., 2006; Schneider et al., 2006). Also, Rtt109 forms a stable complex with a different histone chaperone, Vps75, a NAP1 (nucleosome assembly protein 1) family

protein. *In vivo*, Rtt109-Vps75 contributes to acetylation of H3K9, H3K23 and H3K27 but not H3K56 (Berndsen et al., 2008; Tsubota et al., 2007). However, *in vitro*, Rtt109-Vps75 efficiently acetylates H3K56 (Berndsen et al., 2008; Tsubota et al., 2007). Yeast cells incapable of acetylating H3K56 are extremely sensitive to DNA damage (Driscoll et al., 2007; Hyland et al., 2005; Lopes da Rosa et al., 2010; Masumoto et al., 2005; Xhemalce et al., 2007). Consequently, deletion of *RTT109* in the pathogenic fungus *Candida albicans* causes hypersensitivity to the genotoxic effects of reactive oxygen species (ROS) released by phagocytic cells of the mammalian immune system (Lopes da Rosa et al., 2010). As a result, *C. albicans rtt109* $^{-/-}$ cells are avirulent in the murine model of systemic candidiasis (Lopes da Rosa et al., 2010).

In humans, systemic candidiasis results in approximately 40% mortality, despite currently available anti-fungal medications (Gudlaugsson et al., 2003). *C. albicans* infections are common in hospital settings, especially on implanted surgical devices and in immune-compromised patients (Neofytos et al., 2010; Pfaller and Diekema, 2007). Most clinical drugs used against *C. albicans* intervene with cellular membrane or wall integrity. Unfortunately, anti-fungal drug resistance is common in this organism, involving changes in membrane synthesizing pathways and rapid efflux of the drugs through cellular membrane pumps (Cannon et al., 2007; Cowen et al., 2002). Therefore, discovery of novel anti-fungal drugs to combat this public health issue is merited. Since, loss of RTT109 significantly abolishes *C. albicans* pathogenicity and Rtt109 is solely conserved in fungi, we reasoned that a specific

HAT inhibitor would serve as an appropriate new drug without affecting other HATs conserved throughout Eukaryotes.

Rtt109 has limited primary sequence homology to the three known HAT families: P300/CBP, GNAT (Gcn5- related N-acetyl transferase) and MYST (MOZ, Ybf2/Sas3, Sas2, Tip60). Furthermore, Rtt109 does not possess the canonical Motif A (acetyl coenzyme A binding pocket) as seen in other HATs. However, Rtt109 has a similar tertiary fold structures as the mammalian HAT p300 and a similar central core structure to that of Gcn5 (Lin and Yuan, 2008; Stavropoulos et al., 2008; Tang et al., 2008). Thus far, the catalytic mechanism of known HATs entails de-protonation of the target histone lysine residue to facilitate its nucleophilic attack on the acetyl group of acetyl-coA (Hodawadekar and Marmorstein, 2007; Liu et al., 2008). Current evidence supports that Rtt109, GNAT and MYST family enzymes use a sequential catalytic mechanism involving binding of the substrates to enzyme to form a ternary intermediate complex before these catalytic steps can occur (Albaugh et al., 2010; Berndsen et al., 2007; Tanner et al., 1999; Trievel et al., 1999). In contrast, p300 operates a Theorell-Chance (“hit-and- run”) mechanism that involves association of the enzyme and acetyl-coA first, followed by transient association with the protein substrate (Liu et al., 2008). The transient association of p300 to its substrate correlates with its large pool of target proteins. Despite the similarities between Rtt109 and other HATs, previously described HAT inhibitors, specifically for p300, do not affect Rtt109 catalysis (Bowers et al., 2010; Tang et al., 2008).

Here, I present the discovery of the first compound that specifically inhibits Rtt109 HAT activity, called KB7 (Kaufman-Broad #7). p300 or Gcn5 activities are not affected by KB7. KB7 has a $K_i^{app}$ of 56 nM. Its mechanism of inhibition appears to be noncompetitve with regard to the histone substrate and uncompetitive regarding Ac-CoA. KB7 inhibits Rtt109 in the presence of either Vps75 or Asf1, and inhibits HAT reactions using either N-terminal histone peptide or histone tetramer substrates. Finally, KB7-treated cells exhibit hypersensitivity to the DNA damaging agent campthotecin (CPT), reminiscent of *rtt109Δ* mutant cells. Overall, the data presented strongly supports KB7 as an appropriate candidate for further development into a novel anti-fungal drug.

**Materials and Methods**

Protein expression and purification

Recombinant *S. cerevisiae* 6xHis-Rtt109, 6xHis-Vps75 and co-expressed RTT109-VPS75 with a 6xHis tag on either protein were purified as previously described (Tsubota et al., 2007). Recombinant *S. cerevisiae* FLAG-epitope-tagged Asf1N (N-terminal amino acids 1-155) was purified as previously described (Daganzo et al., 2003). Recombinant *Xenopus laevis* Histone H3 and Histone (H3-H4)$_2$ tetramers were purified as previously described (Luger et al., 1999). All proteins were dialyzed into 20 mM Hepes, 7.5, 25 mM NaCl, 1 mM EDTA, 5% glycerol, ultracentrifuged at 100,000 x g for 45 minutes and stored in small aliquots at -80°C.

A construct encoding recombinant 6xHIS-2xFLAG-P300 (nucleotides 1196-1808) was obtained from Dr. Sharon Cantor. The protein was expressed in BL21 *E. coli* cells and purified through Ni-NTA resin (Qiagen) using the manufacteur's instructions. The peak elutions were pooled and dialyzed in 20 mM Hepes, 7.5, 25 mM NaCl, 1 mM EDTA, 5% glycerol and 1 mM PMSF (phenylmethysulfonyl fluoride) and stored in small aliquots at -80°C.

A construct encoding recombinant *S. cerevisiae* 6xHIS-GCN5 (CP921) was obtained from Dr. Craig Peterson (Boyer et al., 2002). BL21 *E. coli* cells transformed with CP921 were cultures at 37°C and diluted back to $O.D._{600nm}$ = 0.01 in 4 x 1L at 18°C overnight. Cells were induced with 0.2 M IPTG between $O.D._{600nm}$ = 0.38-0.5 for 4 hours at 28°C. Four cell pellets were collected and washed with 25 mL 50 mM $NaPO_4$ pH 7.0, 100 mM NaCl, 1 mM benzamidine, 5 mM beta-mercaptoethanol. Gcn5 was precipitated with 70% $NH_4SO_4$ by slowly adding finely ground $NH_4SO_4$ crystals at 4°C while stirring. The solution was centrifuged at 20,000 x g and the pellet was resuspended in 20 mM Hepes pH 7.5, 1 mM EDTA, 10% glycerol, 0.01% NP40. Gcn5 was dialyzed into 20 mM Hepes, 7.5, 1 mM EDTA, 5% glycerol (no salt), ultracentrifuged at 100,000 x g for 45 minutes and stored in small aliquots at -80°C.

Pilot high throughput screen

Detailed description of the protocol is provided in Table 3.1. Briefly, the pilot HTS was conducted with recombinant proteins in a 384-well plate format consisting

## Table 3.1 Protocol for pilot high-throughput screen

**High-throughput HAT ELISA Assay**

Kaufman lab, JLS

1. Pipet **20** µl/well 2x HAT reaction into 384-conical-well polyprolylene plate (Greiner Bio-One, cat. # 781280) from 96-well *ABgene* storage plate.
2. Add **1.0** µl/well small molecule compounds (or DMSO only control) to wells
3. Add **19** µl/well 16.05 µM Acetyl Coenzyme A (or pure water for negative controls) to wells.
4. Cover with top and incubate plate at **30°** for **30** minutes.
5. Transfer **35** µl of reaction into polystyrene 384-flat-well plate (Greiner Bio-One, cat. # 781061)
6. Cover with top and wrap with parafilm to prevent evaporation
7. Place at **4°**, overnight
8. Discard all well contents
9. Add **80** µl/well blocking buffer (1% BSA, 0.05% Tween, TBS)
10. Cover with top and parafilm. Incubate at **4°**, **2** hours
11. Wash all wells 3 times with **80** µl wash buffer (0.05% Tween, TBS)
12. Add **40** µl/well 1° antibody diluted 10,000-fold in wash buffer
13. Cover with top and incubate at **4°**, **2** hours
14. Wash well 3 times with **80** µl wash buffer
15. Add **40** µl/well 2° HRP-labeled anti-rabbit IgG antibody (G. E. Healthcare) diluted 5,000-fold in wash buffer
16. Cover with parafilm and incubate at **4°**, **1** hour
17. Wash well 3 times with **80** µl wash buffer
18. Add **45** µl/well colorimetric reagent and allow to develop for **15** minutes
19. Stop development reaction with **15** µl/well 1M sulfuric acid
20. Read absorbance at 490 nm

Recipes:

| **2x HAT reaction:** | *Per 384-well plate (= 19.2 ml)* |
|---|---|
| • 50 nM Rtt109-Vps75 | *0.022 ml 22 µM Rtt109-Vps75* |
| • 374 nM $[H3\text{-}H4]_2$ | *0.809 ml 5.81 µM $[H3\text{-}H4]_2$* |
| • 0.2% BSA, 100 mM Tris, pH 8 | *3.84 ml 10x buffer* |
| • 2 mM DTT | *0.038 ml 1 M DTT* |

**Blocking Buffer (1% BSA, 0.05% Tween-20, TBS)**

- 5 g Bovine serum albumin
- 250 µl Tween-20
- 50 ml 10 x TBS
- Adjust to 500 ml

**Wash Buffer (0.05% Tween-20, TBS)**

- 500 µl Tween-20
- 100 ml 10 x TBS
- 899.5 ml MilliQ

**Colorimetric Buffer (Phosphate/ Citric acid, pH 5)**

- 196.5 ml 0.5M $Na_2HPO_4$
- 243 ml 0.2M Citric acid
- 560.5 ml MilliQ

**Colorimetric Reagent**

Immediately prior use add to colorimetric buffer

- 1 mg/ ml ImmunoPure OPD (α-Phenylenediamine Dihydrochloride, Pierce, cat. # 34005)

1 µl/ ml $H_2O_2$ 30% (w/w) solution

of 25 nM Rtt109-Vps75 and 178 µM $(H3-H4)_2$ tetramers. The compounds were added at a final concentration of 125 µM, 2% DMSO. The HAT reactions were initiated with 7.5 µM acetyl-coenzyme A (Ac-CoA) (Sigma Aldrich, catalogue # A2056). Inhibition was quantified by ELISA with respect to each plate's positive control (2% DMSO), using a specific anti-serum raised against an H3K56ac peptide ($21^{st}$ Century Biochemicals, Marlboro, MA).

Broad Institute High throughput screen

*High throughput screen*: Using a BioRaptr robot (Beckman), 80 nM Rtt109-Vps75 (or just reaction buffer) and 50 µM screening compound were joined in 1 µl. Reactions were initiated with the addition of 1 µl 120 µM H3n21 peptide, 150 µM Ac-CoA in reaction buffer. The final composition of the HAT reaction is 40 nM Rtt09-Vps75, 60 µM H3n21 peptide, 75 µM Ac-CoA and 25 µM screening compound in 50 mM Hepes 0.0005% Pluronic F-68, pH8.0. The reaction proceeded for 4 hours at RT° in a humid chamber. Released coenzyme A was detected by the addition of 0.5 µl 370 µM ThioGlo1 in PBS, 0.0005% Pluronic pH 7.4, for a final volume of 2.5 µl at 74 µM. After 10 minutes at RT°, plates were read at ex380/em510 on an Envision (Perkin Elmer) plate reader. Each compound was tested twice. Hits were determined as causing >50% inhibition in duplicate. For data points where only a single reading was available, hits were also determined if >50% inhibition was observed.

*Cherry Picks*: From the HTS, 537 hits were cherry picked for re-testing. Only 449 compounds were available. These compounds were tested 2-3 individual times in

8-point 2-fold dose titrations ranging from 20-0.156 µM in 384-well clear bottom black plates. The reactions were prepared by adding 0.1 µl compound to 25 µl 200 nM Rtt109-Vps75 (or just reaction buffer). The enzyme complex and compound were incubated at RT° for 10 minutes. Reactions were initiated with the addition of 25 µl 120 µM H3n21 peptide, 150 µM ac-CoA in reaction buffer. The final composition of the HAT reaction was 100 nM Rtt09-Vps75, 60 µM H3n21 peptide and 75 µM Ac-CoA in 50 mM Hepes 0.0005% Pluronic F-68, pH 8.0. The reaction proceeded for 2 hours at RT°. Released coenzyme A was detected by the addition of 10 µl 4 mM Ellman's Reagent (DTNB) in PBS, 0.0005% Pluronic pH 7.4, for a final volume of 60µl at 0.66 µM. After 10 minutes at RT°, plates were read at absorbance 405 nm on an Envision (Perkin Elmer) plate reader.

*Powders*: Thirty-two compounds were chosen from the cherry pick data to re-test as freshly ordered powders. Twenty-eight of these were chosen based on yielding an IC50 $\leq$ 20 µM and having medicinal chemistry potential. Four additional compounds were chosen based on chemical expertise. The powder re-test was performed similarly to the cherry picks done in duplicate 8-point dose responses. The criterion for powder re-test was IC50 < 10 µM.

HAT-ELISA assay

End-point enzyme assays analyzed by ELISA were performed with 50 nM Rtt109 and 50 nM Vps75 or 400 nM Asf1-N terminus (amino acids1-155) or 15 µg/mL p300. 300 nM $(H3\text{-}H4)_2$ tetramer substrate was provided. Reactions were

initiated with 30 µM Ac-CoA (Sigma Aldrich, catalogue # A2056). Briefly, the protein mix was assembled on ice in 50 mM Tris, pH 8.0, 0.1 mg/ml BSA, 1 mM DTT to a volume of 323.4 µl. 3.3 µL of Dimethylsulfonate (DMSO) or 100x KB7 was added for a final concentration of 1% DMSO in the reactions. The reaction was placed at 30°C for 5 minutes to allow temperature equilibration before initiating with 3.3 µL of 100x (= 3 mM) Ac-CoA. After 30 minutes, the reactions were placed on ice and 100 µL were plated in triplicate on Immulon B 96-well ELISA plates. The plate were stored overnight at 4°C.

Reactions were decanted and non-specific binding by the antibodies was prevented by incubating the wells with 200 µL 1% BSA, 0.05% tween-20, TBS for 1-2 hrs at 4°C. ELISA detection was performed with 100 µL per well of rabbit anti-serum raised against an H3K56ac peptide (21$^{st}$ Century Biochemicals, Marlboro, MA) diluted at 1:5000 in ELISA buffer (0.05% tween-20, TBS) for 1-2 hrs at 4°C. Anti-rabbit HRP-conjugated IgG was used at 1:2500 in ELISA buffer for 100 µL per well for 1 hr at 4°C. Washes before and after antibody incubations were performed 3 x 200 µL per well with ELISA buffer.

HAT- ThioGlo1 assay

Kinetic measurements of HAT reactions were performed using 50 nM co-expressed Rtt109-Vps75, 15 µM Histone H3 N-terminal peptide residues 1-21 (H3n21; 21$^{st}$ Century Biochemicals, Marlboro, MA. Cat# H3 1-21NT) and 30 µM Ac-CoA (Sigma Aldrich), unless otherwise indicated. In place of R-V, 15 µg/mL

p300 or 3.07 µg/mL Gcn5 was used. Reactions were assembled on ice in 20 mM Hepes, pH 7.5, 0.01% NEM-treated BSA (Trievel et al., 2000), 0.01% triton X-100 to a volume of 646.8 µL in glass tubes. 6.6 µL of Dimethylsulfonate (DMSO) or 100x KB7 was added for a final concentration of 1% DMSO. Unless otherwise indicated, the reaction was place at 30°C for 5 minutes to allow temperature equilibration before initiating with 3.3 µL of 100x (=3 mM) Ac-CoA. 120 µL samples were collected at 2, 4, 6, 8 and 10 minutes after initiation, directly added to 120 µL ice cold isopropanol and vortexed. Stopped reaction time-points were stored at -20°C until further use.

The amount of released coenzyme A upon acetylation was quantified at each collected time point as previously described (Trievel et al., 2000) and plotted on Prism GraphPad software. Briefly, released coenzyme A is detected by a maleimide reagent (ThioGlo1; EMD, catalogue #595501) which fluoresces upon binding to the free sulfhydryl exposed on coenzyme A, but not on Ac-CoA. Rates were determined by comparison with standard curves of fluorescence obtained with known amounts of Coenzyme A (CoA; Sigma Aldrich, catalogue #c3144). Two-fold serial dilutions from 6- 0.5 µM CoA were prepared in HAT reaction buffer for each plate, and an equal volume of isopropanol was added. To measure fluorescence, 100 µL per well of the stopped reactions or standards (in duplicate or triplicate, respectively) were plated in FluoTrac200 medium-binding black plates (Greiner, VWR, catalogue # 655076). 100 µL of 30 µM ThiolGlo1 diluted in 1% Triton X-100 was added and mixed by pipetting. The plate was incubated at RT° for 30 minutes in the dark and read at ex384/em513.

To determine mode of inhibition, reaction rates versus substrate concentration were fitted to a non-linear regression curve and analyzed using the Michaelis-Menten equation by Prism GraphPad. Three concentrations of inhibitor were tested per experiment for each substrate, including a 1% DMSO control (no inhibitor). Eight concentrations of substrate were tested per concentration of inhibitor. Due to day-to-day variation in reaction rates, a single representative experiment is shown for each substrate titration. The trends and conclusions between the individual experiments are consistent.

Microtiter broth growth assay

Overnight yeast cultures grown in YPD at 30 °C were diluted to 0.1 $O.D._{600\ nm}$ and allowed to exit lag phase for 2 hrs. *C. albicans* cells were transferred to 37°C after those initial 2 hrs. *C. albicans* cells were allowed to grow for 4- 5 hrs in log-phase then diluted back to 0.04 $O.D._{600\ nm}$. 100µL cells were plated onto 96-well non-tissue culture treated sterile plates in triplicate. The indicated concentrations of camptothecin diluted in 1.5 N NaOH (or the equivalent amount of NaOH without drug) and KB7 diluted in DMSO (or 1 % DMSO alone) were added to a final volume of 200 µL per well. The plates were incubated at 37°C in a temperature-controlled spectrometer (Synergy HT, Bio-Tek) and $O.D._{595\ nm}$ was measured every 30 minutes for 19 hrs. Growth rates were calculated using KC4 data analysis software (Bio-Tek).

**RESULTS**

**Pilot high-throughput screen for Rtt109 inhibitors**

In order to test the feasibility of finding Rtt109 inhibitors using an *in vitro* histone acetyl-transferase (HAT) assay, I developed a pilot high-throughput screen (HTS) to query the 30,000-compound library at the Small Molecule Facility, UMass Medical School (Worcester, MA). The compounds were queried at 125 µM against the Rtt109-Vps75 (R-V) complex. Levels of acetylated H3K56 (H3K65ac) on $(H3\text{-}H4)_2$ tetramers after an end-point HAT assay were detected by ELISA using a specific anti-H3K56ac anti-serum. The pilot screen averaged a z-factor score of 0.9 per plate and had an initial hit rate of 0.52% with a cutoff of 75% inhibition. Ninety-three primary candidates were repurchased for manual testing. Of these, 8 exhibited ≥ 75% inhibition at 25 µM using a fluorescent detection reagent (ThioGlo1) that quantitatively detects the free sulfhydryl of the coenzyme A released during the acetyl-transferase reaction.

From this pilot screen, the most potent of these eight candidate compounds, termed iPK38, displayed a 50% inhibitory concentration (IC50) value of 4.5 µM and displayed noncompetitive inhibition with respect to both histone H3n21 peptide and Ac-CoA substrates (data not shown). However, iPK38 proved to be inhibitory towards all categories of enzymes tested, including restriction endonucleases (data not shown). Since iPK38 has the same chemical backbone (quinoxaline) as half of the potent inhibitors obtained in this pilot screen, and other potent inhibitors with different chemical backbones were also non-specific, I concluded that a more

sophisticated library needed to be queried to find specific inhibitors of Rtt109 at low micromolar range.

**High-throughput screen conducted at the Broad Institute**

In collaboration with the Chemical Biology Platform at the Broad Institute (Cambridge, MA), we screened 363,843 small molecules at 25 μM for inhibitors of Rtt109 catalysis in end-point HAT assays. The pilot HTS developed in our laboratory using the ThioGlo1-based fluorescent detection of the free sulfhydryl group on released coenzyme A was adapted at the Broad Institute to a 1536-well plate format. The HTS was performed in duplicate, and 224 out of 333,734 compounds yielded > 50% inhibition (0.07% hit rate). For those compounds where only a single measurement was available, 313 out of 30,109 yielded > 50% inhibition (1% hit rate). Of these initial hits, 449 compounds were readily available for re-testing in 8-point 2-fold dose titration. In this case, the free sulfhydryl groups of released CoA were detected using Ellman's reagent (DTNB), via optical absorbance. Using Ellman's reagent should therefore control for non-specific fluorescence quenchers obtained in the initial screen. We observed that 83 compounds produced a dose-dependent response with an estimated IC50 ≤ 20 μM. Thirty-two of these compounds were chosen to re-test as freshly ordered powders based on their medicinal chemistry potential. Again, these compounds were tested in 8-point 2-fold dose response curves. Nine of these compounds exhibited IC50 values below 10 μM. These nine

compounds were sent to our laboratory for further characterization and inhibition kinetics studies.

**KB7 is a specific inhibitor to Rtt109 catalysis**

To test the specificity of the 9 most potent inhibitor candidates, I performed enzyme inhibition kinetic assays comparing Rtt109-Vps75 and p300 in the presence of 0.5 – 2 μM compound (Table 3.2). Only a single chemical, KB7 (Kaufman-Broad #7) inhibited Rtt109 without inhibiting p300. Two compounds (KB5 and KB9) appeared to inhibit the maleimide detection reaction based on no increase of fluorescence with time and similar low ex384/em513 raw values across all 4 experimental conditions lower than protein background. KB7 specifically decreased R-V reaction rates by 80, 77, 87% with 2, 1, 0.5 μM, respectively, compared to 47, > 0, > 0% for p300 rates. KB7 has the following chemical formula $C_{22}H_{23}ClFN_3O_3$ and structure as depicted in Figure 3.1A. **(**IUPAC name N-[(2-chloro-6-fluorophenyl)methyl]-2-(2, 5-dioxo-4-phenyl-4-propylimidazolidin-1-yl)-N-methylacetamide).

To assess an IC50 value for R-V reaction rate, I performed HAT reactions with varying concentrations of KB7 and determined rates during the initial linear phase of the reaction. Each reaction rate was calculated via linear regression of product formed versus time (mean $R^2 = 0.91$, ranging from 0.77-0.99). Non-linear fit of each reaction velocity plotted against KB7 concentration on a semi-log scale

**Table 3.2 Initial assessment of chemical inhibitor (IC50 < 10 µM in end-point assay) from HTS conducted at the Broad Institute.** Percent reaction rates are reported as normalized to 1% DMSO (no inhibitor) reactions performed in parallel. ** Compounds believed to quench the ThioGlo1 detection reaction making these results inconclusive.

| Kaufman-Broad compound | concentration (µM) | % inhibition Rtt109-Vps75 | % inhibition p300 |
|---|---|---|---|
| 1 | 3 | 16 | 59 |
| 2 | 0.5 | 78 | 97 |
| | 2 | 100 | 99 |
| 3 | 4 | 0 | 36 |
| 4 | 4 | 50 | 73 |
| 5** | 2 | 97 | 100 |
| 6 | 2 | 46 | 91 |
| 7 | 0.5 | 87 | > 0 |
| | 1 | 77 | > 0 |
| | 2 | 80 | 47 |
| 8 | 2 | 47 | 90 |
| 9** | 2 | 97 | 100 |

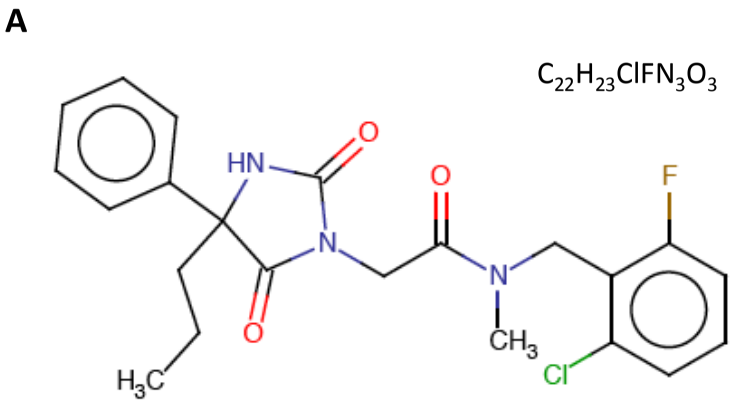


**Figure 3.1. KB7 is a specific inhibitor of Rtt109 HAT catalysis.** (**A**) Chemical structure of KB7. (**B**) KB7 IC50 curve for R-V catalysis. HAT reactions with 50 nM Rtt109-Vps75, 15 µM H3n21 peptide, the indicated concentrations of KB7 and 30 µM Ac-CoA at 30°C. Percent activity of reaction rates were quantified to no inhibitor control reactions and fit onto non-linear regression. IC50 = 56.19 nM, $R^2$ = 0.94. (**C**) HAT percent activity of p300 (15 µg/ml) and Gcn5 (3.1 µg/ml) at the indicated KB7 concentrations were performed as described above.

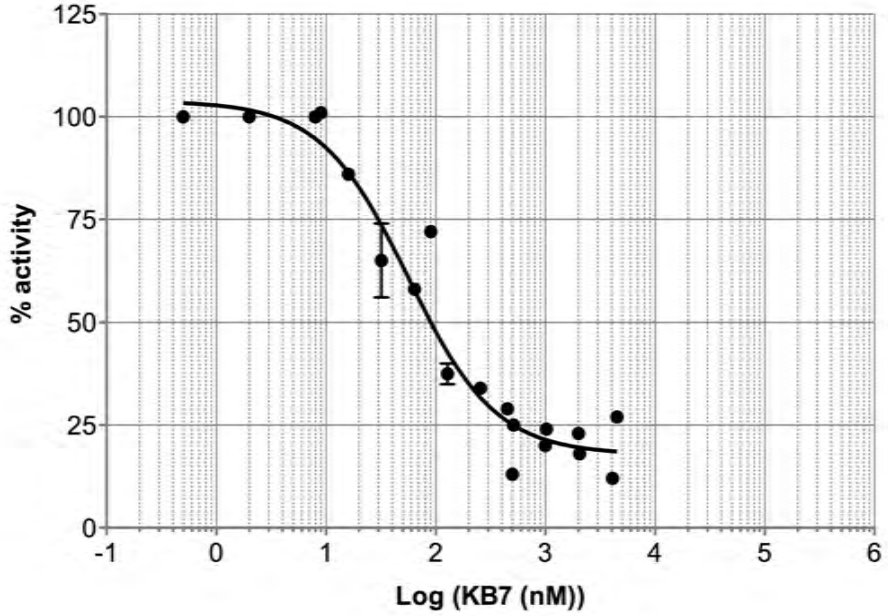


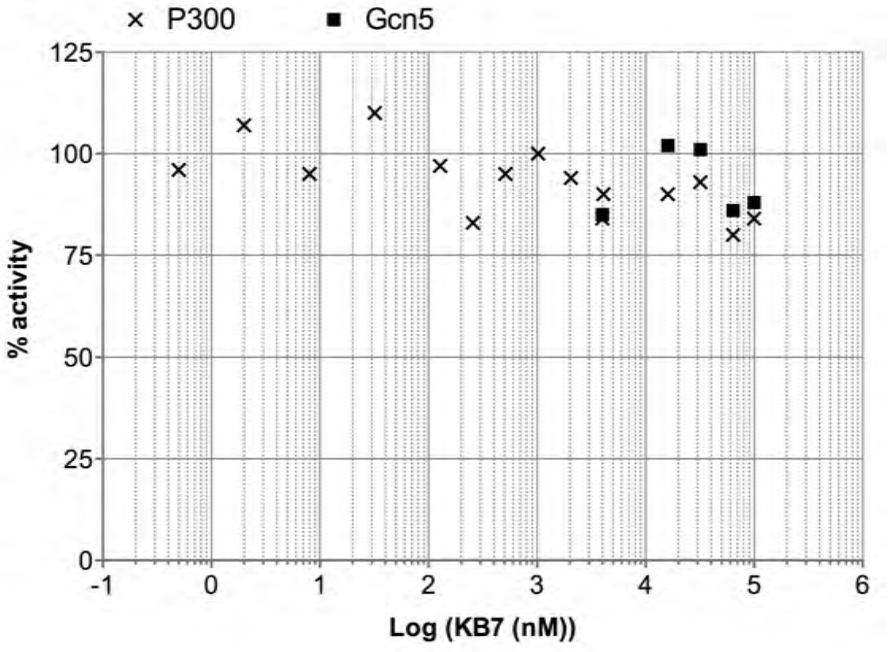

indicates an IC50 of 56.19 nM (1.28 nM SEM; 95% CI 33.25- 94.94 nM) and Hill slope coefficient of -1.09 (0.28 SEM) ($R^2 = 0.94$) (Figure 3.1B).

IC50 values could not be calculated for KB7 inhibition of p300 and Gcn5 enzyme activity. As above, each reaction rate was determined via linear regression of product formed versus time (p300 mean $R^2 = 0.98$, ranging from 0.97-0.99; Gcn5 mean $R^2 = 0.97$, ranging from 0.94-0.99). High concentrations of KB7 (up to 100 μM) did not reduce enzyme reaction rates below 80% activity, with no apparent trend as KB7 concentration was increased (Figure 3.1C). Due to solubility limitations, KB7 was not tested above 100 μM. It is, therefore, possible that stronger inhibition can occur at higher concentrations.

**KB7 inhibits Rtt109 H3K56 acetylation mediated by both Vps75 and Asf1 on $(H3\text{-}H4)_2$ tetramers**

*In vivo*, Rtt109-Vps75 (R-V) acetylates three H3 tail residues (K9, K23, and K27) (Berndsen et al., 2008; Burgess et al., 2010; Fillingham et al., 2008). Only Rtt109 associated with Asf1 (R-A) acetylates H3K56 to promote genome stability (Adkins et al., 2007; Driscoll et al., 2007; Han et al., 2007a; Han et al., 2007b; Recht et al., 2006; Schneider et al., 2006). Vps75's contribution to H3K56ac *in vivo* is undetectable (Han et al., 2007c; Tsubota et al., 2007). However, *in vitro*, R-V very efficiently acetylates H3K56 (Tang et al., 2011; Tsubota et al., 2007). The R-V complex has a catalytic efficiency (Kcat/Km) 20-fold greater than R-A mediated catalysis *in vitro* (Tsubota et al., 2007) and Rtt109 has strong affinity towards Vps75

(Kd = ~10-23 nM; (Albaugh et al., 2010; Berndsen et al., 2008) allowing easy co-expression and purification. Therefore, we chose to perform the HTS and enzyme inhibition studies using R-V. However, point mutation data from structural studies suggest that amino acid residues important for catalysis of R-V do not affect R-A (Tang et al., 2011). To determine whether KB7 also inhibits R-A mediated catalysis, I performed end-point HAT assays using $(H3\text{-}H4)_2$ tetramers as the substrates. I then probed the histones for H3K56ac by ELISA using a specific anti-H3K56ac antibody. In this manner, inhibition of R-V and R-A catalysis were comparable at 87% and 83%, respectively (Figure 3.2A). Importantly, this data also shows that acetylation of the core histone target (H3K56) is specifically inhibited by KB7, a conclusion that we could not make using the histone H3n21 peptide substrate and ThioGlo1 detection assay.

Additionally, using the same end-point HAT-ELISA reaction with p300, I confirmed that p300 activity on histone substrates is not affected by KB7 for acetylation of H4 N-terminal residues (Figure 3.2B). This was another conclusion that could not be made using the peptide substrate, as P300 also acetylates non-histone proteins (Ogryzko et al., 1996).

**KB7 is a noncompetitive inhibitor regarding histone and Ac-CoA substrates**

To determine the mechanism of inhibition of KB7, I performed enzyme kinetic studies by titrating Ac-CoA or H3n21 peptide in the presence of varying concentrations of the inhibitor. For each substrate, three independent experiments

**Figure 3. 2. KB7 specifically inhibits H3K56 acetylation by both Rtt109-Vps75 and Rtt109-Asf1.** (**A**) Acetylation of H3K56 is inhibited by KB7. End-point HAT reactions were performed with 50 nM Rtt109, 300 µM $(H3\text{-}H4)_2$ tetramers, 50 nM Vps75 or 400 nM Asf1N(1-155), with DMSO (vehicle) or 500 nM KB7. Reactions were initiated with 15 µM acetyl coEnzyme A at 30°C for 30 minutes. Acetylated H3K56 was detected by ELISA. n = 2 (**B**) HAT activity of P300 is not inhibited by KB7. End-point reactions were performed with 15 µg/ml P300 as described in **A.** Acetylated histone H4 was detected by ELISA. n = 2.

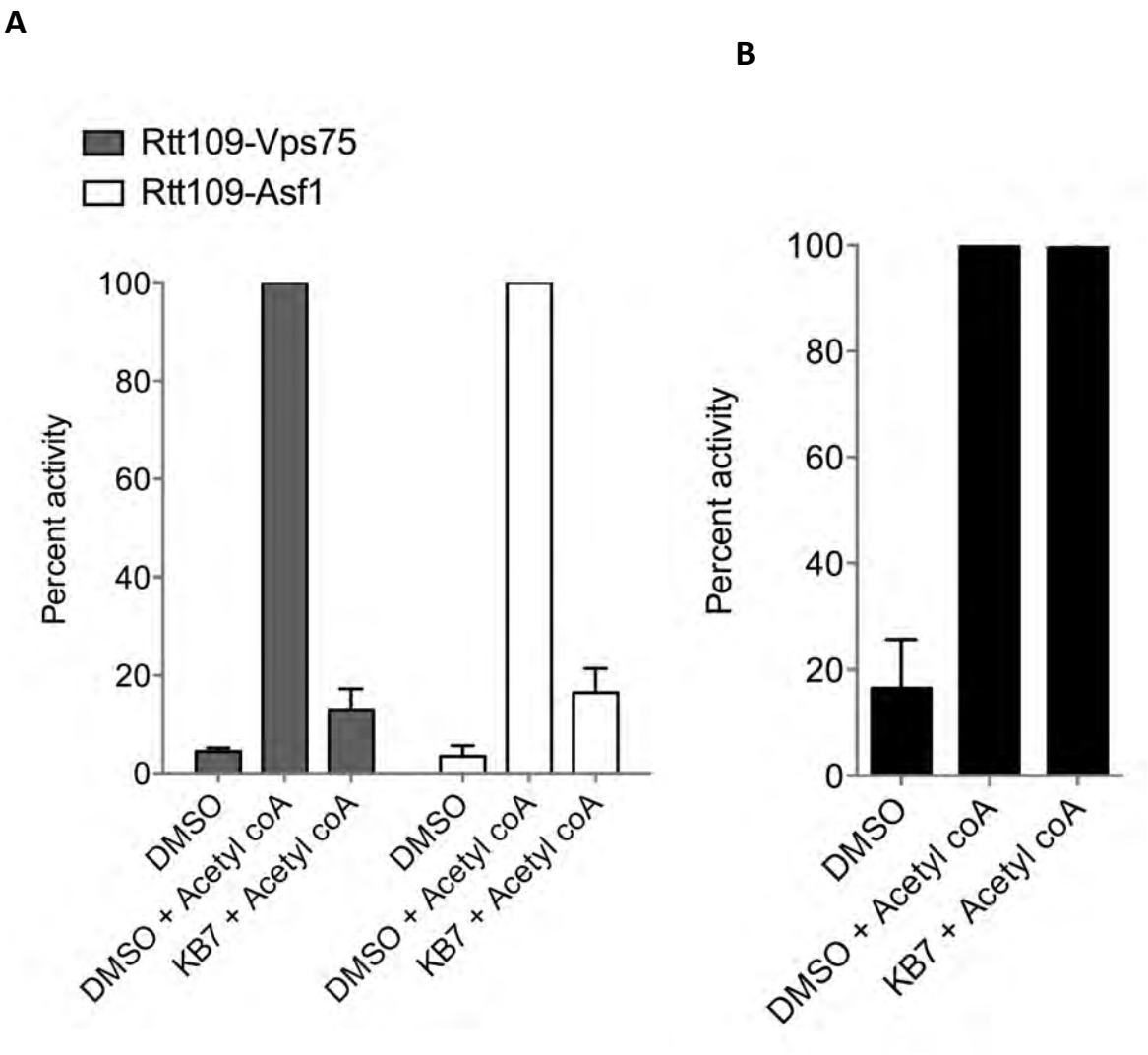

were performed where titration curves with no inhibitor were compared to two concentrations of KB7. A single representative experiment for each substrate is presented due to day-to-day alterations in net velocity. However, trends and conclusions are consistent.

H3n21 peptide was titrated from 0.5- 60 μM in the presence of 0, 40 and 80 nM KB7. Reaction rates (average linear regression $R^2 = 0.89$) were plotted and fit to the Michaelis-Menten equation (Figure 3.3A). Increasing amounts of KB7 reduced Vmax (0 μM KB7, 11.96 pmoles/ min; 40 μM KB7, 5.624 pmoles/ min; 80 μM KB7, 3.852 pmoles/ min). Km was not consistently affected. Graphing the data using the Lineweaver-Burk (double reciprocal) plot yielded more detailed information (Figure 3.3B). Indeed, KB7 decreases Vmax; Linear-regression of the data results in decreasing values of V for the y-intercept as KB7 concentration increases. The value for Km does not significantly change as the lines converge in the third quadrant. This result indicates that $K_{is} > K_{ii}$, (where $K_{is} = K_d$ for free enzyme-inhibitor and $K_{ii} = K_d$ for substrate-bound enzyme- inhibitor) (Purich and Allison, 2000), meaning the dissociation constant for Rtt109 and KB7 is greater than the dissociation constant for Rtt109-H3n21 and KB7. This result suggests that KB7 exhibits mixed inhibition, a type of noncompetitive inhibition where KB7 has greater affinity for the Rtt109-H3n21 intermediate than for free Rtt109. In conclusion, both non-linear regression and double reciprocal linear plots agree that KB7 is acting noncompetitively towards the H3n21 substrate. These results signify that the inhibitor is not competing for the binding site of H3.

**Figure 3.3. KB7 exhibits noncompetitive inhibition towards H3n21 peptide.** (**A**) HAT reaction kinetics with 50 nM Rtt109-Vps75, 30 µM Ac-CoA and the indicated concentrations of KB7 were monitored for the indicated concentrations of H3n21 peptide at 30°C. Non-linear curve fits indicate Vmax =11.96, 5.624, 3.852, Km= 9.708, 6.359, 4.945 and $R^2$ = 0.9916, 0.9699, 0.9140 for reactions with 0 (DMSO), 40 and 80 nM KB7, respectively. (**B**) Data from **A** is fitted to the Lineweaver- Burk equation. $R^2$ = 0.9923, 0.7987, 0.9200 for reactions with 0 (DMSO), 40 and 80 nM KB7, respectively.

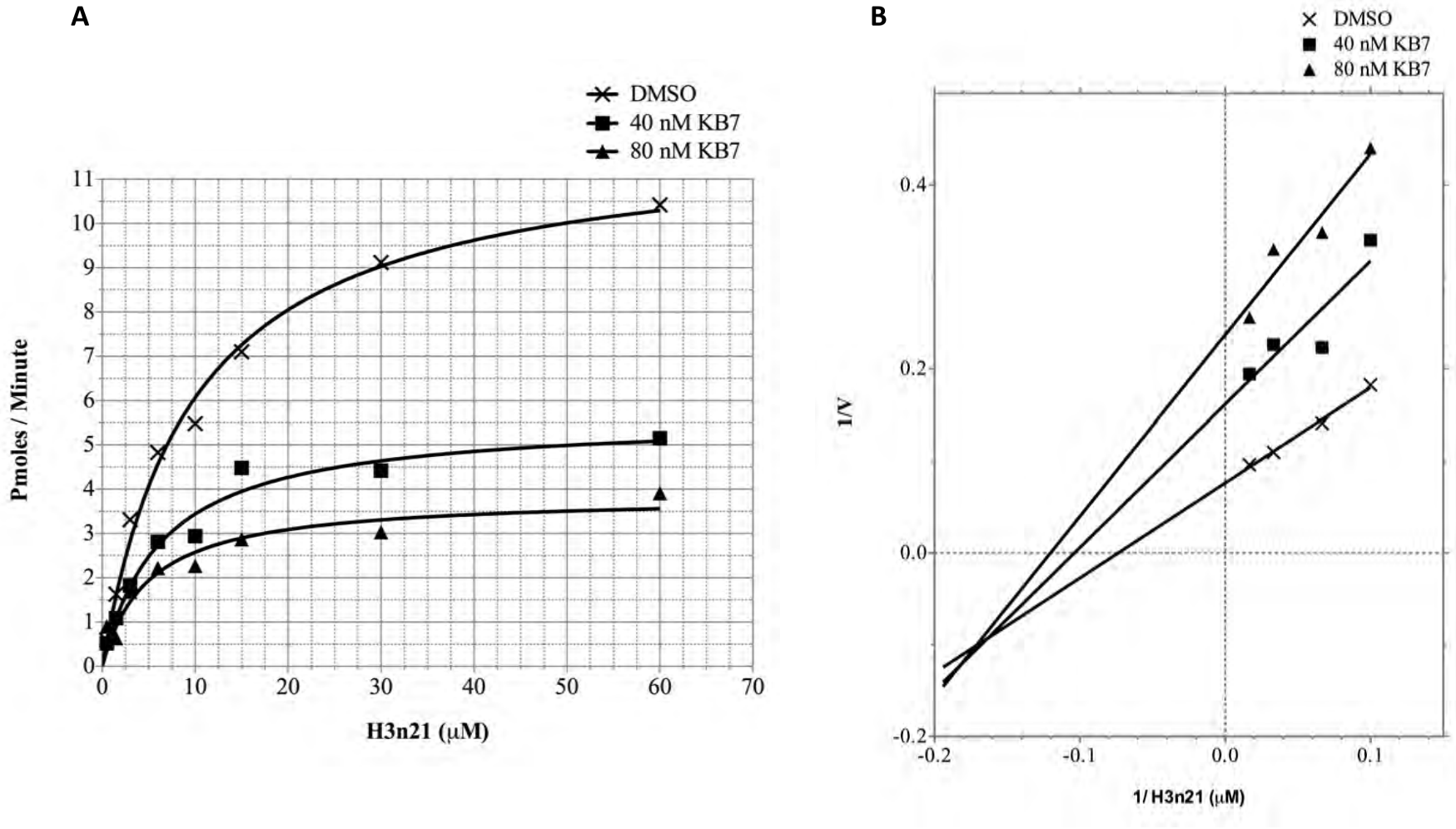

Ac-CoA was titrated in the same fashion from 0.5-10 μM at various concentrations of KB7. Reaction rates (average linear regression $R^2 = 0.95$) were plotted and fit to the Michaelis-Menten equation (Figure 3.4A). KB7 reduced both Vmax (0 μM KB7, 8.122 pmoles/ min; 30 μM KB7, 4.319 pmoles/ min; 60 μM KB7, 2.045 pmoles/ min) and Km (0 μM KB7, 1.607 μM; 30 μM KB7, 0.7726 μM; 60 μM KB7, 0.5994 μM). In a double reciprocal plot, the lines are parallel and do not converge at any point (Figure 3.4B), consistent with the change of both Vmax and Km. These data indicate a specific type of noncompetitive inhibition termed uncompetitive inhibition. Uncompetitive inhibition requires that the enzyme be bound to the substrate in question to accommodate the inhibitor. This conclusion would imply that Rtt109 must be bound to Ac-CoA (with or without H3n21 peptide) in order for KB7 to bind, suggesting that a conformational change may occur upon Ac-CoA binding.

### *In vivo* effects of KB7

The phenotype of yeast cells incapable of acetylating H3K56 either due to loss of functional Rtt109 or point mutations of H3K56 is hypersensitivity to genotoxic agents (Driscoll et al., 2007; Garcia et al., 2007; Hyland et al., 2005; Lopes da Rosa et al., 2010; Xhemalce et al., 2007). To determine if KB7 causes hypersensitivity to DNA damaging agents, growth rates of *C. albicans* cells exposed to 50 and 100 μM KB7 with or without the addition of 100 μM camptothecin (CPT) were monitored. CPT is a topoisomerase I poison that leads to double strand DNA

**Figure 3.4. KB7 exhibits uncompetitive inhibition towards Ac-CoA.** (**A**) HAT reaction kinetics with 50 nM Rtt109-Vps75, 15 μM H3n21 peptide and the indicated concentrations of KB7 were monitored for the indicated concentrations of Ac-CoA at 30°C. Non-linear curve fits indicate Vmax = 7.351, 3.934, 1.819, Km= 1.308, 0.6013, 0.4134 and $R^2$ = 0.9379, 0.8523, 0.6728 for reactions with 0 (DMSO), 30 and 60 nM KB7, respectively. (**B**) Data from **A** is fitted to the Lineweaver- Burk equation. $R^2$ = 0.9688, 0.9785, 0.5889 for reactions with 0 (DMSO), 30 and 60 nM KB7, respectively.

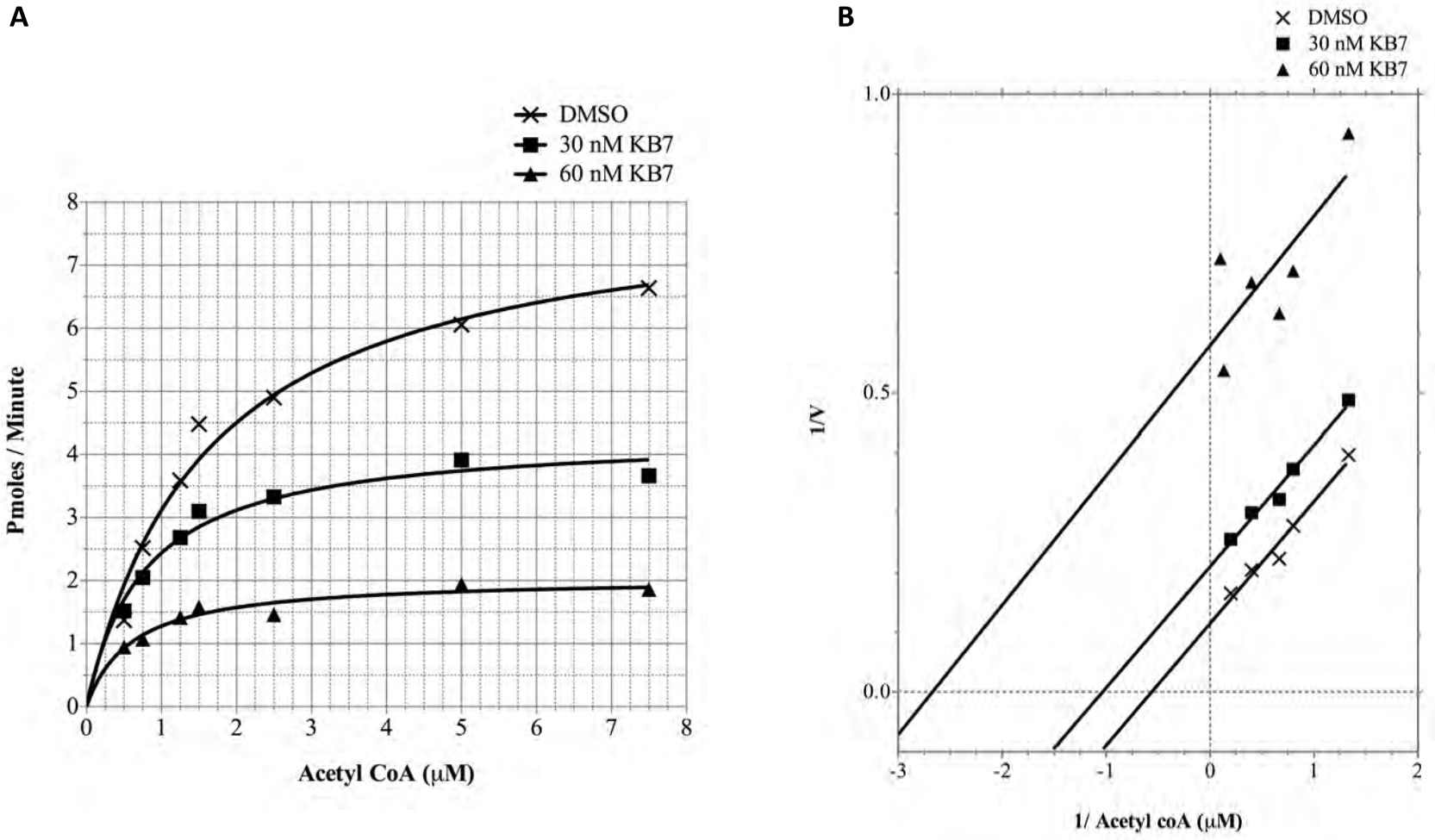

breaks. Wild-type *C. albicans* cells are extremely resilient to this dose of CPT, but *rtt109*$^{-/-}$ cells are sensitive even at 5 μM CPT (Figure 3.5A). We anticipated difficulties in introducing KB7 inside *C. albicans* because of its wide usage of cell membrane efflux pumps to rid itself of toxins. Therefore, we obtained and tested various efflux pump mutants from Dr. Dominique Sanglard that have reduced anti-fungal drug resistance (Ramage, 2002). As shown in Figure 3.5A, *cdr1*$^{-/-}$, *cdr2*$^{-/-}$ (DSY654; (Ramage, 2002)) mutants are already more sensitive to CPT compared to wild-type, suggesting that a mode of resistance to this DNA-damaging drug involves efflux pumps to rid the cells of the toxin. The CDR1, CDR2 genes encode ATP-binding cassette (ABC) pumps that transport multiple drugs across the cellular membrane, specifically promoting azole drug resistance. More interestingly, the presence of KB7 causes a significant synergistic decrease in growth rate in *cdr1*$^{-/-}$, *cdr2*$^{-/-}$ (DSY654; (Ramage, 2002)) mutants (p-values $\leq 0.05$). As expected, KB7 had no effect on rtt109$^{-/-}$ cells and as suspected, no growth defect was detected in wild-type cells (Figure 3.5A).

*rtt109*$^{-/-}$ *C. albicans* cells have a moderate decrease in growth rate (30% decrease in doubling time compared to wild-type; Figure 2.1E; (Lopes da Rosa et al., 2010)). *cdr1*$^{-/-}$, *cdr2*$^{-/-}$ (DSY654; (Ramage, 2002)) cells exhibit clear growth defects on YPD plates embedded with 100 μM KB7 (Figure 3.5B). However, a synergistic effect with embedded 50 μM CPT is not noticeable. This could either be due to the severity of KB7's effect alone or to 50 μM CPT being too low a concentration to cause sufficient DNA damage to this otherwise wild-type cell. Parallel treatment of

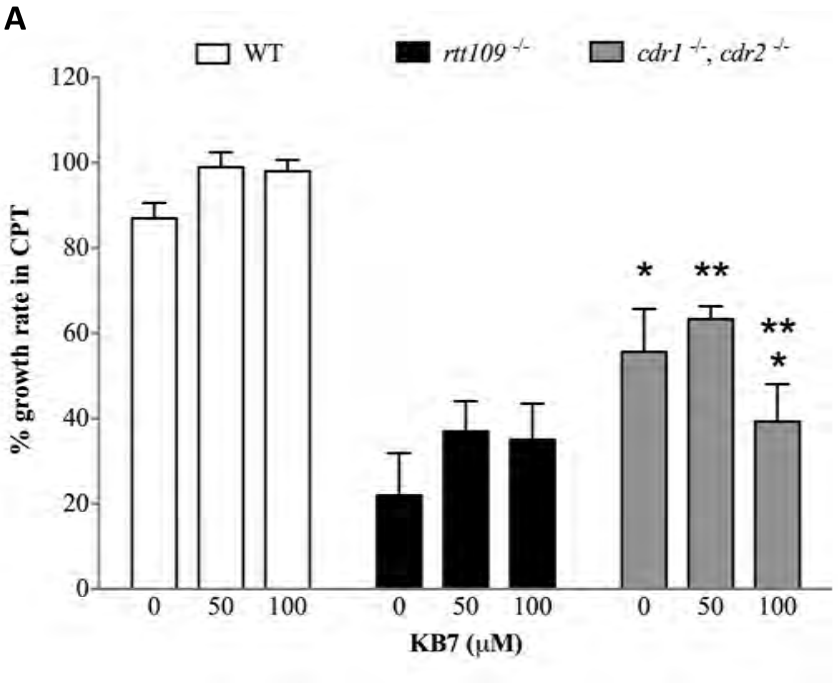


**Figure 3. 5. Cellular effects of KB7.** (**A**) Growth rate of the indicated *C. albicans* strains were monitored by $O.D._{595\ nM}$ for 19 hrs in a microbroth assay at 37°C. Cells were cultured in YPD ± 100 μM CPT (or 5 μM CPT for *rtt109*$^{-/-}$). Average percent growth rate is reported in reference to conditions in vehicle without CPT. (n=3) (p-values * 0.0399, ** 0.0157) (**B**) Spot-assay of 1:5 serial dilutions of the indicated *C. albicans* strains on the indicated YPD plates overnight at 30°C.

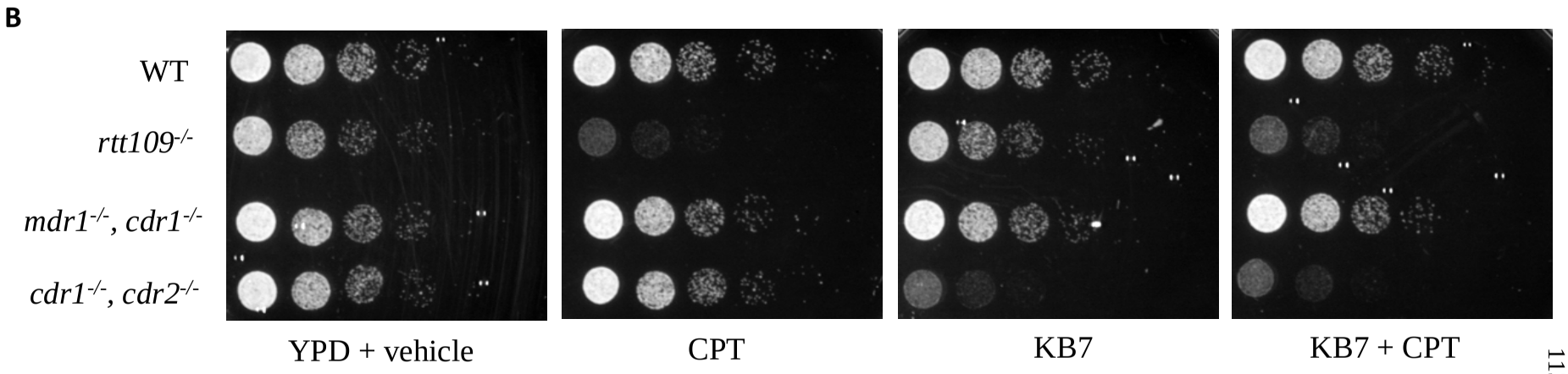

*mdr1*$^{-/-}$, *cdr1*$^{-/-}$ (DSY468; (Ramage, 2002)) cells did not exhibit a growth defect. In addition, *cdr2*$^{-/-}$ (DSY653; (Ramage, 2002)) cells were tested in the microtiter broth assay and showed no phenotype (data not shown). Overall, this suggests that only upon deletion of both CDR genes is efflux action attenuated enough to allow intracellular accumulation of KB7 for an observable phenotype (Figure 3.5B).

**DISCUSSION**

Through a high-throughput screen in collaboration with the Broad Institute, I have identified a specific Rtt109 inhibitor, termed KB7. KB7 inhibits Rtt109 with an apparent IC50 of ~56 nM and is extremely specific to Rtt109 (Figures 3.1 and 3.2). I did not observe significant inhibition of other HATs such as P300 and Gcn5 even at KB7 concentrations of up 100 uM (Figure 3.1C and 3.2B), suggesting that there is at least two orders of magnitude of specificity for Rtt109. Importantly, KB7 inhibits H3K56 acetylation by Rtt109 activated by either Vps75 or Asf1 (Figure 3.2A). H3K56ac is the physiologically relevant PTM for genome stability and efficient pathogenicity of yeast in the face of DNA damage. Since structural studies suggest that Vps75 and Asf1 utilize distinct regions of Rtt109 (Tang et al., 2011), I am confident that KB7 does not simply block interaction between rtt109 and the histone chaperone, but in fact prevents catalysis. Furthermore, the ability of KB7 to inhibit R-V mediated catalysis on H3n21 peptides, representing the N-terminal tail residue H3K9, and H3K56 on full-length histone H3 indicates that positioning of the histone by Vps75 is not restrictive to PTM sites. It supports the conclusion put forth by others

that Asf1 is indeed restrictive in PTM site presentation to Rtt109 for catalysis, allowing only H3K56 acetylation to occur (Lin and Yuan, 2008).

The NIH PubChem database shows that KB7 has been tested in 348 bioassays, but has only been active in one. In that case, 25 μM of KB7 reduced binding of an H4K20 tri-methylated peptide to a jumonji domain (PubChem CID 4785700). Since KB7 concentration was 3 orders of magnitude above the interacting components, a possible conclusion for this result is sequestration of peptide or protein. In our case, KB7 is efficient at nanomolar range, equivalent to Rtt109 concentration, when the substrates are at micromolar range. It is unlikely that sequestration of substrates is occurring.

The inhibition mechanism of KB7 is complex. KB7 decreases the Vmax with respect to both Ac-CoA and H3n21 substrates, indicating that the substrates do not compete with the inhibitor to prevent inhibition (Figure 3.3 and 3.4). The inhibitor is therefore noncompetitive with respect to both substrates and most likely binds allosterically on Rtt109 to prevent catalysis without affecting either substrate (or chaperone) interaction. In more detail, KB7 lowers the Km for Ac-CoA, a behavior characteristic of uncompetitive inhibition (Figure 3.4). As an uncompetitive inhibitor towards Ac-CoA, KB7 can only bind the Rtt109-Ac-CoA intermediate, regardless of the presence of the histone peptide. With regards to the histone substrate, KB7 behaves as a mixed inhibitor (Figure 3.3). KB7 may bind to free Rtt109 or Rtt109-H3 intermediate. However, the double reciprocal plot indicates that $K_{is} > K_{ii}$ , signifying that KB7 has a greater affinity for the Rtt109- H3 intermediate over free Rtt109.

Unifying the two inhibitory mechanisms, one can imagine a model where KB7 preferentially binds to the Rtt109-Ac-CoA- H3n21 ternary intermediate complex. KB7 may also bind to Rtt109-Ac-CoA with less affinity. This model is consistent with data showing that Rtt109 utilizes a random-ordered, sequential mechanism where either substrate can bind Rtt109 in random order to form a ternary complex prior to any catalytic steps (Albaugh et al., 2010).

The goal in finding Rtt109 inhibitors is to provide a lead compound for medicinal chemistry alterations leading to a novel anti-fungal drug. During the course of an infection, pathogenic fungi are subjected to the DNA damaging effects of ROS by phagocytic cells. For *C. albicans*, Rtt109 is essential to survive ROS-mediated DNA damage by macrophages (Figure 2.3E; (Lopes da Rosa et al., 2010)). Most significantly, *rtt109* $^{-/-}$ *C. albicans* cells are avirulent in systemic candidiasis (Figure 2.3A and 2.3B; (Lopes da Rosa et al., 2010; Wurtele et al., 2010)), a bloodborne infection that leads to 49% mortality in humans (Gudlaugsson et al., 2003). On cells, KB7 causes synergistic growth rate defect with the DNA damaging agent CPT, albeit, only in the efflux pump mutant *cdr1*$^{-/-}$, *cdr2* $^{-/-}$ (DSY654; (Ramage, 2002)) (Figure 3.5). However, this data is promising in indicating that Rtt109-mediated DNA damage resistance is compromised by KB7 and would therefore affect pathogenicity. Overall, this initial characterization of KB7 demonstrates outstanding possibilities for further development towards a novel anti-fungal agent. Future studies addressing structural activity relationships (SAR) will focus on improving permeability and retainment of the drug, in order to improve its effective intracellular potential.

# CHAPTER 4

## Concluding Remarks

*Purpose and outcome*

The contributions of chromatin to fungal pathogenesis are just beginning to be elucidated. It is evident from the studies previously discussed that repair of chromatin, transcriptional activation, and manipulation of genome plasticity all promote fungal pathogenicity. In particular, this dissertation focused on a fungal specific chromatin-modifying enzyme that promotes survival from DNA damage and genome stability. The first aim was to establish whether the function of this unique enzyme has biological relevance on pathogenicity. Second, the goal was to determine if this pathway could be exploited for development of novel anti-fungal drugs.

By deleting both alleles of *RTT109* in C. *albicans*, I showed that this particular histone acetyltransferase plays an important role in resistance to genotoxic stress during the course of an infection. This genetic deletion resulted in 100% survival of mice intravenously infected with *rtt109*$^{-/-}$ *C. albicans* cells 20 days post infection, compared to 0% survival in mice infected with wild-type cells by 7 days post infection (Figure 2.3B). Specifically, my data supports that the genotoxic stress caused by reactive oxygen species released from macrophages are detrimental to fungal cells unable to acetylate H3K56 (Figure 2.3E). The connection between H3K56ac and hypersensitivity to DNA damage had already been made in budding and fission yeast (Driscoll et al., 2007; Han et al., 2007a; Masumoto et al., 2005;

Recht et al., 2006; Xhemalce et al., 2007). The data in this dissertation were the first to demonstrate a similar role in a pathogenic fungus and it's implication in pathogenesis (Chapter 2).

Having established a role for Rtt109 and H3K56 acetylation in fungal pathogenesis, I switched my focus to identifying small molecule inhibitors of Rtt109 catalysis. I employed a biochemical enzymatic-based high throughput screen. Out of ~300,000 compounds, I identified a single chemical with inhibitory activity in the nanomolar range and specificity to Rtt109 (chapter 3). This chemical, KB7 reduces Rtt109 catalytic rate by 50% with just ~56 nM (Figure 3.1B). No significant effect was detected on p300 or Gcn5 catalysis at concentrations up to 3 orders of magnitude greater (Figure 3.1C and 3.2B). KB7 inhibits catalysis mediated by the physiologically relevant Rtt109-Asf1 reaction, acetylation of H3K56 on full-length histones and not just N-terminal tail modification mediated by Rtt109-Vps75 complexes (Figure 3.2A). As a consequence, cells treated with KB7 exhibit significant reduction in growth rate in the presence of the DNA damaging agent, camptothecin (Figure 3.5A). The characterization of KB7 as an Rtt109 inhibitor is relatively preliminary in the scope of developing a novel anti-fungal agent. Nonetheless, this dissertation describes the first Rtt109 inhibitor, as thus far attempts to inhibit Rtt109 with other known HAT inhibitors have failed (Bowers et al., 2010; Tang et al., 2008). The specificity of this inhibitor, its potency and intracellular effectiveness make KB7 an outstanding lead compound to directly have come out of a chemical library from a high throughput screen.

*Implications*

It is evident that H3K56 acetylation is crucial for systemic candidiasis, but it is unlikely to be important at other sites of infection, specifically those without activated phagocytes. Circulating monocytes need to be activated by the adaptive immune system to differentiate into non-circulating resident macrophages. This means that in order to take advantage of an Rtt109 defect, the host immune system must be functional. Because a large demographic of people affected by opportunistic candidiasis infections are immuno-compromised, this limitation could be problematic. One way to circumvent this limitation is by combinatorial drug treatment. As shown in chapter 2, *rtt109* $^{-/-}$ cells are sensitive to 5-flucytosine (5-FC), a nucleotide analogue that disrupts the pyrimidine salvage pathway and leads to genotoxic stress (Hope et al., 2004). 5-FC is already a clinically used drug used against *C. albicans*, however with caution due to a ~7-8% incidence of drug resistance (Vermes et al., 2000). As such, 5-FC is recommended primarily for treatment of systemic candidiasis in combination with an additional anti-fungal drug (Vermes et al., 2000). In addition, *rtt109*$^{-/-}$ *C. albicans* cells are sensitive to some but not all classes of clinically approved anti-fungal drugs. *rtt109* $^{-/-}$ cells are sensitive to echinocandins (caspofungin and micafungin) (Wurtele et al., 2010) which interfere with cell wall b-glucan synthesis. However, *rtt109*$^{-/-}$ mutants are not sensitive to azoles (fluconazole) and polyenes (amphothericin B) (Lopes da Rosa et al., 2010), both of which affect cell membrane integrity (Mishra et al., 2007).

An interesting line of research that has not been fully explored is not just the role of chromatin, but in general the role of DNA repair pathways in pathogens that promote pathogenesis. In *C. albicans*, Chauhan, et al. demonstrated that mutants unable to repair DNA through homologous recombination (*rad52*$^{-/-}$) or non-homologuos end-joining (*lig4*$^{-/-}$) are avirulent (Chauhan et al., 2005). However, the authors' emphasis was the role of these DNA repair pathways in generating genetic diversity, not survival from genotoxic stress. No subsequent follow-up studies were undertaken on the aspect of DNA damage and repair. In the field of *Mycobacterium tuberculosis*, DNA repair pathways as it pertains to pathogenesis is intensely being studied, as this bacterium lives inside macrophages and must therefore deal with DNA damage (Reviewed in (Dos Vultos et al., 2009; Gorna et al., 2010; Kurthkoti and Varshney, 2011)). It is accepted that DNA repair is vital to its pathogenesis. However, unlike *M. tuberculosis*, *C. albicans* is an extracellular pathogen. In fact, *C. albicans* colonizes mucosal lining, forms biofilms and damages tissue. However, when *C. albicans* cells are engulfed by macrophages, they readily escape a detrimental fate by filamenting and bursting out of the phagocyte (Lorenz et al., 2004). Despite this difference, it is evident that from the data reported in this dissertation and from other work by Chauhan, et al. and Wurtele, et al. that hypersensitivity to DNA damage is detrimental to *C. albicans* pathogenicity (Chauhan et al., 2005; Wurtele et al., 2010).

*Future directions*

The discovery of a specific Rtt109 inhibitor is exciting in light of the biological consequences towards pathogenicity. However, the inability of KB7 to efficiently cross the cellular membrane of *C. albicans* is challenging. The immediate step to continue characterizing a lead compound from a high throughput screen is structural activity relationship (SAR) studies. We have already obtained 9 structurally similar compounds to KB7 in order to identify which functional groups are required for inhibition. Results from the SAR study may lead to a more permeable compound. However, it is more customary that permeability issues are dealt with purposeful alterations of the compound. Since chemical synthesis of cell permeable version of KB7 could take some time, there are other ways to introduce the chemical inside cells for further preliminary studies. I started some studies with a membrane permealizing agent, geraniol. Geraniol can only be used as a tool to introduce effective amounts of KB7 into yeast cells, as it is eventually toxic to yeast and human cells (Bard et al., 1988; Carnesecchi, 2002). In combination with pump mutant strains, I anticipate an effective accumulation of KB7 intracellularly to cause sufficient Rtt109 inhibition and result in an appreciable decrease in H3K56ac by Western Blot. Upon attaining an inhibitory compound that is cell permeable, the *in vivo* effect of KB7 on pathogenicity can be investigated.

The HTS was performed with recombinant Rtt109 from *S. cerevisiae*, a non-pathogenic fungus. The cellular effects presented are performed on *C. albicans*, a pathogenic fungus. Because of the amino acid sequence conservation of Rtt109 between fungal strains at key residues (Bazan, 2008; Tang et al., 2008), it is likely

that KB7 will also inhibit Rtt109 from other fungal species. This assumption should also be verified.

# References

Adkins, M.W., Carson, J.J., English, C.M., Ramey, C.J., and Tyler, J.K. (2007). The histone chaperone anti-silencing function 1 stimulates the acetylation of newly synthesized histone H3 in S-phase. The Journal of biological chemistry *282*, 1334-1340.

Ahmad, A., Kabir, M.A., Kravets, A., Andaluz, E., Larriba, G., and Rustchenko, E. (2008). Chromosome instability and unusual features of some widely used strains ofCandida albicans. Yeast (Chichester, England) *25*, 433-448.

Albaugh, B.N., Arnold, K.M., Lee, S., and Denu, J.M. (2011). Autoacetylation of the histone acetyltransferase Rtt109. Journal of Biological Chemistry *286*, 24694-24701.

Albaugh, B.N., Kolonko, E.M., and Denu, J.M. (2010). Kinetic mechanism of the Rtt109-Vps75 histone acetyltransferase-chaperone complex. Biochemistry *49*, 6375-6385.

Allard, S., Masson, J.-Y., and Côté, J. (2004). Chromatin remodeling and the maintenance of genome integrity. Biochimica et biophysica acta *1677*, 158-164.

Andaluz, E., Ciudad, T., Gómez-Raja, J., Calderone, R., and Larriba, G. (2006). Rad52 depletion in *Candida albicans* triggers both the DNA-damage checkpoint and filamentation accompanied by but independent of expression of hypha-specific genes. Molecular Microbiology *59*, 1452-1472.

Aratani, Y., Kura, F., Watanabe, H., Akagawa, H., Takano, Y., Suzuki, K., Dinauer, M.C., Maeda, N., and Koyama, H. (2002a). Critical role of myeloperoxidase and nicotinamide adenine dinucleotide phosphate-oxidase in high-burden systemic infection of mice with Candida albicans. The Journal of infectious diseases *185*, 1833-1837.

Aratani, Y., Kura, F., Watanabe, H., Akagawa, H., Takano, Y., Suzuki, K., Dinauer, M.C., Maeda, N., and Koyama, H. (2002b). Relative contributions of myeloperoxidase and NADPH-oxidase to the early host defense against pulmonary infections with Candida albicans and Aspergillus fumigatus. Medical mycology : official publication of the International Society for Human and Animal Mycology *40*, 557-563.

Bai, C., Ramanan, N., Wang, Y.M., and Wang, Y. (2002). Spindle assembly checkpoint component CaMad2p is indispensable for Candida albicans survival and virulence in mice. Molecular Microbiology *45*, 31-44.

Balasubramanyam, K., Swaminathan, V., Ranganathan, A., and Kundu, T.K. (2003). Small molecule modulators of histone acetyltransferase p300. The Journal of biological chemistry *278*, 19134-19140.

Balasubramanyam, K., Varier, R.A., Altaf, M., Swaminathan, V., Siddappa, N.B., Ranga, U., and Kundu, T.K. (2004). Curcumin, a novel p300/CREB-binding protein-specific inhibitor of acetyltransferase, represses the acetylation of histone/nonhistone proteins and histone acetyltransferase-dependent chromatin transcription. The Journal of biological chemistry *279*, 51163-51171.

Bard, M., Albrecht, M.R., Gupta, N., Guynn, C.J., and Stillwell, W. (1988). Geraniol interferes with membrane functions in strains of Candida and Saccharomyces. Lipids *23*, 534-538.

Battu, A., Ray, A., and Wani, A.A. (2011). ASF1A and ATM regulate H3K56-mediated cell-cycle checkpoint recovery in response to UV irradiation. Nucleic acids research *39*, 7931-7945.

Bazan, J.F. (2008). An old HAT in human p300/CBP and yeast Rtt109. Cell cycle *7*, 1884-1886.

Benjamini, Y., and Hochberg, Y. (1995). Controlling the False Discovery Rate - a Practical and Powerful Approach to Multiple Testing. Journal of the Royal Statistical Society Series B-Methodological *57*, 289-300.

Berman, J. (2006). Morphogenesis and cell cycle progression in Candida albicans. Current opinion in microbiology *9*, 595-601.

Berndsen, C.E., Albaugh, B.N., Tan, S., and Denu, J.M. (2007). Catalytic mechanism of a MYST family histone acetyltransferase. Biochemistry *46*, 623-629.

Berndsen, C.E., and Denu, J.M. (2008). Catalysis and substrate selection by histone/protein lysine acetyltransferases. Current Opinion In Structural Biology *18*, 682-689.

Berndsen, C.E., Tsubota, T., Lindner, S.E., Lee, S., Holton, J.M., Kaufman, P.D., Keck, J.L., and Denu, J.M. (2008). Molecular functions of the histone acetyltransferase chaperone complex Rtt109-Vps75. Nature Structural & Molecular Biology *15*, 948-956.

Bowers, E.M., Yan, G., Mukherjee, C., Orry, A., Wang, L., Holbert, M.A., Crump, N.T., Hazzalin, C.A., Liszczak, G., Yuan, H., *et al.* (2010). Virtual Ligand Screening of the p300/CBP Histone Acetyltransferase: Identification of a Selective Small Molecule Inhibitor. Chemistry & Biology *17*, 471-482.

Boyer, L.A., Langer, M.R., Crowley, K.A., Tan, S., Denu, J.M., and Peterson, C.L. (2002). Essential role for the SANT domain in the functioning of multiple chromatin remodeling enzymes. Molecular cell *10*, 935-942.

Brand, A. (2012). Hyphal growth in human fungal pathogens and its role in virulence. International journal of microbiology *2012*, 517529.

Briggs, S.D., Bryk, M., Strahl, B.D., Cheung, W.L., Davie, J.K., Dent, S.Y., Winston, F., and Allis, C.D. (2001). Histone H3 lysine 4 methylation is mediated by Set1 and required for cell growth and rDNA silencing in Saccharomyces cerevisiae. Genes & Development *15*, 3286-3295.

Brown, A.J.P., Odds, F.C., and Gow, N.A.R. (2007). Infection-related gene expression in Candida albicans. Current opinion in microbiology *10*, 307-313.

Brownell, J.E., Zhou, J., Ranalli, T., Kobayashi, R., Edmondson, D.G., Roth, S.Y., and Allis, C.D. (1996). Tetrahymena histone acetyltransferase A: a homolog to yeast Gcn5p linking histone acetylation to gene activation. Cell *84*, 843-851.

Burgess, R.J., Zhou, H., Han, J., and Zhang, Z. (2010). A role for Gcn5 in replication-coupled nucleosome assembly. Molecular cell *37*, 469-480.

Calderone, R.A., and Fonzi, W.A. (2001). Virulence factors of Candida albicans. Trends in microbiology *9*, 327-335.

Cannon, R.D., Lamping, E., Holmes, A.R., Niimi, K., Tanabe, K., Niimi, M., and Monk, B.C. (2007). Candida albicans drug resistance another way to cope with stress. Microbiology *153*, 3211-3217.

Carnesecchi, S. (2002). Perturbation by Geraniol of Cell Membrane Permeability and Signal Transduction Pathways in Human Colon Cancer Cells. Journal of Pharmacology and Experimental Therapeutics *303*, 711-715.

Castaño, I., Pan, S.-J., Zupancic, M., Hennequin, C., Dujon, B., and Cormack, B. (2005). Telomere length control and transcriptional regulation of subtelomeric adhesins in Candida glabrata. Molecular Microbiology *55*, 1246-1258.

Celic, I., Masumoto, H., Griffith, W.P., Meluh, P., Cotter, R.J., Boeke, J.D., and Verreault, A. (2006). The sirtuins Hst3 and Hst4p preserve genome integrity by controlling histone H3 lysine 56 deacetylation. Current biology *16*, 1280-1289.

Chauhan, N., Ciudad, T., Rodríguez-Alejandre, A., Larriba, G., Calderone, R., and Andaluz, E. (2005). Virulence and karyotype analyses of rad52 mutants of Candida albicans: regeneration of a truncated chromosome of a reintegrant strain (rad52/RAD52) in the host. Infection and immunity *73*, 8069-8078.

Cheeseman, I.M., and Desai, A. (2008). Molecular architecture of the kinetochore-microtubule interface. Nature reviews Molecular cell biology *9*, 33-46.

Chen, C.-C., Carson, J.J., Feser, J., Tamburini, B., Zabaronick, S., Linger, J., and Tyler, J.K. (2008). Acetylated lysine 56 on histone H3 drives chromatin assembly after repair and signals for the completion of repair. Cell *134*, 231-243.

Chen, C.-C., and Tyler, J. (2008). Chromatin reassembly signals the end of DNA repair. Cell cycle *7*, 3792-3797.

Cheng, S., Clancy, C.J., Checkley, M.A., Handfield, M., Hillman, J.D., Progulske-Fox, A., Lewin, A.S., Fidel, P.L., and Nguyen, M.H. (2003). Identification of Candida albicans genes induced during thrush offers insight into pathogenesis. Molecular Microbiology *48*, 1275-1288.

Cole, P.A. (2008). Chemical probes for histone-modifying enzymes. Nature chemical biology *4*, 590-597.

Collins, S.R., Miller, K.M., Maas, N.L., Roguev, A., Fillingham, J., Chu, C.S., Schuldiner, M., Gebbia, M., Recht, J., Shales, M., *et al.* (2007). Functional dissection of protein complexes involved in yeast chromosome biology using a genetic interaction map. Nature *446*, 806-810.

Cormack, B., Ghori, N., and Falkow, S. (1999). An adhesin of the yeast pathogen Candida glabrata mediating adherence to human epithelial cells. Science *285*, 578-582.

Côté, J., Quinn, J., Workman, J.L., and Peterson, C.L. (1994). Stimulation of GAL4 derivative binding to nucleosomal DNA by the yeast SWI/SNF complex. Science *265*, 53-60.

Cowen, L.E., Anderson, J.B., and Kohn, L.M. (2002). Evolution of drug resistance in Candida albicans. Annual review of microbiology *56*, 139-165.

Cuenca-Estrella, M., Moore, C.B., Barchiesi, F., Bille, J., Chryssanthou, E., Denning, D.W., Donnelly, J.P., Dromer, F., Dupont, B., Rex, J.H., *et al.* (2003). Multicenter evaluation of the reproducibility of the proposed antifungal susceptibility testing method for fermentative yeasts of the Antifungal Susceptibility Testing Subcommittee of the European Committee on Antimicrobial Susceptibility Testing

(AFST-EUCAST). Clinical microbiology and infection : the official publication of the European Society of Clinical Microbiology and Infectious Diseases *9*, 467-474.

Cui, L., and Miao, J. (2010). Chromatin-mediated epigenetic regulation in the malaria parasite Plasmodium falciparum. Eukaryotic Cell *9*, 1138-1149.

Cui, L., Miao, J., and Cui, L. (2007). Cytotoxic effect of curcumin on malaria parasite Plasmodium falciparum: inhibition of histone acetylation and generation of reactive oxygen species. Antimicrobial agents and chemotherapy *51*, 488-494.

Daganzo, S.M., Erzberger, J.P., Lam, W.M., Skordalakes, E., Zhang, R., Franco, A.A., Brill, S.J., Adams, P.D., Berger, J.M., and Kaufman, P.D. (2003). Structure and function of the conserved core of histone deposition protein Asf1. Current biology *13*, 2148-2158.

Davey, C.A., Sargent, D.F., Luger, K., Maeder, A.W., and Richmond, T.J. (2002). Solvent Mediated Interactions in the Structure of the Nucleosome Core Particle at 1.9Å Resolution. Journal of molecular biology *319*, 1097-1113.

De Las Peñas, A., Pan, S.-J., Castaño, I., Alder, J., Cregg, R., and Cormack, B. (2003). Virulence-related surface glycoproteins in the yeast pathogen Candida glabrata are encoded in subtelomeric clusters and subject to RAP1- and SIR-dependent transcriptional silencing. Genes & Development *17*, 2245-2258.

de Repentigny, L. (2004). Animal models in the analysis of Candida host-pathogen interactions. Current opinion in microbiology *7*, 324-329.

Dekker, F.J., and Haisma, H.J. (2009). Histone acetyl transferases as emerging drug targets. Drug discovery today, 1-7.

Dixon, S.E., Stilger, K.L., Elias, E.V., Naguleswaran, A., and Jr, W.J.S. (2010). A decade of epigenetic research in Toxoplasma gondii. Molecular & Biochemical Parasitology *173*, 1-9.

Dokmanovic, M., Clarke, C., and Marks, P.A. (2007). Histone Deacetylase Inhibitors: Overview and Perspectives. Molecular Cancer Research *5*, 981-989.

Domergue, R., Castaño, I., De Las Peñas, A., Zupancic, M., Lockatell, V., Hebel, J.R., Johnson, D., and Cormack, B. (2005). Nicotinic acid limitation regulates silencing of Candida adhesins during UTI. Science *308*, 866-870.

Donini, M., Zenaro, E., Tamassia, N., and Dusi, S. (2007). NADPH oxidase of human dendritic cells: role in Candida albicans killing and regulation by interferons, dectin-1 and CD206. European journal of immunology *37*, 1194-1203.

Dos Vultos, T., Mestre, O., Tønjum, T., and Gicquel, B. (2009). DNA repair in Mycobacterium tuberculosisrevisited. FEMS Microbiology Reviews *33*, 471-487.

Dovey, O.M., Foster, C.T., and Cowley, S.M. (2010). Histone deacetylase 1 (HDAC1), but not HDAC2, controls embryonic stem cell differentiation. Proceedings of the National Academy of Sciences of the United States of America *107*, 8242-8247.

Driscoll, R., Hudson, A., and Jackson, S.P. (2007). Yeast Rtt109 promotes genome stability by acetylating histone H3 on lysine 56. Science (New York, NY) *315*, 649-652.

Drogaris, P., Villeneuve, V., Pomiès, C., Lee, E.-H., Bourdeau, V., Bonneil, E., Ferbeyre, G., Verreault, A., and Thibault, P. (2012). Histone Deacetylase Inhibitors Globally Enhance H3/H4 Tail Acetylation Without Affecting H3 Lysine 56 Acetylation. Scientific Reports *2*, 1-12.

Duraisingh, M.T., Voss, T.S., Marty, A.J., Duffy, M.F., Good, R.T., Thompson, J.K., Freitas-Junior, L.H., Scherf, A., Crabb, B.S., and Cowman, A.F. (2005). Heterochromatin silencing and locus repositioning linked to regulation of virulence genes in Plasmodium falciparum. Cell *121*, 13-24.

Duro, E., Vaisica, J.A., Brown, G.W., and Rouse, J. (2008). Budding yeast Mms22 and Mms1 regulate homologous recombination induced by replisome blockage. DNA repair *7*, 811-818.

Dutta, D., Ray, S., Home, P., Saha, B., Wang, S., Sheibani, N., Tawfik, O., Cheng, N., and Paul, S. (2010). Regulation of angiogenesis by histone chaperone HIRA-mediated incorporation of lysine 56-acetylated histone H3.3 at chromatin domains of endothelial genes. Journal of Biological Chemistry *285*, 41567-41577.

English, C.M., Adkins, M.W., Carson, J.J., Churchill, M.E.A., and Tyler, J.K. (2006). Structural basis for the histone chaperone activity of Asf1. Cell *127*, 495-508.

Enjalbert, B., Nantel, A., and Whiteway, M. (2003). Stress-induced gene expression in Candida albicans: absence of a general stress response. Molecular biology of the cell *14*, 1460-1467.

Enjalbert, B., Smith, D.A., Cornell, M.J., Alam, I., Nicholls, S., Brown, A.J.P., and Quinn, J. (2006). Role of the Hog1 stress-activated protein kinase in the global transcriptional response to stress in the fungal pathogen Candida albicans. Molecular biology of the cell *17*, 1018-1032.

Erkmann, J.A., and Kaufman, P.D. (2009). A negatively charged residue in place of histone H3K56 supports chromatin assembly factor association but not genotoxic stress resistance. DNA repair *8*, 1371-1379.

Ernst, J.F. (2000). Transcription factors in Candida albicans - environmental control of morphogenesis. Microbiology (Reading, England) *146 ( Pt 8)*, 1763-1774.

Faucher, D., and Wellinger, R.J. (2010). Methylated H3K4, a transcription-associated histone modification, is involved in the DNA damage response pathway. PLoS genetics *6*, 1-16.

Ferrante, A. (1989). Tumor necrosis factor alpha potentiates neutrophil antimicrobial activity: increased fungicidal activity against Torulopsis glabrata and Candida albicans and associated increases in oxygen radical production and lysosomal enzyme release. Infection and immunity *57*, 2115-2122.

Figueiredo, L.M., Cross, G.A.M., and Janzen, C.J. (2009). Epigenetic regulation in African trypanosomes: a new kid on the block. Nature reviews Microbiology *7*, 504-513.

Fillingham, J., Kainth, P., Lambert, J.-P., van Bakel, H., Tsui, K., Peña-Castillo, L., Nislow, C., Figeys, D., Hughes, T.R., Greenblatt, J., *et al.* (2009). Two-color cell array screen reveals interdependent roles for histone chaperones and a chromatin boundary regulator in histone gene repression. Molecular cell *35*, 340-351.

Fillingham, J., Recht, J., Silva, A.C., Suter, B., Emili, A., Stagljar, I., Krogan, N.J., Allis, C.D., Keogh, M.-C., and Greenblatt, J.F. (2008). Chaperone control of the activity and specificity of the histone H3 acetyltransferase Rtt109. Molecular And Cellular Biology *28*, 4342-4353.

Finley, K.R., and Berman, J. (2005). Microtubules in Candida albicans hyphae drive nuclear dynamics and connect cell cycle progression to morphogenesis. Eukaryotic Cell *4*, 1697-1711.

Finley, K.R., Bouchonville, K.J., Quick, A., and Berman, J. (2008). Dynein-dependent nuclear dynamics affect morphogenesis in Candida albicans by means of the Bub2p spindle checkpoint. Journal of cell science *121*, 466-476.

Fradin, C., De Groot, P., MacCallum, D., Schaller, M., Klis, F., Odds, F.C., and Hube, B. (2005). Granulocytes govern the transcriptional response, morphology and proliferation of Candida albicans in human blood. Molecular Microbiology *56*, 397-415.

Freitas-Junior, L.H., Hernandez-Rivas, R., Ralph, S.A., Montiel-Condado, D., Ruvalcaba-Salazar, O.K., Rojas-Meza, A.P., Mancio-Silva, L., Leal-Silvestre, R.J.,

Gontijo, A.M., Shorte, S., *et al.* (2005). Telomeric heterochromatin propagation and histone acetylation control mutually exclusive expression of antigenic variation genes in malaria parasites. Cell *121*, 25-36.

Frohner, I.E., Bourgeois, C., Yatsyk, K., Majer, O., and Kuchler, K. (2009). Candida albicans cell surface superoxide dismutases degrade host-derived reactive oxygen species to escape innate immune surveillance. Molecular Microbiology *71*, 240-252.

Garcia, B.A., Hake, S.B., Diaz, R.L., Kauer, M., Morris, S.A., Recht, J., Shabanowitz, J., Mishra, N., Strahl, B.D., Allis, C.D., *et al.* (2007). Organismal differences in post-translational modifications in histones H3 and H4. The Journal of biological chemistry *282*, 7641-7655.

Gardner, K.E., Allis, C.D., and Strahl, B.D. (2011). Operating on chromatin, a colorful language where context matters. Journal of molecular biology *409*, 36-46.

Gorna, A.E., Bowater, R.P., and Dziadek, J. (2010). DNA repair systems and the pathogenesis of Mycobacterium tuberculosis: varying activities at different stages of infection. Clinical Science *119*, 187-202.

Gow, N.A.R., van de Veerdonk, F.L., Brown, A.J.P., and Netea, M.G. (2012). Candida albicans morphogenesis and host defence: discriminating invasion from colonization. Nature reviews Microbiology *10*, 112-122.

Groth, A., Rocha, W., Verreault, A., and Almouzni, G. (2007). Chromatin challenges during DNA replication and repair. Cell *128*, 721-733.

Gudlaugsson, O., Gillespie, S., Lee, K., Vande Berg, J., Hu, J., Messer, S., Herwaldt, L., Pfaller, M., and Diekema, D. (2003). Attributable mortality of nosocomial candidemia, revisited. Clinical infectious diseases : an official publication of the Infectious Diseases Society of America *37*, 1172-1177.

Guillemette, B., Drogaris, P., Lin, H.-H.S., Armstrong, H., Hiragami-Hamada, K., Imhof, A., Bonneil, E., Thibault, P., Verreault, A., and Festenstein, R.J. (2011). H3 lysine 4 is acetylated at active gene promoters and is regulated by H3 lysine 4 methylation. PLoS genetics *7*, e1001354.

Haghnazari, E., and Heyer, W.D. (2004). The Hog1 MAP kinase pathway and the Mec1 DNA damage checkpoint pathway independently control the cellular responses to hydrogen peroxide. DNA repair *3*, 769-776.

Han, J., Zhou, H., Horazdovsky, B., Zhang, K., Xu, R.M., and Zhang, Z. (2007a). Rtt109 Acetylates Histone H3 Lysine 56 and Functions in DNA Replication. Science *315*, 653-655.

Han, J., Zhou, H., Li, Z., Xu, R.-M., and Zhang, Z. (2007b). Acetylation of lysine 56 of histone H3 catalyzed by RTT109 and regulated by ASF1 is required for replisome integrity. The Journal of biological chemistry *282*, 28587-28596.

Han, J., Zhou, H., Li, Z., Xu, R.-M., and Zhang, Z. (2007c). The Rtt109-Vps75 histone acetyltransferase complex acetylates non-nucleosomal histone H3. The Journal of biological chemistry *282*, 14158-14164.

Hancock, J.T., and Jones, O.T. (1987). The inhibition by diphenyleneiodonium and its analogues of superoxide generation by macrophages. The Biochemical journal *242*, 103-107.

Hnisz, D., Majer, O., Frohner, I.E., Komnenovic, V., and Kuchler, K. (2010). The Set3/Hos2 histone deacetylase complex attenuates cAMP/PKA signaling to regulate morphogenesis and virulence of Candida albicans. PLoS pathogens *6*, 1-18.

Hnisz, D., Schwarzmüller, T., and Kuchler, K. (2009). Transcriptional loops meet chromatin: a dual-layer network controls white-opaque switching in Candida albicans. Molecular Microbiology *74*, 1-15.

Hodawadekar, S.C., and Marmorstein, R. (2007). Chemistry of acetyl transfer by histone modifying enzymes: structure, mechanism and implications for effector design. Oncogene *26*, 5528-5540.

Hope, W.W., Tabernero, L., Denning, D.W., and Anderson, M.J. (2004). Molecular mechanisms of primary resistance to flucytosine in Candida albicans. Antimicrobial agents and chemotherapy *48*, 4377-4386.

Horwitz, G.A., Zhang, K., McBrian, M.A., Grunstein, M., Kurdistani, S.K., and Berk, A.J. (2008). Adenovirus small e1a alters global patterns of histone modification. Science *321*, 1084-1085.

Hu, Y., Farah, C.S., and Ashman, R.B. (2006). Effector function of leucocytes from susceptible and resistant mice against distinct isolates of Candida albicans. Immunology and cell biology *84*, 455-460.

Hyland, E.M., Cosgrove, M.S., Molina, H., Wang, D., Pandey, A., Cottee, R.J., and Boeke, J.D. (2005). Insights into the role of histone H3 and histone H4 core modifiable residues in Saccharomyces cerevisiae. Molecular and Cellular Biology *25*, 10060-10070.

Janbon, G., Sherman, F., and Rustchenko, E. (1998). Monosomy of a specific chromosome determines L-sorbose utilization: a novel regulatory mechanism in Candida albicans. Proceedings of the National Academy of Sciences of the United States of America *95*, 5150-5155.

Kamieniarz, K., and Schneider, R. (2009). Tools to tackle protein acetylation. Chemistry & Biology *16*, 1027-1029.

Kaplan, T., Liu, C.L., Erkmann, J.A., Holik, J., Grunstein, M., Kaufman, P.D., Friedman, N., and Rando, O.J. (2008). Cell cycle- and chaperone-mediated regulation of H3K56ac incorporation in yeast. PLoS genetics *4*, 1-16.

Karanam, B., Jiang, L., Wang, L., Kelleher, N.L., and Cole, P.A. (2006). Kinetic and mass spectrometric analysis of p300 histone acetyltransferase domain autoacetylation. The Journal of biological chemistry *281*, 40292-40301.

Keck, K.M., and Pemberton, L.F. (2011). Interaction with the histone chaperone Vps75 promotes nuclear localization and HAT activity of Rtt109 in vivo. Traffic *12*, 826-839.

Ketel, C., Wang, H.S.W., McClellan, M., Bouchonville, K., Selmecki, A., Lahav, T., Gerami-Nejad, M., and Berman, J. (2009). Neocentromeres form efficiently at multiple possible loci in Candida albicans. PLoS genetics *5*, 1-18.

Kim, J.-A., and Haber, J.E. (2009). Chromatin assembly factors Asf1 and CAF-1 have overlapping roles in deactivating the DNA damage checkpoint when DNA repair is complete. Proceedings of the National Academy of Sciences *106*, 1151-1156.

Klar, A.J., Srikantha, T., and Soll, D.R. (2001). A histone deacetylation inhibitor and mutant promote colony-type switching of the human pathogen Candida albicans. Genetics *158*, 919-924.

Kolonko, E.M., Albaugh, B.N., Lindner, S.E., Chen, Y., Satyshur, K.A., Arnold, K.M., Kaufman, P.D., Keck, J.L., and Denu, J.M. (2010). Catalytic activation of histone acetyltransferase Rtt109 by a histone chaperone. Proceedings of the National Academy of Sciences *107*, 20275-20280.

Kong, S., Kim, S.-J., Sandal, B., Lee, S.-M., Gao, B., Zhang, D.D., and Fang, D. (2011). The type III histone deacetylase Sirt1 protein suppresses p300-mediated histone H3 lysine 56 acetylation at Bclaf1 promoter to inhibit T cell activation. Journal of Biological Chemistry *286*, 16967-16975.

Kottom, T.J., Han, J., Zhang, Z., and Limper, A.H. (2011). Pneumocystis carinii expresses an active Rtt109 histone acetyltransferase. American journal of respiratory cell and molecular biology *44*, 768-776.

Kouzarides, T. (2007). Chromatin modifications and their function. Cell *128*, 693-705.

Kumamoto, C.A. (2008). Niche-specific gene expression during C. albicans infection. Current opinion in microbiology *11*, 325-330.

Kumamoto, C.A., and Vinces, M.D. (2005). Contributions of hyphae and hypha-co-regulated genes to Candida albicans virulence. Cellular Microbiology *7*, 1546-1554.

Kurthkoti, K., and Varshney, U. (2011). Base excision and nucleotide excision repair pathways in mycobacteria. Tuberculosis *91*, 533-543.

Kushnirov, V.V. (2000). Rapid and reliable protein extraction from yeast. Yeast *16*, 857-860.

Kwon, H., Imbalzano, A.N., Khavari, P.A., Kingston, R.E., and Green, M.R. (1994). Nucleosome disruption and enhancement of activator binding by a human SW1/SNF complex. Nature *370*, 477-481.

Laprade, L., Boyartchuk, V.L., Dietrich, W.F., and Winston, F. (2002). Spt3 plays opposite roles in filamentous growth in Saccharomyces cerevisiae and Candida albicans and is required for C. albicans virulence. Genetics *161*, 509-519.

Lau, O.D., Kundu, T.K., Soccio, R.E., Ait-Si-Ali, S., Khalil, E.M., Vassilev, A., Wolffe, A.P., Nakatani, Y., Roeder, R.G., and Cole, P.A. (2000). HATs off: selective synthetic inhibitors of the histone acetyltransferases p300 and PCAF. Molecular cell *5*, 589-595.

Legrand, M., Chan, C.L., Jauert, P.A., and Kirkpatrick, D.T. (2008). Analysis of base excision and nucleotide excision repair in Candida albicans. Microbiology *154*, 2446-2456.

Li, B., Carey, M., and Workman, J.L. (2007). The role of chromatin during transcription. Cell *128*, 707-719.

Li, Q., Zhou, H., Wurtele, H., Davies, B., Horazdovsky, B., Verreault, A., and Zhang, Z. (2008). Acetylation of histone H3 lysine 56 regulates replication-coupled nucleosome assembly. Cell *134*, 244-255.

Lin, C., and Yuan, Y.A. (2008). Structural insights into histone H3 lysine 56 acetylation by Rtt109. Structure *16*, 1503-1510.

Liu, X., Wang, L., Zhao, K., Thompson, P.R., Hwang, Y., Marmorstein, R., and Cole, P.A. (2008). The structural basis of protein acetylation by the p300/CBP transcriptional coactivator. Nature *451*, 846-850.

Lo, H.J., Köhler, J.R., DiDomenico, B., Loebenberg, D., Cacciapuoti, A., and Fink, G.R. (1997). Nonfilamentous C. albicans mutants are avirulent. Cell *90*, 939-949.

Lo, K.A., Bauchmann, M.K., Baumann, A.P., Donahue, C.J., Thiede, M.A., Hayes, L.S., des Etages, S.A.G., and Fraenkel, E. (2011). Genome-wide profiling of H3K56 acetylation and transcription factor binding sites in human adipocytes. PloS one *6*, 1-12.

Lohse, M.B., and Johnson, A.D. (2009). White-opaque switching in Candida albicans. Current opinion in microbiology *12*, 650-654.

Lopes da Rosa, J., Boyartchuk, V.L., Zhu, L.J., and Kaufman, P.D. (2010). Histone acetyltransferase Rtt109 is required for Candida albicans pathogenesis. Proceedings of the National Academy of Sciences *107*, 1594-1599.

Lopez-Rubio, J.J., Riviere, L., and Scherf, A. (2007). Shared epigenetic mechanisms control virulence factors in protozoan parasites. Current opinion in microbiology *10*, 560-568.

Lorenz, M.C., Bender, J.A., and Fink, G.R. (2004). Transcriptional response of Candida albicans upon internalization by macrophages. Eukaryotic Cell *3*, 1076-1087.

Lu, Y., Su, C., Mao, X., Raniga, P.P., Liu, H., and Chen, J. (2008). Efg1-mediated recruitment of NuA4 to promoters is required for hypha-specific Swi/Snf binding and activation in Candida albicans. Molecular biology of the cell *19*, 4260-4272.

Luger, K., Mäder, A.W., Richmond, R.K., Sargent, D.F., and Richmond, T.J. (1997). Crystal structure of the nucleosome core particle at 2.8 A resolution. Nature *389*, 251-260.

Luger, K., Rechsteiner, T.J., and Richmond, T.J. (1999). Expression and purification of recombinant histones and nucleosome reconstitution. Methods in molecular biology *119*, 1-16.

Maas, N.L., Miller, K.M., DeFazio, L.G., and Toczyski, D.P. (2006). Cell cycle and checkpoint regulation of histone H3 K56 acetylation by Hst3 and Hst4. Molecular cell *23*, 109-119.

Mansour, M.K., and Levitz, S.M. (2002). Interactions of fungi with phagocytes. Current opinion in microbiology *5*, 359-365.

Mantelingu, K., Reddy, B.A.A., Swaminathan, V., Kishore, A.H., Siddappa, N.B., Kumar, G.V.P., Nagashankar, G., Natesh, N., Roy, S., Sadhale, P.P., *et al.* (2007). Specific inhibition of p300-HAT alters global gene expression and represses HIV replication. Chemistry & Biology *14*, 645-657.

Mao, X., Cao, F., Nie, X., Liu, H., and Chen, J. (2006). The Swi/Snf chromatin remodeling complex is essential for hyphal development in Candida albicans. FEBS letters *580*, 2615-2622.

Marcu, M.G., Jung, Y.-J., Lee, S., Chung, E.-J., Lee, M.-J., Trepel, J., and Neckers, L. (2006). Curcumin is an inhibitor of p300 histone acetylatransferase. Medicinal chemistry *2*, 169-174.

Marmorstein, R., and Trievel, R.C. (2009). Histone modifying enzymes: structures, mechanisms, and specificities. Biochimica et biophysica acta *1789*, 58-68.

Martchenko, M., Alarco, A.-M., Harcus, D., and Whiteway, M. (2004). Superoxide dismutases in Candida albicans: transcriptional regulation and functional characterization of the hyphal-induced SOD5 gene. Molecular biology of the cell *15*, 456-467.

Masumoto, H., Hawke, D., Kobayashi, R., and Verreault, A. (2005). A role for cell-cycle-regulated histone H3 lysine 56 acetylation in the DNA damage response. Nature *436*, 294-298.

McAinsh, A.D., Tytell, J.D., and Sorger, P.K. (2003). Structure, function, and regulation of budding yeast kinetochores. Annual review of cell and developmental biology *19*, 519-539.

Merrick, C.J., and Duraisingh, M.T. (2006). Heterochromatin-mediated control of virulence gene expression. Molecular Microbiology *62*, 612-620.

Mersfelder, E.L., and Parthun, M.R. (2006). The tale beyond the tail: histone core domain modifications and the regulation of chromatin structure. Nucleic acids research *34*, 2653-2662.

Millar, C.B., and Grunstein, M. (2006). Genome-wide patterns of histone modifications in yeast. Nature reviews Molecular cell biology *7*, 657-666.

Miller, K.M., Tjeertes, J.V., Coates, J., Legube, G., Polo, S.E., Britton, S., and Jackson, S.P. (2010). Human HDAC1 and HDAC2 function in the DNA-damage response to promote DNA nonhomologous end-joining. Nature Structural & Molecular Biology *17*, 1144-1151.

Mishra, N.N., Prasad, T., Sharma, N., Payasi, A., Prasad, R., Gupta, D.K., and Singh, R. (2007). Pathogenicity and drug resistance in Candida albicans and other yeast species. A review. Acta microbiologica et immunologica Hungarica *54*, 201-235.

Missall, T.A., Lodge, J.K., and McEwen, J.E. (2004). Mechanisms of resistance to oxidative and nitrosative stress: implications for fungal survival in mammalian hosts. Eukaryotic Cell *3*, 835-846.

Moore, J.D., and Krebs, J.E. (2004). Histone modifications and DNA double-strand break repair. Biochemistry and cell biology = Biochimie et biologie cellulaire *82*, 446-452.

Morschhäuser, J. (2010). Regulation of white-opaque switching in Candida albicans. Medical microbiology and immunology *199*, 165-172.

Nasution, O., Srinivasa, K., Kim, M., Kim, Y.-J., Kim, W., Jeong, W., and Choi, W. (2008). Hydrogen Peroxide Induces Hyphal Differentiation in Candida albicans. Eukaryotic Cell *7*, 2008-2011.

Neofytos, D., Fishman, J.A., Horn, D., Anaissie, E., Chang, C.-H., Olyaei, A., Pfaller, M., Steinbach, W.J., Webster, K.M., and Marr, K.A. (2010). Epidemiology and outcome of invasive fungal infections in solid organ transplant recipients. Transplant infectious disease : an official journal of the Transplantation Society *12*, 220-229.

Netea, M.G., Brown, G.D., Kullberg, B.J., and Gow, N.A.R. (2008). An integrated model of the recognition of Candida albicans by the innate immune system. Nature reviews Microbiology *6*, 67-78.

Neumann, H., Hancock, S.M., Buning, R., Routh, A., Chapman, L., Somers, J., Owen-Hughes, T., van Noort, J., Rhodes, D., and Chin, J.W. (2009). A Method for Genetically Installing Site-Specific Acetylation in Recombinant Histories Defines the Effects of H3 K56 Acetylation. Molecular cell *36*, 153-163.

O'Meara, T.R., Hay, C., Price, M.S., Giles, S., and Alspaugh, J.A. (2010). Cryptococcus neoformans histone acetyltransferase Gcn5 regulates fungal adaptation to the host. Eukaryotic Cell *9*, 1193-1202.

Ogryzko, V.V., Schiltz, R.L., Russanova, V., Howard, B.H., and Nakatani, Y. (1996). The transcriptional coactivators p300 and CBP are histone acetyltransferases. Cell *87*, 953-959.

Ozdemir, A., Masumoto, H., Fitzjohn, P., Verreault, A., and Logie, C. (2006). Histone H3 lysine 56 acetylation: a new twist in the chromosome cycle. Cell cycle *5*, 2602-2608.

Park, Y.-J., and Luger, K. (2008). Histone chaperones in nucleosome eviction and histone exchange. Current Opinion In Structural Biology *18*, 282-289.

Pereira, H.A., and Hosking, C.S. (1984). The role of complement and antibody in opsonization and intracellular killing of Candida albicans. Clinical and experimental immunology *57*, 307-314.

Pérez-Martín, J., Uría, J.A., and Johnson, A.D. (1999). Phenotypic switching in Candida albicans is controlled by a SIR2 gene. The EMBO journal *18*, 2580-2592.

Peterson, C., and Laniel, M.-A. (2004). Histones and histone modifications. Current biology *14*, R546-551.

Pfaller, M., and Diekema, D.J. (2007). Epidemiology of invasive candidiasis: a persistent public health problem. Clinical microbiology reviews *20*, 133-163.

Pfaller, M., Moet, G.J., Messer, S.A., Jones, R.N., and Castanheira, M. (2011). Candida bloodstream infections: comparison of species distributions and antifungal resistance patterns in community-onset and nosocomial isolates in the SENTRY Antimicrobial Surveillance Program, 2008-2009. Antimicrobial agents and chemotherapy *55*, 561-566.

Pijnappel, W., Schaft, D., Roguev, A., Shevchenko, A., Tekotte, H., Wilm, M., Rigaut, G., Seraphin, B., Aasland, R., and Stewart, A. (2001). The S-cerevisiae SET3 complex includes two histone deacetylases, Hos2 and Hst1, and is a meiotic-specific repressor of the sporulation gene program. Genes & Development *15*, 2991-3004.

Polak, A., and Scholer, H.J. (1975). Mode of action of 5-fluorocytosine and mechanisms of resistance. Chemotherapy *21*, 113-130.

Prado, F., Cortés-Ledesma, F., and Aguilera, A. (2004). The absence of the yeast chromatin assembly factor Asf1 increases genomic instability and sister chromatid exchange. EMBO reports *5*, 497-502.

Pukkila-Worley, R., Peleg, A.Y., Tampakakis, E., and Mylonakis, E. (2009). Candida albicans hyphal formation and virulence assessed using a Caenorhabditis elegans infection model. Eukaryotic Cell *8*, 1750-1758.

Purich, D.L., and Allison, R. (2000). Handbook of Biochemical Kinetics - Daniel L. Purich, R. Donald Allison, 1 edition edn (Academic Press).

Ramage, G. (2002). Investigation of multidrug efflux pumps in relation to fluconazole resistance in Candida albicans biofilms. Journal of Antimicrobial Chemotherapy *49*, 973-980.

Raman, S.B., Nguyen, M.H., Zhang, Z., Cheng, S., Jia, H.Y., Weisner, N., Iczkowski, K., and Clancy, C.J. (2006). Candida albicans SET1 encodes a histone 3 lysine 4

methyltransferase that contributes to the pathogenesis of invasive candidiasis. Molecular Microbiology *60*, 697-709.

Ransom, M., Dennehey, B.K., and Tyler, J.K. (2010). Chaperoning histones during DNA replication and repair. Cell *140*, 183-195.

Recht, J., Tsubota, T., Tanny, J.C., Diaz, R.L., Berger, J.M., Zhang, X., Garcia, B.A., Shabanowitz, J., Burlingame, A.L., Hunt, D.F., *et al.* (2006). Histone chaperone Asf1 is required for histone H3 lysine 56 acetylation, a modification associated with S phase in mitosis and meiosis. Proceedings of the National Academy of Sciences of the United States of America *103*, 6988-6993.

Redon, C., Pilch, D.R., Rogakou, E.P., Orr, A.H., Lowndes, N.F., and Bonner, W.M. (2003). Yeast histone 2A serine 129 is essential for the efficient repair of checkpoint-blind DNA damage. EMBO reports *4*, 678-684.

Reuss, O., Vik, A., Kolter, R., and Morschhäuser, J. (2004). The SAT1 flipper, an optimized tool for gene disruption in Candida albicans. Gene *341*, 119-127.

Romani, L., Bistoni, F., and Puccetti, P. (2003). Adaptation of Candida albicans to the host environment: the role of morphogenesis in virulence and survival in mammalian hosts. Current opinion in microbiology *6*, 338-343.

Rufiange, A., Jacques, P.-E., Bhat, W., Robert, F., and Nourani, A. (2007). Genome-wide replication-independent histone H3 exchange occurs predominantly at promoters and implicates H3K56 acetylation and Asf1. Molecular cell *27*, 393-405.

Rustchenko, E., Howard, D.H., and Sherman, F. (1994). Chromosomal alterations of Candida albicans are associated with the gain and loss of assimilating functions. Journal of bacteriology *176*, 3231-3241.

Ruthenburg, A.J., Li, H., Patel, D.J., and Allis, C.D. (2007). Multivalent engagement of chromatin modifications by linked binding modules. Nature reviews Molecular cell biology *8*, 983-994.

Salmon, T.B., Evert, B.A., Song, B., and Doetsch, P.W. (2004). Biological consequences of oxidative stress-induced DNA damage in Saccharomyces cerevisiae. Nucleic acids research *32*, 3712-3723.

Sasada, M., and Johnston, R.B. (1980). Macrophage microbicidal activity. Correlation between phagocytosis-associated oxidative metabolism and the killing of Candida by macrophages. The Journal of experimental medicine *152*, 85-98.

Sasada, M., Kubo, A., Nishimura, T., Kakita, T., Moriguchi, T., Yamamoto, K., and Uchino, H. (1987). Candidacidal activity of monocyte-derived human macrophages:

relationship between Candida killing and oxygen radical generation by human macrophages. Journal of leukocyte biology *41*, 289-294.

Schneider, J., Bajwa, P., Johnson, F.C., Bhaumik, S.R., and Shilatifard, A. (2006). Rtt109 is required for proper H3K56 acetylation: a chromatin mark associated with the elongating RNA polymerase II. The Journal of biological chemistry *281*, 37270-37274.

Scholes, D.T., Banerjee, M., Bowen, B., and Curcio, M.J. (2001). Multiple regulators of Ty1 transposition in Saccharomyces cerevisiae have conserved roles in genome maintenance. Genetics *159*, 1449-1465.

Sellam, A., Askew, C., Epp, E., Lavoie, H., Whiteway, M., and Nantel, A. (2009). Genome-wide mapping of the coactivator Ada2p yields insight into the functional roles of SAGA/ADA complex in Candida albicans. Molecular biology of the cell *20*, 2389-2400.

Selmecki, A., Bergmann, S., and Berman, J. (2005). Comparative genome hybridization reveals widespread aneuploidy in Candida albicans laboratory strains. Molecular Microbiology *55*, 1553-1565.

Selmecki, A., Forche, A., and Berman, J. (2006). Aneuploidy and isochromosome formation in drug-resistant Candida albicans. Science *313*, 367-370.

Sexton, J.A., Brown, V., and Johnston, M. (2007). Regulation of sugar transport and metabolism by the Candida albicans Rgt1 transcriptional repressor. Yeast *24*, 847-860.

Shi, Q.-M., Wang, Y.-M., Zheng, X.-D., Lee, R.T.H., and Wang, Y. (2007). Critical role of DNA checkpoints in mediating genotoxic-stress-induced filamentous growth in Candida albicans. Molecular biology of the cell *18*, 815-826.

Shogren-Knaak, M., Ishii, H., Sun, J.-M., Pazin, M.J., Davie, J.R., and Peterson, C.L. (2006). Histone H4-K16 acetylation controls chromatin structure and protein interactions. Science *311*, 844-847.

Sinha, M., and Peterson, C.L. (2009). Chromatin dynamics during repair of chromosomal DNA double-strand breaks. Epigenomics *1*, 371-385.

Slutsky, B., Staebell, M., Anderson, J., Risen, L., Pfaller, M., and Soll, D.R. (1987). "White-opaque transition": a second high-frequency switching system in Candida albicans. Journal of bacteriology *169*, 189-197.

Smith, C.L., and Peterson, C. (2005). ATP-dependent chromatin remodeling. Current topics in developmental biology *65*, 115-148.

Smyth, G.K. (2004). Linear models and empirical bayes methods for assessing differential expression in microarray experiments. Statistical applications in genetics and molecular biology *3*.

Soll, D. (2009). Why does Candida albicans switch? FEMS Yeast Research *9*, 973-989.

Spellberg, B., Ibrahim, A.S., Edwards, J.E., and Filler, S.G. (2005). Mice with disseminated candidiasis die of progressive sepsis. The Journal of infectious diseases *192*, 336-343.

Srikantha, T., Tsai, L., Daniels, K., Klar, A.J., and Soll, D.R. (2001). The histone deacetylase genes HDA1 and RPD3 play distinct roles in regulation of high-frequency phenotypic switching in Candida albicans. Journal of bacteriology *183*, 4614-4625.

Staib, P., Kretschmar, M., Nichterlein, T., Hof, H., and Morschhäuser, J. (2000). Differential activation of a Candida albicans virulence gene family during infection. Proceedings of the National Academy of Sciences of the United States of America *97*, 6102-6107.

Stavropoulos, P., Nagy, V., Blobel, G., and Hoelz, A. (2008). Molecular basis for the autoregulation of the protein acetyl transferase Rtt109. Proceedings of the National Academy of Sciences *105*, 12236-12241.

Stevenhagen, A., and van Furth, R. (1993). Interferon-gamma activates the oxidative killing of Candida albicans by human granulocytes. Clinical and experimental immunology *91*, 170-175.

Stevenson, J.S., and Liu, H. (2011). Regulation of white and opaque cell-type formation in Candida albicans by Rtt109 and Hst3. Molecular Microbiology *81*, 1078-1091.

Su, D., Hu, Q., Li, Q., Thompson, J.R., Cui, G., Fazly, A., Davies, B.A., Botuyan, M.V., Zhang, Z., and Mer, G. (2012). Structural basis for recognition of H3K56-acetylated histone H3-H4 by the chaperone Rtt106. Nature *483*, 104-107.

Sudbery, P., Gow, N., and Berman, J. (2004). The distinct morphogenic states of Candida albicans. Trends in microbiology *12*, 317-324.

Sudbery, P.E. (2011). Growth of Candida albicans hyphae. Nature reviews Microbiology *9*, 737-748.

Sun, Y., Jiang, X., Chen, S., Fernandes, N., and Price, B.D. (2005). A role for the Tip60 histone acetyltransferase in the acetylation and activation of ATM. Proceedings

of the National Academy of Sciences of the United States of America *102*, 13182-13187.

Sun, Y., Jiang, X., Chen, S., and Price, B.D. (2006). Inhibition of histone acetyltransferase activity by anacardic acid sensitizes tumor cells to ionizing radiation. FEBS letters *580*, 4353-4356.

Tang, Y., Holbert, M.A., Delgoshaie, N., Wurtele, H., Guillemette, B., Meeth, K., Yuan, H., Drogaris, P., Lee, E.-H., Durette, C., *et al.* (2011). Structure of the Rtt109-AcCoA/Vps75 complex and implications for chaperone-mediated histone acetylation. Structure *19*, 221-231.

Tang, Y., Holbert, M.A., Wurtele, H., Meeth, K., Rocha, W., Gharib, M., Jiang, E., Thibault, P., Verreault, A., Verrault, A., *et al.* (2008). Fungal Rtt109 histone acetyltransferase is an unexpected structural homolog of metazoan p300/CBP. Nature Structural & Molecular Biology *15*, 738-745.

Tanner, K.G., Langer, M.R., Kim, Y., and Denu, J.M. (2000). Kinetic mechanism of the histone acetyltransferase GCN5 from yeast. The Journal of biological chemistry *275*, 22048-22055.

Tanner, K.G., Trievel, R.C., Kuo, M.H., Howard, R.M., Berger, S.L., Allis, C.D., Marmorstein, R., and Denu, J. (1999). Catalytic mechanism and function of invariant glutamic acid 173 from the histone acetyltransferase GCN5 transcriptional coactivator. The Journal of biological chemistry *274*, 18157-18160.

Thaminy, S., Newcomb, B., Kim, J., Gatbonton, T., Foss, E., Simon, J., and Bedalov, A. (2007). Hst3 is regulated by Mec1-dependent proteolysis and controls the S phase checkpoint and sister chromatid cohesion by deacetylating histone H3 at lysine 56. The Journal of biological chemistry *282*, 37805-37814.

Thompson, H.L., and Wilton, J.M. (1992). Interaction and intracellular killing of Candida albicans blastospores by human polymorphonuclear leucocytes, monocytes and monocyte-derived macrophages in aerobic and anaerobic conditions. Clinical and experimental immunology *87*, 316-321.

Thompson, P.R., Wang, D., Wang, L., Fulco, M., Pediconi, N., Zhang, D., An, W., Ge, Q., Roeder, R.G., Wong, J., *et al.* (2004). Regulation of the p300 HAT domain via a novel activation loop. Nature Structural & Molecular Biology *11*, 308-315.

Timmermann, S., Lehrmann, H., Polesskaya, A., and Harel-Bellan, A. (2001). Histone acetylation and disease. Cellular and Molecular Life Sciences *58*, 728-736.

Tjeertes, J.V., Miller, K.M., and Jackson, S.P. (2009). Screen for DNA-damage-responsive histone modifications identifies H3K9Ac and H3K56Ac in human cells. The EMBO journal *28*, 1878-1889.

Tonkin, C.J., Carret, C.K., Duraisingh, M.T., Voss, T.S., Ralph, S.A., Hommel, M., Duffy, M.F., da Silva, L.M., Scherf, A., Ivens, A., *et al.* (2009). Sir2 Paralogues Cooperate to Regulate Virulence Genes and Antigenic Variation in Plasmodium falciparum. PLoS biology *7*, 771-788.

Trievel, R.C., Li, F.Y., and Marmorstein, R. (2000). Application of a fluorescent histone acetyltransferase assay to probe the substrate specificity of the human p300/CBP-associated factor. Analytical biochemistry *287*, 319-328.

Trievel, R.C., Rojas, J.R., Sterner, D.E., Venkataramani, R.N., Wang, L., Zhou, J., Allis, C.D., Berger, S.L., and Marmorstein, R. (1999). Crystal structure and mechanism of histone acetylation of the yeast GCN5 transcriptional coactivator. Proceedings of the National Academy of Sciences of the United States of America *96*, 8931-8936.

Tsubota, T., Berndsen, C.E., Erkmann, J.A., Smith, C.L., Yang, L., Freitas, M.A., Denu, J.M., and Kaufman, P.D. (2007). Histone H3-K56 acetylation is catalyzed by histone chaperone-dependent complexes. Molecular cell *25*, 703-712.

Vázquez-Torres, A., and Balish, E. (1997). Macrophages in resistance to candidiasis. Microbiology and molecular biology reviews *61*, 170-192.

Vempati, R.K. (2011). DNA damage in the presence of chemical genotoxic agents induce acetylation of H3K56 and H4K16 but not H3K9 in mammalian cells. Molecular biology reports.

Vempati, R.K., Jayani, R.S., Notani, D., Sengupta, A., Galande, S., and Haldar, D. (2010). p300-mediated acetylation of histone H3 lysine 56 functions in DNA damage response in mammals. Journal of Biological Chemistry *285*, 28553-28564.

Vermes, A., Guchelaar, H.J., and Dankert, J. (2000). Flucytosine: a review of its pharmacology, clinical indications, pharmacokinetics, toxicity and drug interactions. The Journal of antimicrobial chemotherapy *46*, 171-179.

Verstrepen, K.J., and Fink, G.R. (2009). Genetic and Epigenetic Mechanisms Underlying Cell-Surface Variability in Protozoa and Fungi. Annual Review of Genetics *43*, 1-24.

Wang, L., Tang, Y., Cole, P.A., and Marmorstein, R. (2008). Structure and chemistry of the p300/CBP and Rtt109 histone acetyltransferases: implications for histone

acetyltransferase evolution and function. Current Opinion In Structural Biology *18*, 741-747.

Watanabe, S., Resch, M., Lilyestrom, W., Clark, N., Hansen, J.C., Peterson, C., and Luger, K. (2010). Structural characterization of H3K56Q nucleosomes and nucleosomal arrays. Biochimica et biophysica acta *1799*, 480-486.

Whiteway, M., and Bachewich, C. (2007). Morphogenesis in Candida albicans*. Annual review of microbiology *61*, 529-553.

Williams, S.K., Truong, D., and Tyler, J.K. (2008). Acetylation in the globular core of histone H3 on lysine-56 promotes chromatin disassembly during transcriptional activation. Proceedings of the National Academy of Sciences *105*, 9000-9005.

Wurtele, H., Kaiser, G.S., Bacal, J., St-Hilaire, E., Lee, E.-H., Tsao, S., Dorn, J., Maddox, P., Lisby, M., Pasero, P., *et al.* (2012). Histone h3 lysine 56 acetylation and the response to DNA replication fork damage. Molecular And Cellular Biology *32*, 154-172.

Wurtele, H., Tsao, S., Lépine, G., Mullick, A., Tremblay, J., Drogaris, P., Lee, E.-H., Thibault, P., Verreault, A., and Raymond, M. (2010). Modulation of histone H3 lysine 56 acetylation as an antifungal therapeutic strategy. Nature medicine *16*, 774-780.

Wysong, D.R., Christin, L., Sugar, A.M., Robbins, P.W., and Diamond, R.D. (1998). Cloning and sequencing of a Candida albicans catalase gene and effects of disruption of this gene. Infection and immunity *66*, 1953-1961.

Xhemalce, B., Miller, K.M., Driscoll, R., Masumoto, H., Jackson, S.P., Kouzarides, T., Verreault, A., and Arcangioli, B. (2007). Regulation of histone H3 lysine 56 acetylation in Schizosaccharomyces pombe. The Journal of biological chemistry *282*, 15040-15047.

Xie, W., Song, C., Young, N.L., Sperling, A.S., Xu, F., Sridharan, R., Conway, A.E., Garcia, B.A., Plath, K., Clark, A.T., *et al.* (2009). Histone H3 Lysine 56 Acetylation Is Linked to the Core Transcriptional Network in Human Embryonic Stem Cells. Molecular cell *33*, 417-427.

Xu, D., Jiang, B., Ketela, T., Lemieux, S., Veillette, K., Martel, N., Davison, J., Sillaots, S., Trosok, S., Bachewich, C., *et al.* (2007a). Genome-wide fitness test and mechanism-of-action studies of inhibitory compounds in Candida albicans. PLoS pathogens *3*.

Xu, F., Zhang, K., and Grunstein, M. (2005). Acetylation in histone H3 globular domain regulates gene expression in yeast. Cell *121*, 375-385.

Xu, F., Zhang, Q., Zhang, K., Xie, W., and Grunstein, M. (2007b). Sir2 deacetylates histone H3 lysine 56 to regulate telomeric heterochromatin structure in yeast. Molecular cell *27*, 890-900.

Yan, Y., Harper, S., Speicher, D.W., and Marmorstein, R. (2002). The catalytic mechanism of the ESA1 histone acetyltransferase involves a self-acetylated intermediate. Nature structural biology *9*, 862-869.

Yang, B., Miller, A., and Kirchmaier, A.L. (2008). HST3/HST4-dependent Deacetylation of Lysine 56 of Histone H3 in Silent Chromatin. Molecular biology of the cell *19*, 4993-5005.

Yang, X., Figueiredo, L.M., Espinal, A., Okubo, E., and Li, B. (2009). RAP1 is essential for silencing telomeric variant surface glycoprotein genes in Trypanosoma brucei. Cell *137*, 99-109.

Yu, Y., Song, C., Zhang, Q., DiMaggio, P.A., Garcia, B.A., York, A., Carey, M.F., and Grunstein, M. (2012). Histone H3 Lysine 56 Methylation Regulates DNA Replication through Its Interaction with PCNA. Molecular cell, 1-11.

Yuan, J., Pu, M., Zhang, Z., and Lou, Z. (2009). Histone H3-K56 acetylation is important for genomic stability in mammals. Cell cycle *8*, 1747-1753.

Zhang, L., Eugeni, E.E., Parthun, M.R., and Freitas, M.A. (2003). Identification of novel histone post-translational modifications by peptide mass fingerprinting. Chromosoma *112*, 77-86.

Zhu, Q., and Wani, A.A. (2010). Histone modifications: crucial elements for damage response and chromatin restoration. Journal of cellular physiology *223*, 283-288.

Zunder, R.M., Antczak, A.J., Berger, J.M., and Rine, J. (2012). Two surfaces on the histone chaperone Rtt106 mediate histone binding, replication, and silencing. Proceedings of the National Academy of Sciences *109*, 144-153.